Validation Report for the PGE01-02-03 of the SAFNWC/MSG

SAF/NWC/IOP/MFL/SCI/VAL/01, Issue 1, Rev. 1

14 September 2006

Prepared by Météo-France / Centre de Météorologie Spatiale

REPORT SIGNATURE TABLE

Function	Name	Signature	Date
Prepared by	MF/DP/CMS		
Reviewed by	MF/DP/CMS		
Authorised by	L. F. López Cotín SAFNWC Project Manager		*14 September 2006*

DOCUMENT CHANGE RECORD

Version	Date	Pages	CHANGE(S)
1.0	1 September 2005	87	Initial
1.1	14 September 2006	87	Results of comparisons with interactive data set were not those of version 1.2 of the software. Tables 4 and 5 and figures 16,17,18,19 have been corrected accordingly.

Table of contents

List of Tables and Figures

1. INTRODUCTION

1.1 SCOPE OF THE DOCUMENT

An extensive validation of prototyped algorithms using AVHRR, HIRS, GOES and MODIS data has been performed during the SAFNWC development phase, and documented in Scientific Reports (AD. 1, AD. 2, AD. 3).

No real SEVIRI data were available during the SAFNWC development phase, due to the delay of MSG launch. The validation phase has therefore been postponed to the Initial Operational Phase.

The algorithm has been tuned with real SEVIRI data (AD. 4, AD. 5), before being validated.

This document successively presents the validation of CMa, CT and CTTH using SEVIRI/MSG-1 data.

1.2 SOFTWARE VERSION IDENTIFICATION

The validation results presented in this document apply to the algorithms implemented in the release 1.2 of the SAFNWC/MSG SW package.

1.3 DEFINITIONS, ACRONYMS AND ABBREVIATIONS

ARPEGE	French weather forecast model
BUFR	European Centre for Medium range Weather Forecast
CMa	Cloud Mask (also PGE01)
CMS	Centre de Météorologie Spatiale (Météo-France, satellite reception and processing centre in Lannion)
CT	Cloud Type
CTTH	Cloud Top Temperature and Height
ECMWF	
GOES	Geostationary Operational Environmental Satellite
IR	Infrared
MSG	Meteosat Second Generation
SAFNWC	Satellite Application Facility for support to NoWcasting
SEVIRI	Spinning Enhanced Visible & Infrared Imager
SIRTA	Site Instrumental de Télédetection Atmosphérique (located near Paris)
SYNOP	Synoptic observation
SW	SoftWare
WAVE	Image processing commercial software
WMO	World Meteorological Organisation

1.4 REFERENCES

1.4.1 Applicable Documents

Reference	Title	Code	Vers	Date
[AD. 1]	Prototype Scientific Description for Meteo-France/CMS. February 2000.	SAF/NWC/MFCMS/MTR/PSD	1.0	01/02/00
[AD. 2]	Use of MODIS to enhance the PGE01-02 of the SAFNWC / MSG.	SAF/NWC/MFL/SCI/PSD/02	1.0	17/12/01
[AD. 3]	SAFNWC/MSG PGE01-02 tuning using GOES and MODIS	SAF/NWC/IOP/MFL/SCI/TUN/01	0.1	22/10/02
[AD. 4]	Scientific report on First checking and Tuning for MSG PGE01-02-03	SAF/NWC/IOP/MFL/SCI/RP/01	1.0	17/12/03
[AD. 5]	Scientific report on additional tuning of MSG PGE01-02-03 following validation activities	SAF/NWC/IOP/MFL/SCI/RP/02	0.1	03/05/05

Table 1 List of Applicable Documents

1.4.2 Reference Documents

Reference	Title	Code	Vers	Date
[RD.1]				
[RD.2]				

Table 2 List of Referenced Documents

2. CMA VALIDATION

2.1 OVERVIEW

2.1.1 General objectives of the validation

The following extensive validation of the CMa product is performed:

- ✓ The CMa cloud mask is validated for all seasons, various atmospheric conditions (mid-latitude and nordic), and in different geographical areas
- ✓ The CMa dust detection is validated on numerous selected cases
- ✓ The CMa volcanic ash detection is illustrated on two volcanic events whereas false alarm ratios are estimated in various conditions

The validation is mainly performed using objective methods, but results from visual inspection are also available.

2.1.2 Methodology outline

A first estimation of the CMa product's quality is done using the Interactive Target Database, although this database has been used during the tuning process.

The main validation of the CMa cloud mask consists in a comparison with surface observations (SYNOP).

Visual inspection is also performed by skilled forecasters using a dedicated visualisation tool to complement automatic validation methods.

In all these validation studies, CMa is retrieved over the MSG full disk using NWP fields forecast by the French model ARPEGE four times per day (0h, 6h, 12h and 18h) at a 1.5 degree horizontal resolution.

2.2 CMA CLOUD MASK: COMPARISON WITH INTERACTIVE TARGET DATABASE

As a first step towards verification of the CMa cloud mask, contingency tables and statistical scores are computed using results of the CMa applied to the SEVIRI data from the Interactive Target Database gathered over MSG full disk as soon as SEVIRI data were available (see Annex 1).

This can't be strictly a verification, as a great part of CMa tuning is based on the use of the interactive file which makes them dependent, and therefore may lead to artificially change the real skill of CMa. Moreover, most cases in interactive target database have been manually selected because they were presenting a difficulty for CMa algorithm (excessive numbers of cloud non-detection), therefore the statistical indicators are biased and must be handled with care when measuring the CMa performance. On the other hand, this interactive target database will be useful to quantify the improvement when changing algorithm version). From the initial data set we have removed targets related to dust identification.

Each interactive target is analysed using CMa results of its 3x3 pixels according to the following rules; a cloudy target is detected when at least 7 pixels are detected cloudy by CMa, a clear target is detected when at least 7 pixels are detected clear by CMa. Therefore the other cases (only 6.2% of useful targets) are not taken into account in the statistics.

	Cloud detected	Clear detected
Cloud observed	n_a	n_b
Clear observed	n_c	n_d

Table 3 Contingency table conventions for CMa validation

The following statistical indicators derived from the contingency tables (see Table 3) are computed:

- PC= $[(n_a+n_d)/(n_a+n_b+n_c+n_d)]$, is the percentage of correct detections (PC)

Two indicators stratified by observation qualify producer's accuracy, should be as low as possible

- $(1.\text{-POD}_{Cloud})=[n_b/(n_a+n_b)]$, is the rate of missed cloud observations, i.e. targets classified as cloud-free but observed cloudy (it expresses cloud underdetection errors).
- $(1.\text{-POD}_{Clear})=[n_c/(n_c+n_d)]$, is the rate of missed clear observations or false flagging of clouds, i.e. the targets classified as cloudy but observed clear (it expresses cloud overdetection errors)

Two indicators stratified by detection qualify user's accuracy, should be as low as possible

- $(FAR_{Cloud})=[n_c/(n_a+n_c)]$, is the rate of false detections of cloudy events
- $(FAR_{Clear})=[n_b/(n_b+n_d)]$, is the rate of false detections of clear events

The statistical indicators are associated with changes in latitudes, (for Nordic (latitude larger than 55 degrees) and mid-latitude (latitude between 20 and 55 degrees) conditions), scene background (land or sea) and illumination conditions (day, night, twilight, sunglint).

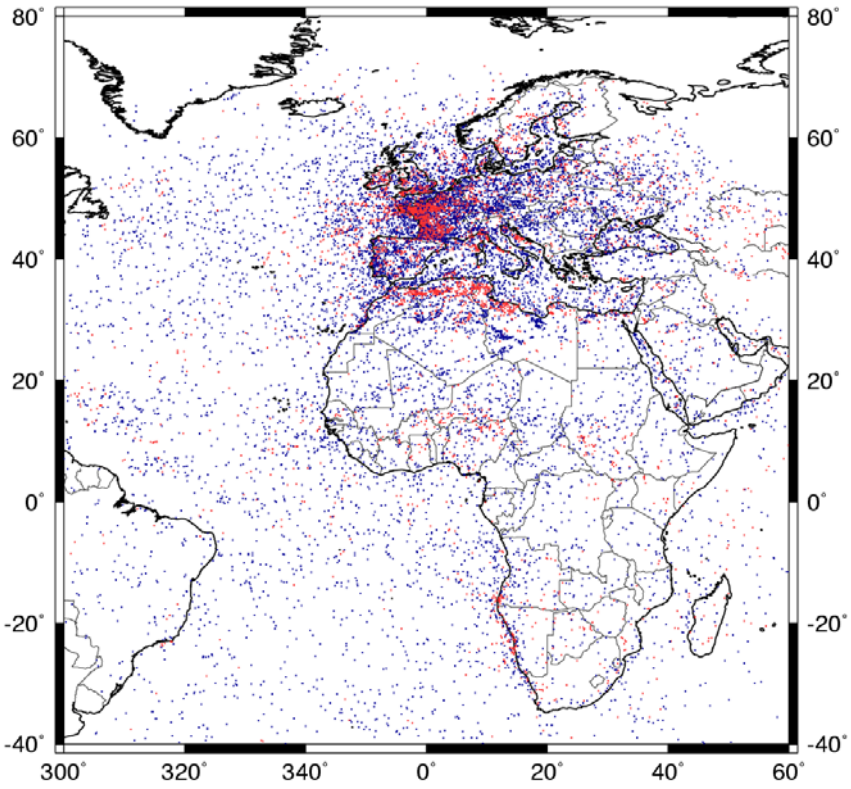

Figure 1 Localisation of the interactive targets used for CMa validation, red and blue dots correspond respectively to manually assigned clear (including snow) and cloudy targets.

According to the results shown by Table 4, as observed when validating GOES prototype during SAFNWC development phase see [AD. 1], CMa algorithm performs better over ocean than over land at night and twilight. Considering the disparity observed between the different stratifications it is not possible to state that over ocean night algorithm is better than day (this was one conclusion of GOES prototype validation). Nevertheless Table 5 indicates that over sea in night-time condition CMa seems better for Nordic cases than mid-latitude ones. But one must keep in mind that the interactive target database have been manually selected when presenting a difficulty for CMa or CT algorithm.

	Contingency table		**PC (%)**	**1-PODCloud (%)**	**1-PODClear (%)**	**FARCloud (%)**	**FARClear (%)**
All targets	7242	2821	80.4	28.0	5.4	4.2	33.3
	324	5661					
Sea	3586	498	90.7	12.2	4.0	2.4	18.7
	90	2165					
Land	3656	2323	73.7	38.9	6.3	6.0	39.9
	234	3496					
Day over Sea	1783	90	95.0	4.8	5.4	2.8	9.2
	51	893					
Day over Land	1728	156	93.9	8.3	3.8	3.7	8.4
	67	1712					
Night over Sea	1554	325	88.4	17.3	2.3	1.7	22.3
	27	1132					
Night over Land	1548	1508	63.8	49.3	8.9	7.9	52.8
	132	1346					
Twilight over Sea	249	83	80.4	25.0	7.9	4.6	37.2
	12	140					
Twilight over Land	380	659	54.1	63.4	7.4	8.4	60.1
	35	438					
Sunglint	45	9	95.5	16.7	0.6	2.2	5.2
	1	165					

Table 4 CMa performance in the detection of cloudy and cloud-free events from interactive target database; stratification with illumination and land/sea conditions.

	Contingency table		PC (%)	1-PODCloud (%)	1-PODClear (%)	FARCloud (%)	FARClear (%)
Nordic Sea Day	245	2	96.1	0.8	11.1	4.7	2.0
	12	96					
Nordic Sea Night	161	3	98.4	1.8	1.2	0.6	3.5
	1	83					
Nordic Sea Twilight	92	19	84.8	17.1	4.8	1.1	48.7
	1	20					
Midlatitude Sea Day	1035	40	95.8	3.7	5.1	2.5	7.4
	27	498					
Midlatitude Sea Night	784	251	84.3	24.3	2.0	1.6	28.5
	13	630					
Midlatitude Sea Twilight	131	60	77.4	31.4	7.9	6.4	36.4
	9	105					

Table 5 CMa performance in the detection of cloudy and cloud-free events over sea from interactive target database; stratification with illumination and latitude

2.3 CMA CLOUD MASK: COMPARISON WITH SURFACE OBSERVATION (SYNOP)

The quantitative comparison of the CMa cloud mask with surface synoptic observations is made possible thanks to the use of the coincident satellite targets and SYNOP data gathered from 1st November 2003 up to 28th February 2005 from terrestrial stations over Europe and North Africa, (as shown in Figure 36: unless specified only manned stations (the selected station dataset (SSD) subset) are retained in the statistics). This dataset is not used when training and developing CMa algorithms, so that the quality indicators and skill scores computed with this dataset should not be suspected to be overestimated.

From the SYNOP data set, ground-based total cloud cover (N) and partial cloud cover from low, medium and high clouds are available. Satellite cloud coverage is estimated from CMa applied to the pixels of the satellite targets. To simulate the surface observations from the satellite pixels, no attempt is made to take into account the complexity of the observation, and the 25 pixels inside the satellite data target are used for the evaluation.

2.3.1 CMa and SYNOP cloud cover comparison

The total cloudiness over SYNOP station is very roughly simulated from CMa results over the 5x5 target centred on the station by counting each pixel detected as cloud contaminated as 100% covered. This CMa-based cloud cover simulation can be compared with SYNOP total cloud cover through contingency tables as Table 6 and statistical indicators computed for several stratifications of the dataset and presented below through figures and tables.

obs/sat	0	1	2	3	4	5	6	7	8	total
0	**60706**	7908	2744	1446	984	815	756	719	2893	78971
1	41020	**7590**	3222	1827	1243	814	699	517	1656	58588
2	24101	6824	**4009**	2833	2242	1693	1448	1198	3550	47898
3	14643	5935	4222	**3494**	3192	2862	2722	2276	6030	45376
4	7043	3759	3175	3132	**3065**	3144	3208	3316	9102	38944
5	4493	2765	2749	2967	3306	**3731**	4427	5275	18117	47830
6	2434	1882	2101	2479	3087	3864	**5244**	7145	39992	68228
7	1859	1505	1700	2210	3010	3861	5703	**9466**	137168	166482
8	1502	992	1006	1222	1614	2000	3015	4776	**140349**	156476
total	157801	39160	24928	21610	21743	22784	27222	34688	358857	708793

Table 6 Contingency table for SSD subset (manned stations) from collocated surface and MSG-1/SEVIRI observations from 01/11/2003 to 28/02/2005.

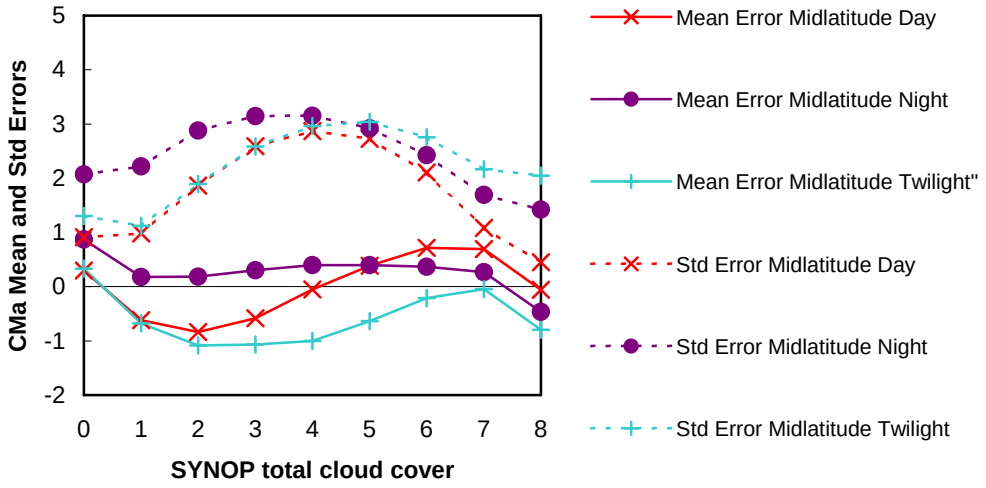

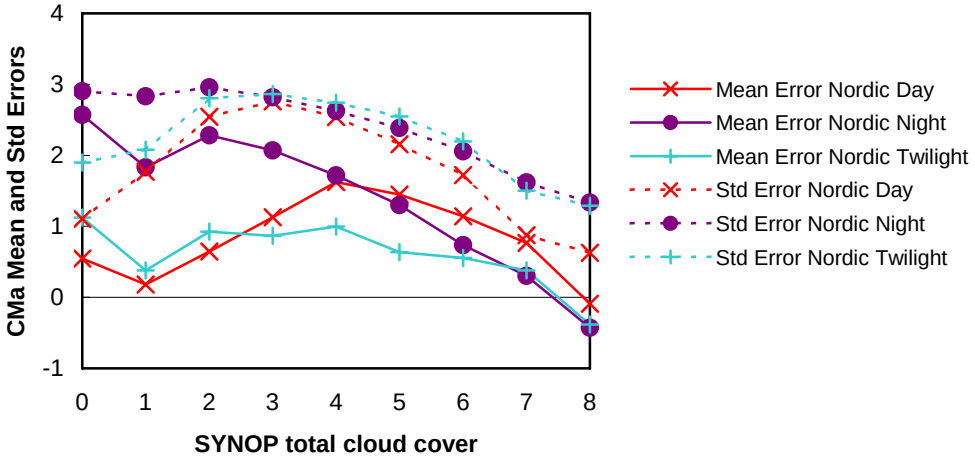

Figure 2 CMa Cloud cover Mean error (satellite-synop) and standard deviation against SYNOP cloud cover for midlatitude (top) and Nordic(bottom) matchups according to illumination ; day (red x), night (purple circle), twilight (blue +) with SSD subset from 01/11/2003 to 28/02/2005

Figure 2, top, shows that there is a rather good agreement in midlatitude regions between satellite and SYNOP cloud covers. The mean error (satellite-synop) ranging between -1 and +1 octas, is quite constant and slightly positive at night except for overcast situations, globally negative at twilight, negative at low cloudiness but positive at large ones for daytime matchups. Figure 2, bottom, illustrates the impact of latitude (but mixing also resolution, viewing angles and climatic effects). We see that the cloud cover overestimation becomes systematic for Nordic cases, reaching more than 2 octas at night for low cloudiness, less than 1 octa at daytime for low cloudiness but a little more for high cloudiness, and being in general positive but less than 1 octa at twilight. The dispersion of the CMa and SYNOP cloud covers relative behaviours is also expressed through histograms plotted in Figure 3 and Figure 4 below.

These behaviours are confirmed by Table 7, quantifying also the underestimation of CMa-based cloud cover simulation for midlatitude at twilight, and its overestimation for Nordic cases at daytime and night-time, keeping in mind that the imbalance between low and high cloudiness populations among the subsets affects the statistics.

	All matchups				Midlatitude				Nordic			
	All	Day	Night	Twil	All	Day	Night	Twil	All	Day	Night	Twil
Matchups	708793	318289	290897	99607	596371	281939	240643	73789	112422	36350	50254	25818
MAE	1.36	1.27	1.43	1.47	1.36	1.27	1.41	1.54	1.36	1.25	1.48	1.27
BIAS	.169	.201	.288	-.281	.094	.143	.212	-.473	.564	.652	.651	.269
Δ =0	33.5	29.3	38.7	32.0	33.0	29.0	38.4	30.8	36.2	31.1	40.1	35.6
Δ =1	67.7	68.6	67.1	66.3	67.3	68.4	67.0	64.4	69.3	69.9	67.8	71.5
Δ=2	82.4	85.3	79.8	80.5	82.4	85.3	80.0	79.2	82.4	85.7	79.0	84.4

Table 7 Summary statistics of CMa cloud cover errors (satellite-synop) stratified by illumination and latitude from SSD subset from 01/11/2003 to 28/02/2005; MAE (mean absolute error, expressing in octas the magnitude of the errors) and bias (expressing in octas the direction of the errors, detection minus observation); Percentage of CMa cloud cover restitutions having a tolerance Δ= 0,1,2 octas with the SYNOP observation.

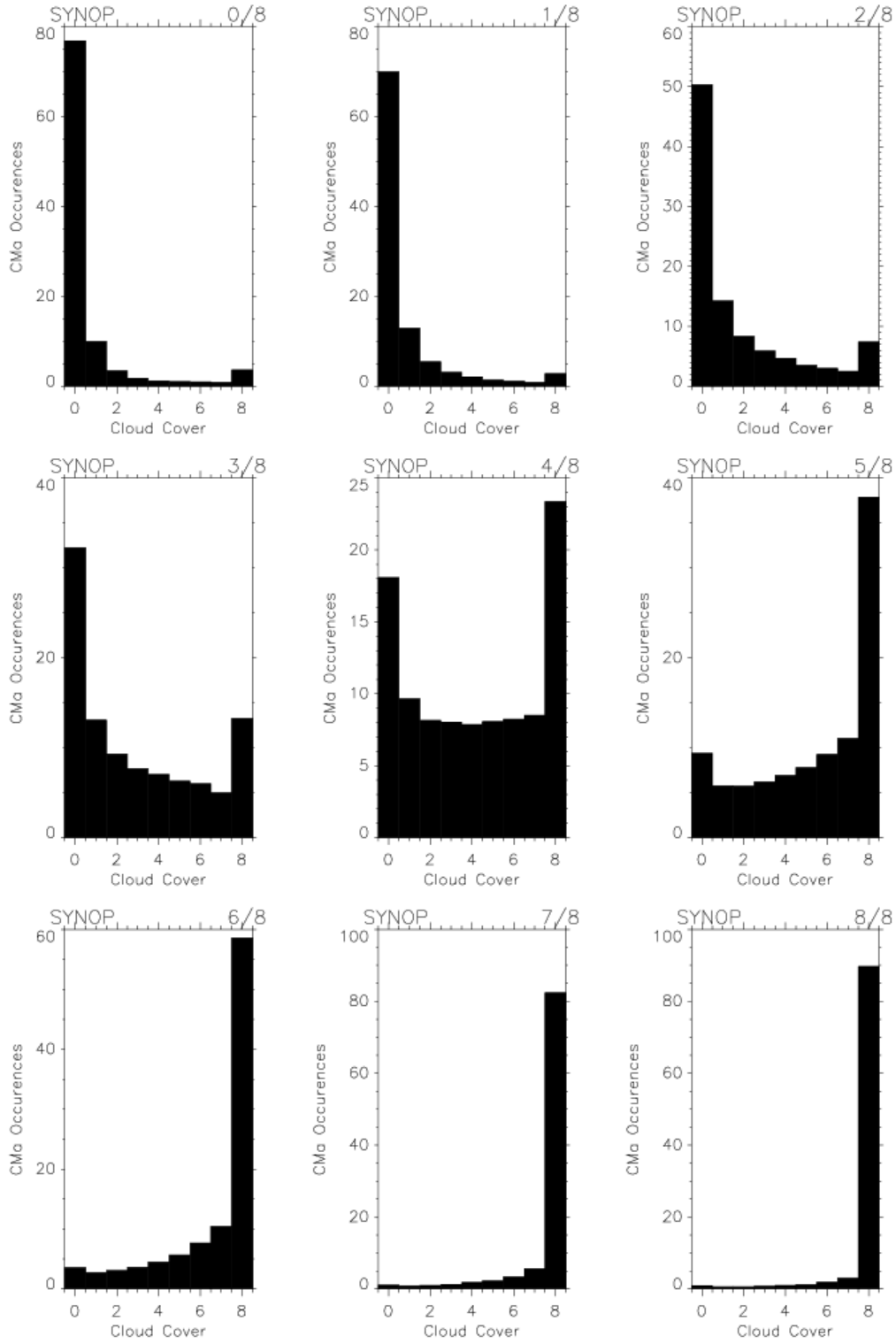

Figure 3 Percentage of occurrences of CMa cloudiness restitution for a given SYNOP cloud cover

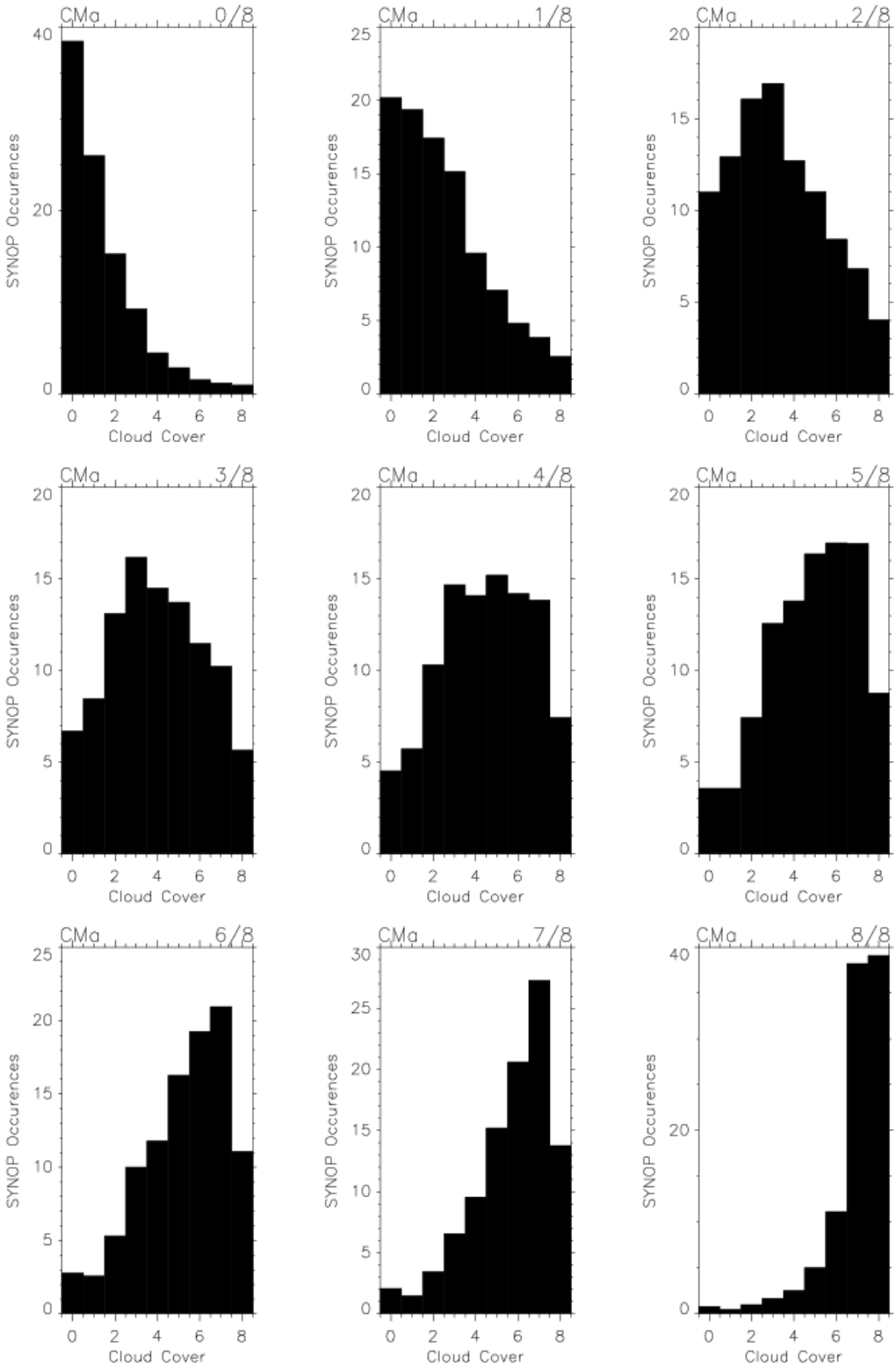

Figure 4 Percentage of occurrences of SYNOP cloud cover for a given CMa cloudiness restitution

2.3.2 CMa evaluation for clear and cloudy events detection

The second part of CMa evaluation examines only cases that show disagreement with SYNOP cloud cover, i.e. when CMa misses clouds reported almost overcast by the ground observer and when CMa detects clouds where SYNOP report no or insignificant cloud cover. For this purpose we build up two-by-two contingency tables counting "cloudy" and "clear" events. An observation is cloudy if N from SYNOP is strictly more than 5 octas, clear if N is strictly less than 3 octas. A detection is cloudy if more than 16/25 pixels are flagged cloud contaminated, clear if less than 8/25 are clear. Consequently all events with N=3,4,5 and equivalent CMa cloud covers expressed in octas are not taken into account in these statistics. An observed event is "missed" if not detected (accuracy indicators interesting the producer), a detection is "false" if not observed (accuracy indicators interesting the user). This study relies on analysis of contingency tables and comparison of statistical scores.

The following statistical indicators derived from the contingency tables (see Table 3) are computed:

- PC= $[(n_a+n_d)/(n_a+n_b+n_c+n_d)]$, is the percentage of correct detections (PC)

Two indicators stratified by observation qualify producer's accuracy, should be as low as possible

- $(1.-POD_{Cloud})=[n_b/(n_a+n_b)]$, is the rate of missed cloud observations, i.e. targets classified as cloud-free but observed cloudy (it expresses cloud underdetection errors).
- $(1.-POD_{Clear})=[n_c/(n_c+n_d)]$, is the rate of missed clear observations or false flagging of clouds, i.e. the targets classified as cloudy but observed clear (it expresses cloud overdetection errors)

Two indicators stratified by detection qualify user's accuracy, should be as low as possible

- $(FAR_{Cloud})=[n_c/(n_a+n_c)]$, is the rate of false detections of cloudy events
- $(FAR_{Clear})=[n_b/(n_b+n_d)]$, is the rate of false detections of clear events

A summary skill score

- Heidke skill score (HSS) expresses as a decimal fraction, the percentage of detections which are correct after eliminating those which would have been correct on the basis of chance. It is computed as:
  $[n_a+n_d-[(n_a+n_b)(n_a+n_c)+(n_c+n_d)(n_b+n_d)/total]] / [total-[(n_a+n_b)(n_a+n_c)+(n_c+n_d)(n_b+n_d)/total]]$

HSS requires a period of verification sufficiently long to evaluate the skill of CMa under all conditions. One year of observations should be sufficient to allow its use.

Contingency tables and statistical scores have been computed for various illumination conditions, and different geographic areas for SAFNWC/MSG CMa v1.2 algorithms and are presented below.

	Contingency table		PC (%)	1-PODCloud (%)	1-PODClear (%)	FARCloud (%)	FARClear (%)	HSS
Nordic	67994	1943	93.24	2.78	22.02	5.58	12.00	.7850
	4022	14242						
Midlatitude	284864	13038	95.02	4.38	6.14	3.20	8.31	.8897
	9414	143882						
Nordic Day	21926	274	97.01	1.23	9.76	2.50	5.00	.9069
	563	5205						
Midlatitude Day	140389	3455	97.68	2.40	2.16	1.01	5.04	.9467
	1434	65115						
Nordic Night	29997	1074	89.99	3.46	33.34	8.84	15.59	.6837
	2909	5815						
Midlatitude Night	109405	5626	92.93	4.89	10.66	6.38	8.26	.8489
	7452	62473						
Nordic Twilight	16071	595	94.40	3.57	14.58	3.31	15.59	.8147
	550	3222						
Midlatitude Twilight	35070	3957	91.97	10.14	3.14	1.48	19.54	.8197
	528	16294						

Table 8 CMa performance in the detection of fully cloudy and cloud-free events estimated from collocated surface and MSG-1/SEVIRI observations from 01/11/2003 to 28/02/2005 when NWP are available (from SSD subset: 539399 matchups)

This table shows that the daytime CMa algorithm performs best, both for Nordic and mid-latitude subsets, with an excellent PC around 97%, except a small weakness expressed by (1-POD_{Clear}) around 10% for Nordic subset, confirming a cloud over-detection at low SYNOP cloud covers that was also visible in graphs of Figure 2.

The trend of the night algorithm to overestimation at low cloud amounts is confirmed by (1-POD_{Clear}) values of 10% and 33% in mid-latitude and Nordic regions. One reason is the human observation errors in darkness. In Nordic regions, the higher values must be due to the confusion of cold snowy grounds with snow.

At twilight in mid-latitude regions, the tendency to underestimate cloud cover is confirmed by (1-POD_{Cloud}) values of 10% larger than those for day or night conditions. The main reason is that the T10.8µm-T3.9µm test becomes inoperative due to sun contamination whereas our reflectance-based tests are not enough efficient, thus leading to frequent low clouds non detection. This is not the case in Nordic areas where (1-POD_{Cloud}) values of 3.6% in twilight conditions are very similar to those observed at night and are much lower than those in mid-latitude regions. One explanation for this behaviour is a better performance of T10.8µm-T8.7µm test at large viewing angles (improving the detection of low clouds for Nordic cases both at daytime and twilight).

For the Nordic stations, the overestimation at low cloud covers counts for much in the statistics. It is indicative of the obvious greater difficulty to detect clear grounds when they are in darkness, very cold, and observed with a wider field of view.

2.3.2.1 Impact of station selection

	Contingency table		PC (%)	1-POD Cloud (%)	1-POD Clear (%)	FAR Cloud (%)	FAR Clear (%)	HSS
Nordic	114787	3174	93.53	2.69	21.66	5.25	12.13	.7886
	6356	22991						
Midlatitude	404882	20646	94.48	4.85	6.53	4.33	7.29	.8850
	18354	262701						
Nordic Day	37469	575	96.96	1.51	9.07	2.28	6.15	.9027
	876	8782						
Midlatitude Day	192794	6021	97.30	3.03	2.14	1.29	4.96	.9426
	2521	115341						
Nordic Night	50942	1590	90.57	3.02	33.67	8.40	14.73	.6894
	4670	9201						
Midlatitude Night	160533	8797	92.23	5.19	11.03	8.41	6.89	.8417
	14740	118874						
Nordic Twilight	26376	1009	94.52	3.68	13.92	2.98	16.77	.8130
	810	5008						
Midlatitude Twilight	51555	5828	92.04	10.16	3.69	2.07	16.98	.8293
	1093	28486						

Table 9 CMa performance in the detection of fully cloudy and cloud-free events estimated from collocated surface and MSG-1/SEVIRI observations from 01/11/2003 to 28/02/2005 when NWP are available (from NSASD subset: 853891 matchups)

The comparison of Table 8 and Table 9 above, indicates that reducing the full dataset (called NSASD) to the SYNOP stations presenting statistics of total cloud amount with anomalies at 1 and 7 (called SSD dataset, Figure 36 and annex 3 for explanations) has not a very high impact on the statistical scores. For the midlatitude subset, the number of cloudy cases increase significantly, from 60% to 68%, indicating that reducing this subset changes somehow its nature. This decrease of the number of clear cases plays a role in the slight deterioration of FAR_{Clear} for mid-latitude stations of SSD. In fact the right part of Figure 36 shows that many stations placed in the southern part of mid-latitude subset are not kept by the selection, therefore giving a heavier weight in SSD to stations with a behaviour closer to Nordic. Several assumptions are open to explain that the N1N7 anomaly suppresses more southern stations. One of them is that the climate of many of them is so dry that numerous clear skies don't present this anomaly. Another one is that during the period automation of stations is appearing, then their N1N7 anomaly becomes blurred with time and can't not be tracked by the cloud cover series.

All other scores are very slightly better with SSD, except for Nordic stations at night-time, where both FAR_{Cloud} and FAR_{Clear} indicate a very slight deterioration similar to the one observed for mid-latitude at night. Here the reduction does not change the nature of the subset as cloudy and clear proportions remain similar. In fact 79% of night-time cases are cloudy in NSASD and 78% in SSD. This small decrease may be due to some automatic observations (detecting more clouds) have been removed, increasing by consequence the number of cloud covers underestimated by human observer at night.

2.3.2.2 Impact of CMa quality on cloud free detection for land remote-sensing

This section analyses whether the CMa quality flag may be useful for land remote-sensing to identify really cloud free areas. The statistical analysis is the same as described in 2.3.2, but cloud free pixels with poor quality are considered as cloudy. The comparison of ($1\text{-}POD_{cloud}$) and FAR_{Clear} in Table 8 and Table 10 indicates the impact of using the CMa quality flag on the identification of cloud free areas. The number of correctly clear detected events indicates the loss of available pixels for land remote sensing activities.

	Contingency table		PC (%)	1-POD Cloud (%)	1-POD Clear (%)	FAR Cloud (%)	FAR Clear (%)	HSS
Nordic	68824	1113	90.57	1.17	39.43	9.47	7.47	.6726
	7202	11062						
Midlatitude	289555	8347	92.70	2.30	16.05	7.83	5.16	.8329
	24609	128687						
Nordic Day	21884	216	95.08	0.82	20.13	5.02	4.01	.8399
	1161	4823						
Midlatitude Day	141074	2770	96.54	1.64	6.78	3.10	3.71	.9194
	4514	62035						
Nordic Night	30501	570	86.83	1.3	53.53	13.28	10.25	.5371
	35171	4624						
Midlatitude Night	111645	3386	88.52	2.29	25.53	13.78	4.96	.7455
	17851	52074						
Nordic Twilight	16339	327	91.69	1.39	36.35	7.74	9.43	.6909
	1371	2401						
Midlatitude Twilight	36836	2191	92.06	4.75	13.34	5.74	11.45	.8112
	2244	14578						

Table 10 CMa performance in the detection of fully cloudy and good quality cloud-free events estimated from collocated surface and MSG-1/SEVIRI observations from 01/11/2003 to 28/02/2005 when NWP are available (SSD subset, poor quality cloud-free pixels being merged with cloudy pixels)

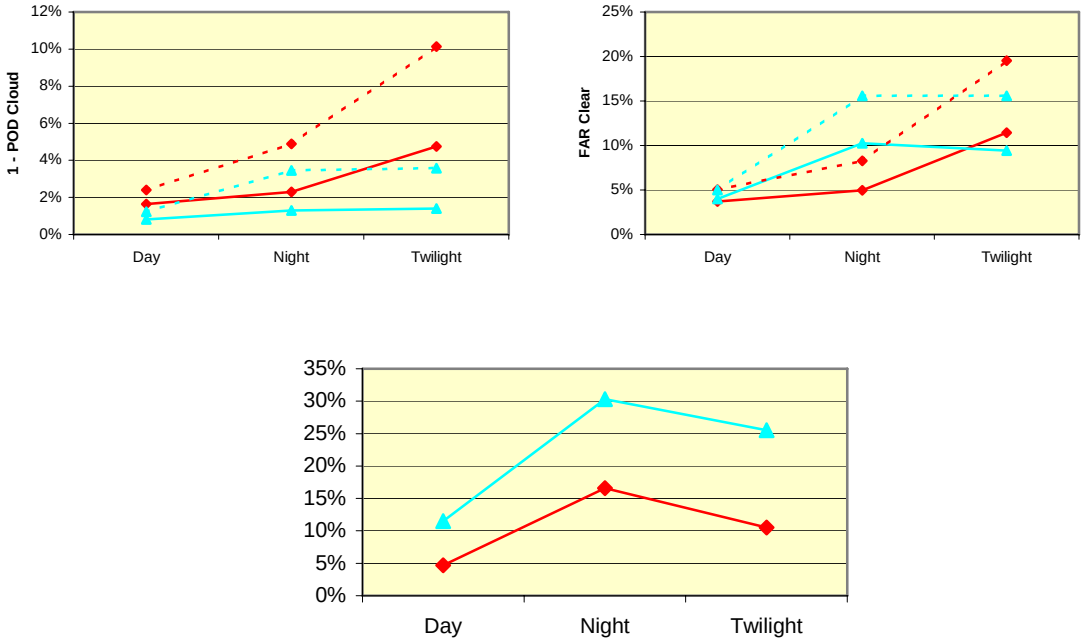

Figure 5 (1-POD_{Cloud}), top left, and FAR_{Clear}, top right, variations against illumination conditions for SSD subset (solid line when poor quality cloud-free pixels are merged with cloudy pixels, dotted when ignoring quality flags). Bottom: Decrease of correct Clear matchups when poor quality cloud-free pixels are merged with cloudy pixels. (mid-latitude in red, Nordic in blue)

2.3.2.3 Impact of missing NWP

The impact of missing NWP data in the algorithms is illustrated by Table 11 (when compared to Table 8) and by Figure 6. Their use is clearly positive as expected, mainly by allowing a decrease of FAR_{Cloud} indicators of 40% indicating that less cloud free areas are confused with clouds (due to the use of forecast surface temperature). As illustrated on Figure 6, the highest gain is for Nordic stations at night and twilight, it is also important at night for mid-latitude stations, and becomes less detectable at daytime.

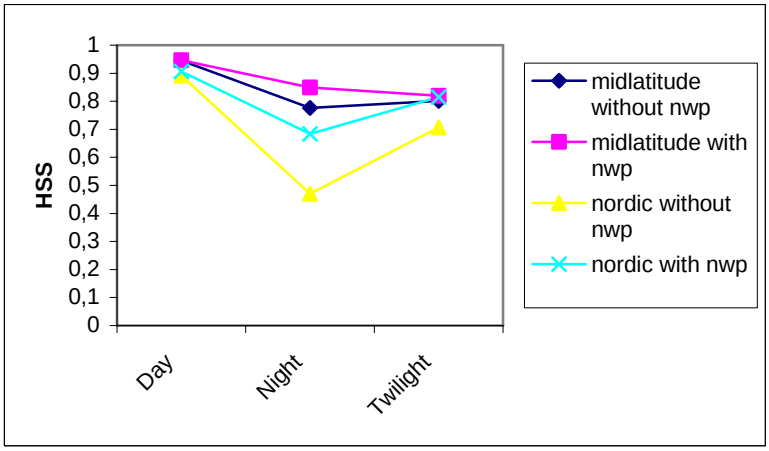

Figure 6 Impact of NWP for geographical subsets against illumination conditions summarised by Heidke Skill Score (HSS); midlatitude stations (square and diamond respectively with and without NWP); Nordic stations (cross and triangle respectively with and without NWP).

	Contingency table		PC (%)	1-POD Cloud (%)	1-POD Clear (%)	FAR Cloud (%)	FAR Clear (%)	HSS
Nordic	70127	1291	90.29	1.81	39.36	9.61	10.29	.6641
	7461	11258						
Midlatitude	292006	11331	93.67	3.74	11.43	5.68	7.76	.8569
	17599	136389						
Nordic Day	21985	276	96.57	1.24	11.94	3.02	5.19	.8918
	684	5045						
Midlatitude Day	142190	3408	97.63	2.34	2.42	1.14	4.93	.9456
	1637	65793						
Nordic Night	31420	617	85.13	1.93	60.00	14.93	14.39	.4700
	5513	3675						
Midlatitude Night	113537	4428	89.87	3.75	2.09	11.38	7.43	.7765
	14582	55167						
Nordic Twilight	16722	398	92.06	2.33	33.25	7.03	13.56	.7069
	1264	2538						
Midlatitude Twilight	36279	3495	91.38	8.78	8.21	3.66	18.47	.8009
	1380	15429						

Table 11 CMa performance in the detection of fully cloudy and cloud-free events estimated from collocated surface and MSG-1/SEVIRI observations for targets from 01/11/2003 to 28/02/2005 without using NWP information

2.3.2.4 Impact of land/coast

Introducing sea as background should tend to ease cloud detection when it is the most difficult, this may explain why for Nordic cases, dominated by cloud cases, CMa accuracy is in general better for coastal stations especially at day and night. But statistics over coast may be blurred by navigation errors in images, as these errors may lead to detect true clear land pixels as cloudy if the error shifts land over sea, this can play a small role in FAR_{Cloud} increase. A clear coast line is also often detected as cloudy by CMa algorithm, particularly during daytime, this fact is more frequent in mid-latitude dataset where clear reports are more frequent and land/sea contrasts are higher, both in IR and VIS bands especially during summer.

	Contingency table		PC (%)	1-POD Cloud (%)	1-POD Clear (%)	FAR Cloud (%)	FAR Clear (%)	HSS
Nordic	51169	1687	92.53	3.19	23.64	6.07	13.65	.7642
	3304	10670						
Midlatitude	304986	14873	94.61	4.65	6.65	3.96	7.78	.8848
	12565	176378						
Nordic Day	17067	238	96.83	1.38	10.62	2.54	5.99	.8968
	444	3736						
Midlatitude Day	147127	4212	97.40	2.78	2.24	1.17	5.23	.9426
	1745	76332						
Nordic Night	22601	970	88.89	4.11	34.76	9.69	17.57	.6597
	2425	4552						
Midlatitude Night	118659	6220	92.45	4.98	11.1	7.80	7.19	.8441
	10035	80342						
Nordic Twilight	11501	479	93.82	4.00	15.44	3.64	16.74	.8008
	435	2382						
Midlatitude Twilight	39200	4441	91.85	10.18	3.83	1.96	18.39	.8211
	785	19704						

Table 12 CMa performance in the detection of fully cloudy and cloud-free events estimated from collocated surface and MSG-1/SEVIRI observations for strictly land stations from 01/11/2003 to 28/02/2005 when NWP are available

	Contingency table		PC (%)	1-POD Cloud (%)	1-POD Clear (%)	FAR Cloud (%)	FAR Clear (%)	HSS
Nordic	58556	1414	94.35	2.36	19.72	4.51	11.17	.8091
	2763	11250						
Midlatitude	95952	5726	94.10	5.63	6.20	5.47	6.39	.8816
	5547	83957						
Nordic Day	18932	310	97.12	1.61	7.79	2.01	6.32	.9113
	388	4592						
Midlatitude Day	44214	1805	96.99	3.92	1.93	1.66	4.53	.9395
	746	37993						
Nordic Night	25955	595	92.01	2.24	32.31	7.25	12.28	.7170
	2029	4251						
Midlatitude Night	40038	2544	91.66	5.97	10.76	10.12	6.36	.8332
	4506	37469						
Nordic Twilight	13669	509	94.95	3.59	12.57	2.47	17.46	.8189
	346	2407						
Midlatitude Twilight	11700	1377	92.35	10.53	3.36	2.46	13.95	.8441
	295	8495						

Table 13 CMa performance in the detection of fully cloudy and cloud-free events estimated from collocated surface and MSG-1/SEVIRI observations from 01/11/2003 to 28/02/2005 with NWP, for coastal stations.

2.3.2.5 Geographical distribution of the errors

It is interesting to look at the spatial distribution of the errors. For this purpose we have computed the errors by station and plotted them on a map using a colour code showing worst, average and best behaviour related to the considered error.

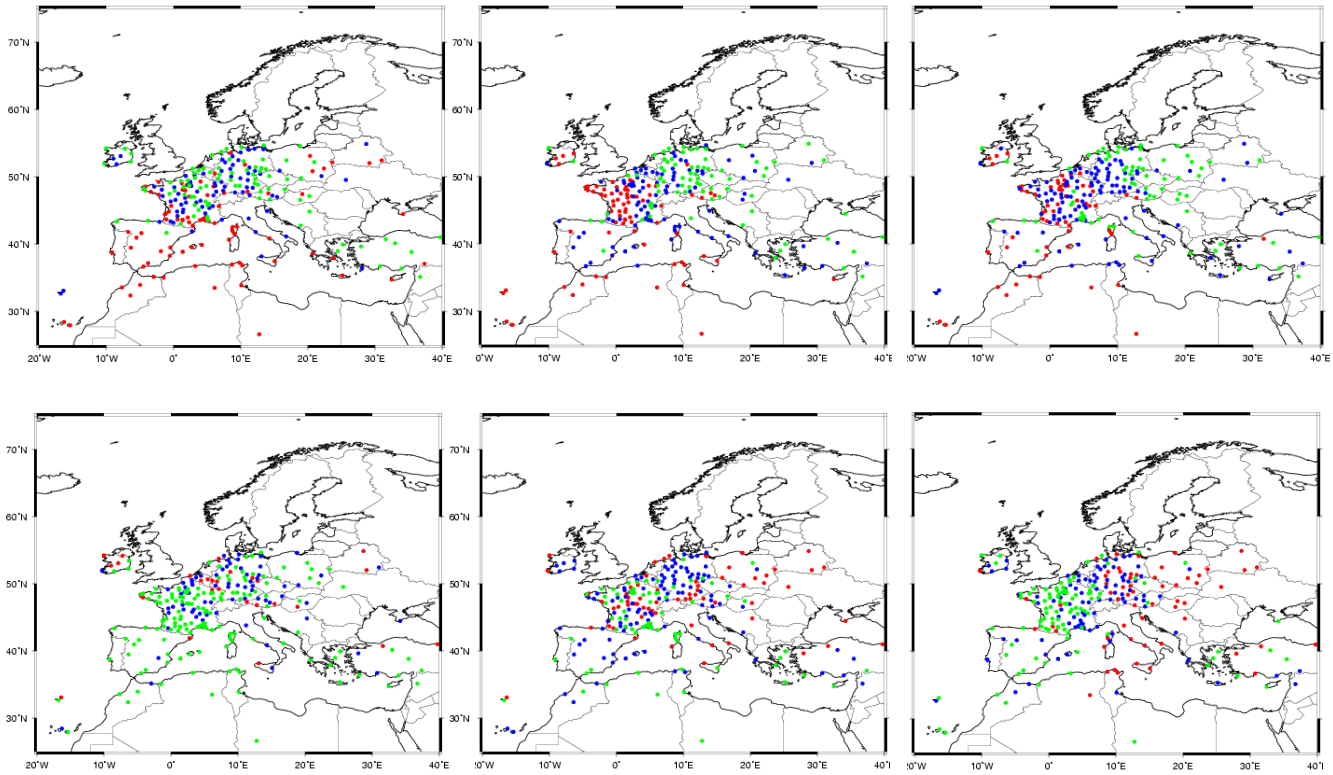

Figure 7 Spatial distribution of underdetection (Top) and overdetection errors (Bottom) for midlatitude stations, (left day, centre night, right twilight). red is used for high errors, blue for average errors and green for low errors.

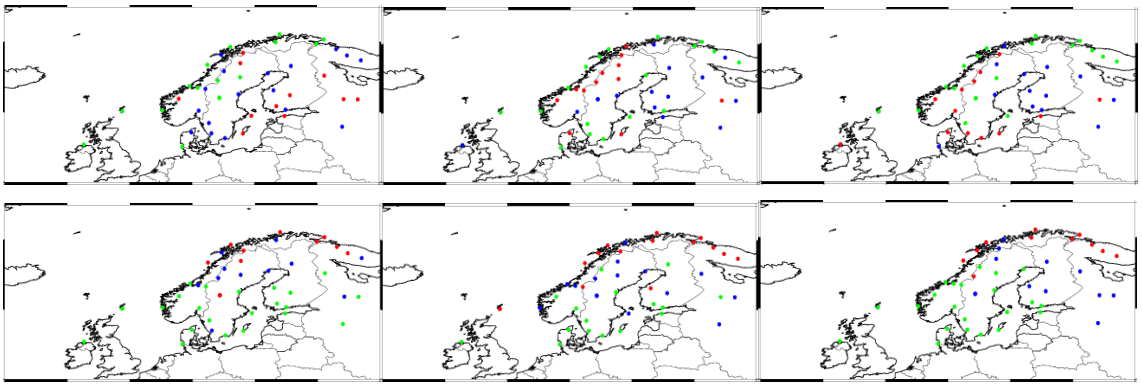

Figure 8 Spatial distribution of underdetection (Top) and overdetection errors (Bottom) for Nordic stations, (left day, centre night, right twilight). red is used for high errors, blue for average errors and green for low errors.

The systematic cloud under-detection errors observed at daytime on Figure 7 can be explained by a worse performance of CMa to detect clouds generally thin and rather not large over barren or desert areas. At night-time, the concentration of under-detections errors over western Europe

(mainly France and Eire) illustrates the difficulty of CMa algorithm over areas where maritime low, rather warm, sometimes not very thick but extensive, cloud layers dominate. For Nordic stations, Figure 8 illustrates that over-detection errors concentrated mainly above 65N are spread out along the coast. At night-time under-detection errors occur more frequently over mountainous stations of central Scandinavia.

2.3.2.6 Impact of target size on the analysis

Its influence is rather weak for FAR_{Cloud} as when overdetections occur they have in general a spatial extension wider than the considered sizes. FAR_{Clear} is more sensitive to a size reduction. As 5x5 is the target size of the database we can't measure the effect of a larger enhancement.

	FAR_{Cloud}		FAR_{Clear}	
	5x5	3x3	5x5	3x3
Midlatitude	3.6	3.7	8.2	9.5
Nordic	5.9	5.9	12.8	14.6

Table 14 Sensitivity of FAR_{Cloud} and FAR_{Clear} to target sizes of 3x3 and 5x5 SEVIRI pixels

2.3.3 CMa and MPEF CLM comparison through SYNOP evaluation

MPEF Cloud Mask (CLM) was required by users and therefore is available through EUMETCast diffusion. It has been added to SYNOP dataset at CMS on 22/05/2004, allowing evaluation of SAFNWC/CMa and MPEF/CLM performance limited to European area, as the two schemes can be compared with exactly the same SYNOP cloud cover observations. On 23/08/2004 MPEF activated the VIS tests in their algorithm to improve CLM results, so that we can analyse the complete dataset since May 2004, knowing CLM was not optimal at the beginning of the period, and a subset starting on 24 August 2004 as soon as CLM behaviour is settled down. The method for this evaluation is the same as in 2.3.2. Matchups are retained when both CLM and CMa fulfil conditions for cloud and clear events contingency tables. CLM is not processed for high satellite zenith angles, hence the stations of the Northern part of the Nordic subset are not taken into account. This contributes to modify somehow the nature of the dataset when compared with previous section.

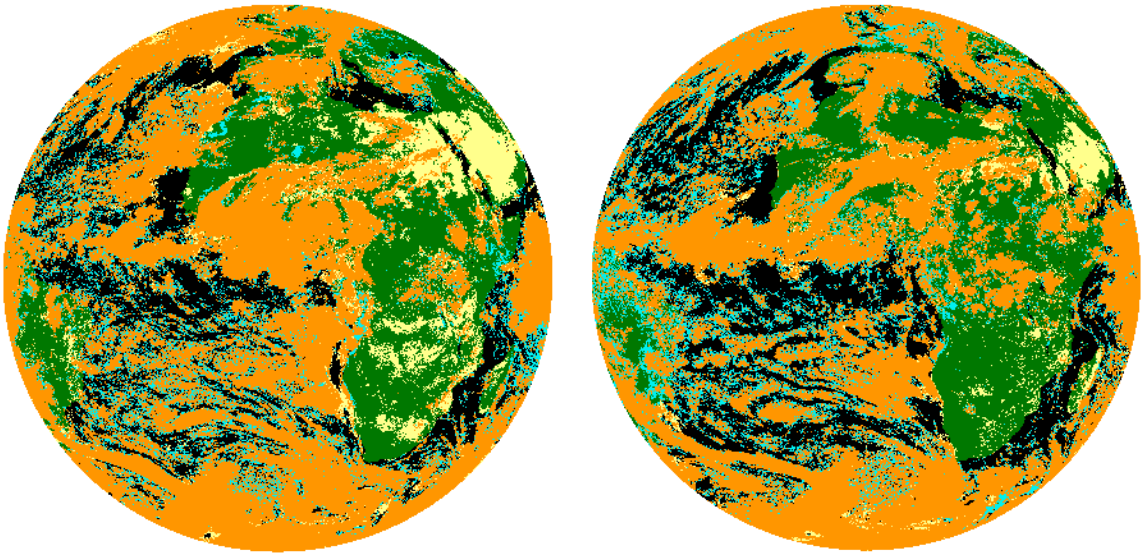

Figure 9 Example of MPEF CLM and SAFNWC CMa comparison 31/05/2005 at 03h45 (left) and 15h30 UTC (right), in black, green and orange both schemes agree for respectively clear sea, clear land and clouds; disagreements are in blue when CMa is cloudy and CLM clear, in yellow when CMa is clear whereas CLM is cloudy.

CMa	Contingency table		PC (%)	1-POD Cloud (%)	1-POD Clear (%)	FAR Cloud (%)	FAR Clear (%)
Nordic	6119	163	95.84	2.59	8.97	2.90	8.07
	183	1857					
Midlatitude	88233	4338	95.92	4.69	3.20	2.29	6.49
	2067	62500					
Nordic Day	2869	26	98.30	0.90	4.21	1.34	2.85
	39	887					
Midlatitude Day	50034	1541	97.73	2.99	1.19	0.80	4.38
	405	33606					
Nordic Night	1991	62	93.29	3.02	17.47	5.81	9.64
	123	581					
Midlatitude Night	27231	1480	94.33	5.15	6.31	5.10	6.38
	1462	21722					
Nordic Twilight	1259	75	94.50	5.62	5.12	1.64	16.16
	21	389					
Midlatitude Twilight	10968	1317	92.28	10.72	2.71	1.79	15.51
	200	7172					

CLM	Contingency table		PC (%)	1-POD Cloud (%)	1-POD Clear (%)	FAR Cloud (%)	FAR Clear (%)
Nordic	5748	534	90.18	8.5	13.87	4.69	23.31
	283	1757					
Midlatitude	81552	11019	91.70	11.9	3.14	2.43	14.98
	2028	62539					
Nordic Day	2656	239	92.46	8.26	5.29	1.81	21.42
	49	877					
Midlatitude Day	45899	5676	93.00	11.01	0.93	0.68	14.42
	315	33696					
Nordic Night	1897	156	87.31	7.60	27.56	9.28	23.42
	194	510					
Midlatitude Night	25359	3352	90.51	11.67	6.78	5.83	13.43
	1571	21613					
Nordic Twilight	1195	139	89.74	10.42	9.76	3.24	27.31
	40	370					
Midlatitude Twilight	10294	1991	89.15	16.21	1.93	1.36	21.59
	142	7230					

Table 15 CMa (Top table) and CLM (bottom table) comparison in the detection of fully cloudy and cloud-free events estimated from same collocated SYNOP and MSG-1/SEVIRI observations from 22/05/2004 till 28/02/2005, (165460 matchups)

CMa	Contingency table		PC (%)	1-POD Cloud (%)	1-POD Clear (%)	FAR Cloud (%)	FAR Clear (%)
Nordic	3175	94	94.6	2.88	16.62	3.70	13.31
	122	612					
Midlatitude	44284	2389	95.05	5.12	4.62	2.45	9.42
	1113	22790					
Nordic Day	737	8	98.25	1.07	6.31	0.94	7.14
	7	104					
Midlatitude Day	17152	400	98.05	2.28	1.30	0.66	4.40
	114	8689					
Nordic Night	1718	48	93.13	2.72	21.79	5.86	11.11
	107	384					
Midlatitude Night	20230	1056	94.02	4.96	7.79	4.43	8.69
	937	11093					
Nordic Twilight	720	38	94.83	5.01	6.06	1.10	23.46
	8	124					
Midlatitude Twilight	6902	933	91.02	11.01	1.91	0.89	22.64
	62	3188					

CLM	Contingency table		PC (%)	1-POD Cloud (%)	1-POD Clear (%)	FAR Cloud (%)	FAR Clear (%)
Nordic	3039	230	89.33	7.04	26.84	6.08	29.99
	197	537					
Midlatitude	41127	5546	90.26	11.88	5.59	3.17	19.61
	1346	22737					
Nordic Day	703	42	93.81	5.64	9.91	1.54	29.58
	11	100					
Midlatitude Day	15900	1652	93.18	9.41	1.66	0.91	16.02
	146	8657					
Nordic Night	1641	125	87.06	7.08	34.01	9.24	27.84
	167	324					
Midlatitude Night	18876	2410	89.43	11.32	9.24	5.56	18.08
	1111	10919					
Nordic Twilight	695	63	90.79	8.31	14.39	2.66	35.80
	19	113					
Midlatitude Twilight	6351	1484	85.81	18.94	2.73	1.38	31.95
	89	3161					

Table 16 CMa (Top table) and CLM (bottom table) comparison in the detection of fully cloudy and cloud-free events estimated from same collocated SYNOP and MSG-1/SEVIRI observations from 25/08/2004 till 28/02/2005 (74759 matchups)

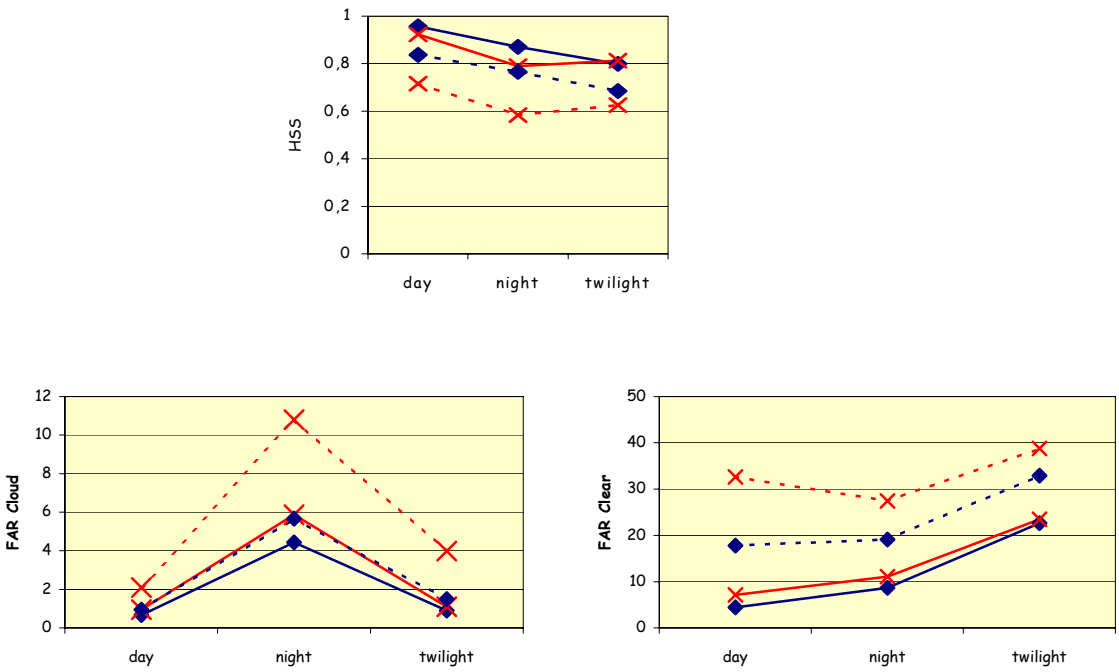

Figure 10 Graphs of Heidke Skill scores (top), FAR Cloud (bottom left) and FAR Clear (bottom right) of MPEF/CLM (dotted lines) and SAFNWC/CMa (solid lines) for midlatitude (blue) and Nordic (red) against illumination, in the detection of fully cloudy and cloud-free events estimated from the same collocated SYNOP and MSG1/SEVIRI observations from 25/08/2004 till 28/02/2005 (74759 matchups)

This comparison shows that the SAFNWC CMa cloud detection performs better than MPEF CLM on European area in all illumination conditions and is also less sensitive to latitude effect. We note also that for the two schemes the degradation of accuracy in twilight conditions is more important for mid-latitude cases than for Nordic.

2.3.4 Evaluation of CMa snow cover identification at daytime

Besides cloud cover, SYNOP data also contains thickness of snow layer measured at the meteorological station. Combined to cloud cover, it can be used to reduce the dataset by keeping a NOSNOW subset (clear cases without snow (snow thickness equal 0 cm)) and a SNOW subset (clear cases with snow thickness larger than 1cm). Satellite cloud and snow cover are estimated from CMa over the target centred on the meteorological station: the target is classified as “snow” if at least 20% of its pixels are classified as snow by CMa. The main problem of this reduced SYNOP matchup data base is illustrated on Figure 11 which shows that the snow thickness is mainly reported in SYNOP at 06h, when most of them are in darkness, especially the Nordic regions, best climatic candidates for frequent snow falls. Bottom left graph shows that CMa snow identification performs best around 12h, and is more frequent during morning than afternoon.

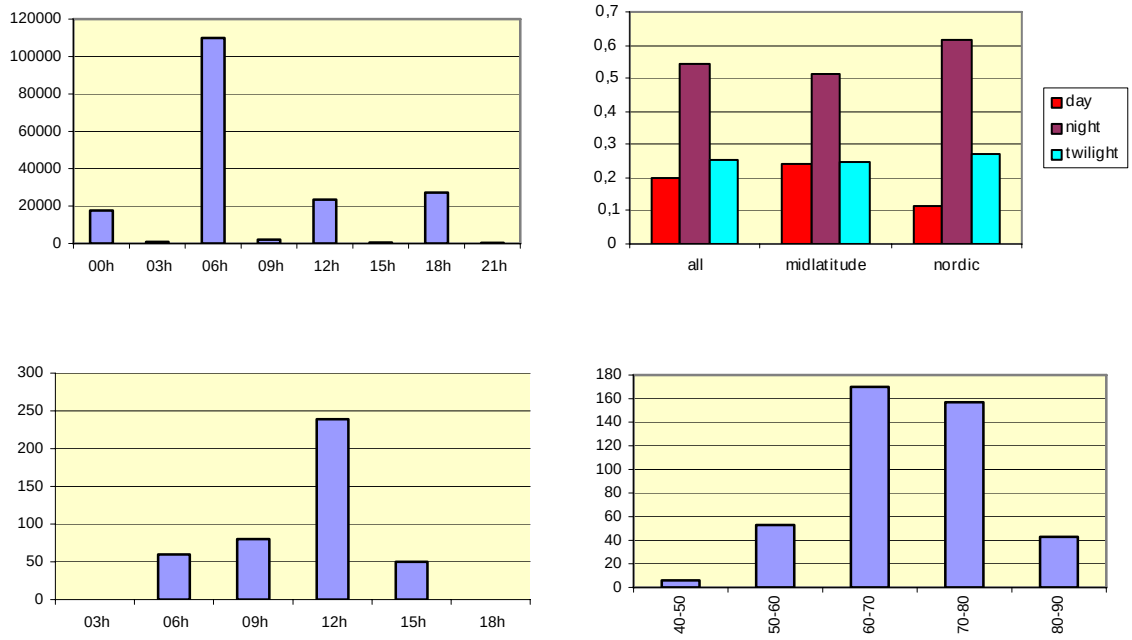

Figure 11 Top left: Number of SYNOP matchups with a snow thickness of 0 cm or greater according to their UTC observation hour (SNOW+NOSNOW subsets). Top right: Their frequency according to geographical and illumination conditions. Bottom left: Number of correct CMa snow identifications against observation time. Bottom right: Same against sun zenith angle.

We restrict the study to daytime and twilight conditions, as snow identification with SEVIRI is not possible at night-time. From the SNOW subset we can estimate a probability of detection (POD) for snow, while its probability of false detection (POFD) is obtained by statistics from NOSNOW subset. We keep in mind that this approach has some drawbacks linked to the nature of the two spatial scales, as SYNOP gives the snow thickness in one point and CMa a probability of snow inside SEVIRI FOV wider than 15 km^2 at European latitudes.

Figure 12 shows that snow detections performs better at daytime for mid-latitude cases (POD 55.9%) than for Nordic (POD 16.7%). We have in mind that Nordic POD is artificially decreased by the fact that snow is detected only when sun zenith angle is lower than 85° (for v1.2). When snow is not correctly detected, it is in general classified as cloud (48%, mainly low clouds) or cloud-free (52%). A very low false detection rate 0.03%, as only 17 matchups among 62904 are badly classified as snow when snow is reported at 0 cm in SYNOP, indicates that CMa snow algorithm does not overestimate snow cover.

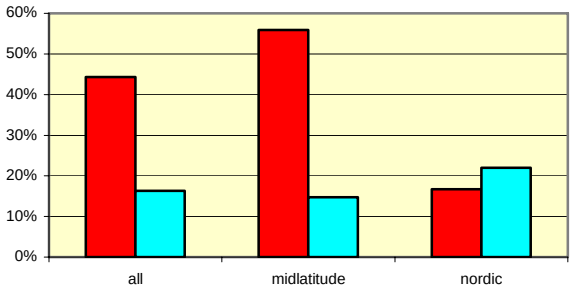

Figure 12 POD of snow by CMa for observed snow cover thicker than 1cm, daytime (red), twilight with a sun zenith angle below 85° (blue).

At night-time, when snow is not detected by CMa, the errors are distributed as following; 63% are classified as cloud-free, 14% as low or medium clouds, 15% as semi-transparent clouds. For midlatitude subset, 75% are classified as cloud-free, 11% as low or medium clouds, 10% as semi-transparent, the repartition becoming respectively 50%, 14%and 23% for Nordic cases.

2.4 CMA CLOUD MASK: PROBLEMS DETECTED BY VISUAL INSPECTION

A systematic long-term visual inspection over Europe and adjacent seas allows to identify main failures to detect clouds or false flagging of clouds by CMa algorithm.

It shows that two problems dominate CMa errors

- Some low clouds are not detected over land and even sea in twilight conditions during day to night and night to day transitions. This effect usually lasts 4 successive 15 minute SEVIRI scenes, during which the sun is too low for the visible bands to be useful, but sufficiently high to contaminate the 3.9µm brightness temperature. This problem can be detected when animating sequences of CT images. For numerical applications, until an improvement in twilight algorithm, CMa information should be considered doubtful when clear in twilight conditions.
- Large areas of low warm clouds at night-time over land, less frequently over sea, may be undetected by CMa. These clouds are generally Sc layers in rather warm oceanic air over continental surfaces with very weak (or no) night cooling. Spring and autumn, over mid-latitude western regions are favourable conditions to encounter this matter.

The following problems are of less importance

- Low clouds surmounted by thin cirrus may remain undetected at night-time
- During night, snow is not detected and is generally classified as clear but also as cloudy (low or fractional) especially over northern countries.
- At daytime, snowy areas are often surrounded by a narrow band of pixels classified as clouds.
- A trend to cloud over-detection over sea in clear coastal areas, particularly at daytime during summer in presence of hot lands, is observed.
- Over Africa a trend to miss clouds, especially at night, is observed.

2.5 CMA DUST FLAG VALIDATION

The only database available at CMS to quantify the CMa dust flag is the Interactive Target Database (see annex) which gathers about 3800 targets corresponding to dust events located over Africa and adjacent seas. This can't be strictly a real validation, as a part of the CMa dust detection tuning is based on the use of the interactive file which makes them dependent. Statistical scores are indicators of how much the automated CMa dust flag agrees with the interactively manned targets types. Note that no attempt to quantify the thin dust clouds detection over Europe has been performed as all the targets corresponds to dust storms over Africa or adjacent seas.

The following statistical scores are computed from contingency tables built from this database (see Table 17 for conventions; "dust detected" corresponds to more than half the pixels of the target flagged as dust by CMa; "no dust detected" corresponds to less than half the pixels of the target flagged as dust by CMa):

- False Alarm Ratio (FAR) quantifies the dust detections that are not correct. FAR= $n_c/(n_a+n_c)$.

- The Percentage Of Detection (POD) quantifies the dust observations that are correctly detected. POD=$n_a/(n_a+n_b)$.

	Dust detected	No dust Detected
Dust observed	n_a	n_b
No dust observed	n_c	n_d

Table 17 Contingency table conventions.

Database is stratified according to solar zenith angle ([0-20], [20-40], [40-60] and [60-80], dust flag is not computed for solar zenith angle higher than 80 degrees). Results are sum up in Table 18 and Table 19.

Angle range (degrees)	Contingency table		FAR (%)	POD (%)
[0-80]	476	835	3.8	36.3
	19	2658		
[0-20]	56	71	15.2	44.1
	10	166		
[20-40]	279	390	0.3	41.7
	1	697		
[40-60]	99	206	2.9	32.5
	3	934		
[60-80]	42	167	10.6	20.1
	5	858		

Table 18 Dust flag performance over sea estimated from the Interactive Target Database

Angle range (degrees)	Contingency table		FAR (%)	POD (%)
[0-80]	1338	874	1.9	60.5
	26	3125		
[0-20]	292	139	1.0	67.7
	3	266		
[20-40]	714	238	1.8	75.0
	13	650		
[40-60]	316	377	3.1	45.6
	10	935		
[60-80]	15	120	0.0	11.1
	0	1274		

Table 19 Dust flag performance over land estimated from the Interactive Target Database

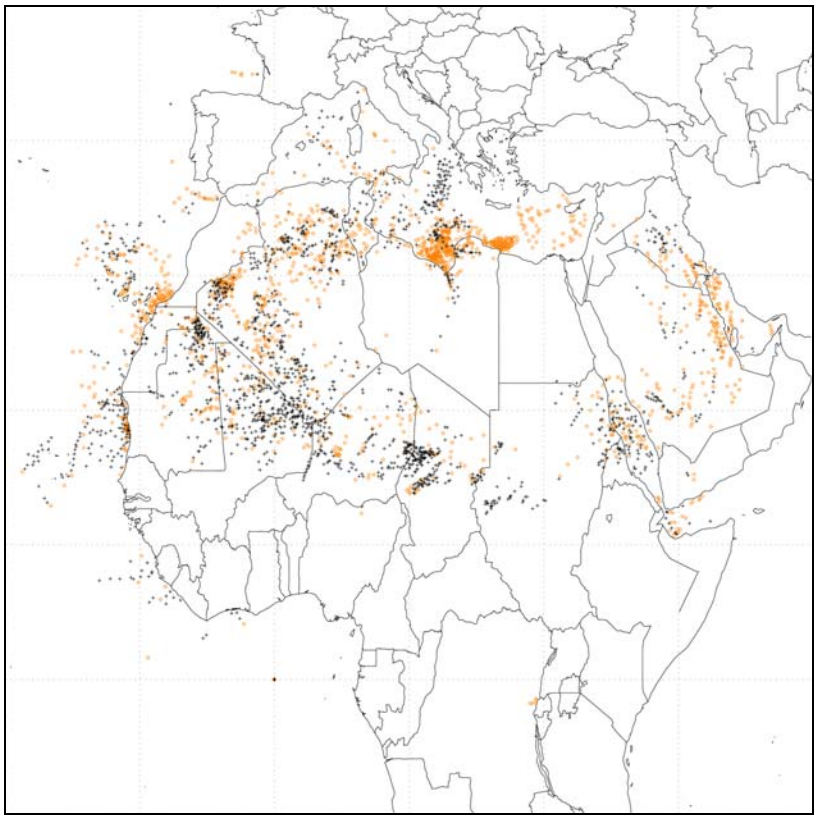

Figure 13 Localisation of the interactive targets corresponding to dust events. Black symbol and orange diamond correspond respectively to detected and non detected by the CMa dust flag.

Over sea:

- The dust flag only allows the identification of 36.3% of dust targets (see Table 18). In fact the difficulty relies in the separation between dust and cloud. 86.5% of the dust targets are separated from cloud free targets either by the CMa cloud mask or by the CMa dust flag, but only 36.3% are classified as dust by the CMa dust flag.
- Some dust events may remain completely unclassified, as for example near Libya coast (see Figure 13). The main reason is a too weak signature in brightness temperature differences which may be due to a too low thermal contrast between oceanic surface and dust cloud.
- False alerts mainly correspond to cloud free surface (16 upon 19) and low clouds.
- The dust flag is illustrated on the Atlantic Ocean on 22nd July 2004 at 18UTC on Figure 14.

Over land:

- The detection performs better at low solar zenith angles as shown on Table 19. In fact, the detection method assumes highly negative T10.8µm-T12.0µm brightness temperature differences which occur when the continental surface is warmer than the dust cloud, not usually the case at low solar elevation.
- False alerts mainly correspond to cloud free areas (14 upon 26) and low clouds.

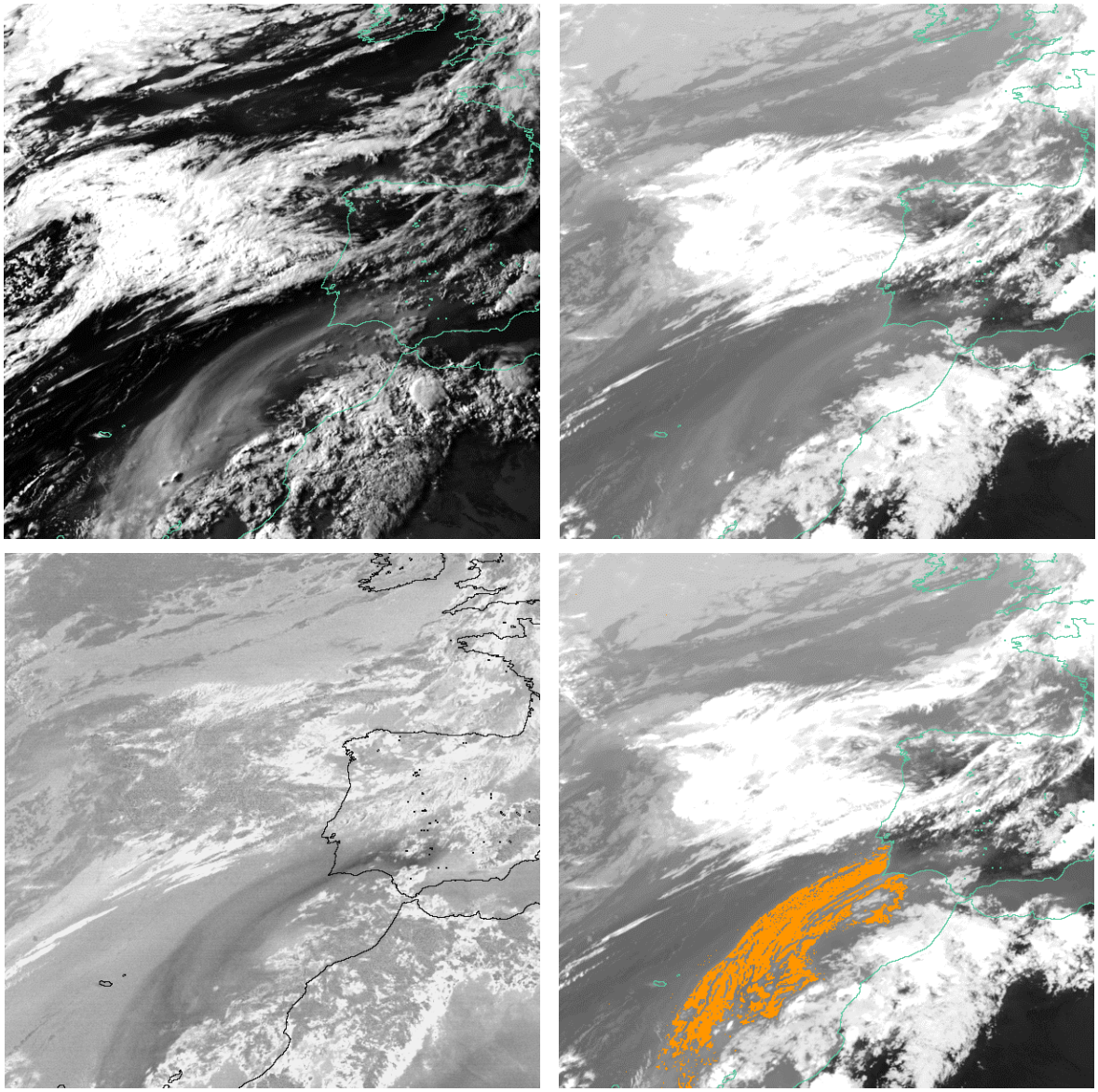

Figure 14 Illustration of the dust flag over the Atlantic Ocean. Top left: R0.6µm; Top right: T10.8µm; bottom left: T10.8µm-T12.0µm; bottom right: dust flag superimposed on T10.8µm.

2.6 CMA VOLCANIC ASH FLAG VALIDATION

Two main volcanic events occurred in the MSG disk in 2004: the eruption of the Nyaragongo in Democratic Republic of Congo, Africa (started on 8th May 2004) and that of the Grimsvotn in Island (1st and 2nd of November 2004); no ash cloud could be detected by CMa volcanic ash flag as T10.8µm-T12.0µm brightness temperature differences did not reveal highly negative values which would have indicated volcanic ash.

The frequency of false alarm can be estimated from the interactive target database using the same logic as for CMa dust flag (see 2.5) to classify targets. Apart from dust clouds being very frequently wrongly detected as volcanic ash, only 16 and 33 targets over land (upon 7990) have been wrongly flagged as volcanic ash by CMa at respectively daytime and night (6 and 43 respectively at daytime and night upon 6066 targets over the ocean). These wrong detections mainly correspond to Cu/Cb/St/Sc over land, and to Cu/Cb/Ac/As over sea.

We can therefore conclude that the false alarm are very infrequent. We still have to wait until next main volcanic eruptions to analyse whether the volcanic ash cloud flag may be useful.

During the Nyaragongo eruption in the Democratic Republic of Congo (Africa), it has been shown that SO_2 gaz emission could be visualized using the 8.7µm channel. This is illustrated in Figure 15, where the SO_2 gaz cloud is clearly identified by its low T8.7µm-T10.8µm (in black on the image). The implementation of an automatic SO_2 flag detection in CMa, which could be a useful complement to the volcanic ash flag, would request a careful study (to avoid false alarm over cloud free desertic areas or over clouds), but also the modification of the CMa output format to include a new SO_2 flag.

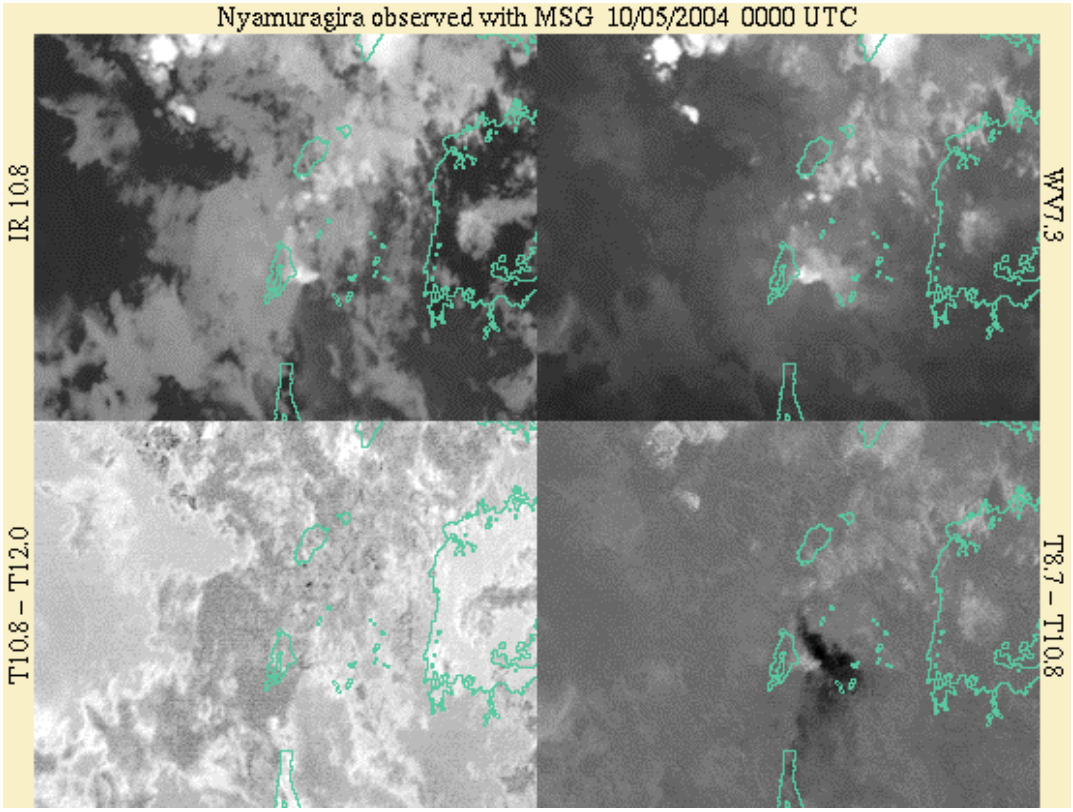

Figure 15 Illustration of SO2 mapping with MSG/SEVIRI. The scales from black to white are the following: T10.8µm (+40°C to –50°C), WV7.3µm (0°C to –50°C), T10.8µm-T12.0µm (-4°C to 4°C) and T8.7µm-T10.8µm (-10°C to 10°C)

2.7 CONCLUSION

2.7.1 Assessment of algorithm quality

A general assessment of the algorithm quality is given in this section.

- There is a clear relationship between CMa quality and illumination:
  - Best performance at daytime
  - Cloud over-detection at night is partly explained by human error observation in darkness.
  - Worst performance at twilight and especially mid-latitude regions (bias -0.5 octa) with under-detection of low clouds.
- The best skill is observed over mid-latitude regions; cloudiness is overestimated over Nordic regions especially when cloudiness is low.

- CMa algorithm performs better when NWP fields are used. Their impact is maximum at night and over Nordic regions.
- Snow identification is not possible at night. At daytime, its POD (56%) when compared to SYNOP snow thickness, shows an under-detection with a very low false detection rate (0.03%). Visual inspection, noting that a narrow band of pixels classified as clouds often surrounds snowy areas, doesn't really confirm such a systematic under-detection behaviour. The very different scales of SYNOP and satellite snow cover estimations impact greatly the relatively bad POD of snow cover.
- The performance of SAFNWC/CMa is superior to MPEF/CLM on European area in all illumination conditions and is also less sensitive to latitude.
- Rather thick dust clouds identification performs better over land than over sea at low sun zenith angles and when thermal contrast between dust cloud and ground is high. False alarms, more frequent over sea, are mainly cloud-free and low clouds.
- No ash cloud could be detected by CMa among the 2 events occurred in 2004 (unexpected T10.8µm-T12.0µm brightness temperature differences), but the false alarms are very infrequent.

2.7.2 Proposal for algorithm modification

The first priority is to improve CMa algorithm for low clouds detection in twilight conditions. We propose to study the temporal behaviour of cloud-free and cloudy scenes around sunrise and sunset, taking benefit from a detection when solar illumination is sufficient or when the sun is well below the horizon.

For validation purposes, we will improve SYNOP database:

- have a more homogeneous repartition over Europe of stations providing human-based observations.
- add HRV data and two SEVIRI slots before SYNOP report

3. CT VALIDATION

3.1 OVERVIEW

3.1.1 General objectives of the validation

The following extensive validation of the CT product is performed:

- ✓ The CT cloud types (the separation between stratiform and cumuliform clouds is not implemented in the release 1.2 of the SAFNWC/MSG SW package) are validated for all seasons, various atmospheric conditions (mid-latitude and nordic), and in different geographical areas
- ✓ The CT cloud phase is not available in the release 1.2 of the SAFNWC/MSG SW package

The validation is mainly performed using automatic methods, but results from visual inspection are also available.

3.1.2 Methodology outline

A first estimation of the CT cloud types' quality is done using the Interactive Target Database, although this database has been partly used during the tuning process.

The validation of the CT cloud types also includes a comparison with surface observations (SYNOP).

Visual inspection of CT cloud types is performed by skilled forecasters using a dedicated visualisation tool to complement automatic validation methods.

In all these validation studies, CT is retrieved over the MSG full disk using NWP fields forecast by the French model ARPEGE four times per day (0h, 6h, 12h and 18h) at a 1.5 degree horizontal resolution.

3.2 COMPARISON WITH INTERACTIVE TARGET DATABASE

The Interactive Target Database (gathered over MSG full disk as soon as SEVIRI data are available (see annex 1) allows the comparison of the CT cloud types and the cloud class manually labelled from SEVIRI imagery. This comparison is an indicator of the CT algorithm's quality but also of the separability of the cloud classes, and a way to understand how the CT algorithm manages classes.

Contingency tables and statistical scores (producer's accuracy (probability of a target being correctly classified), and user's accuracy (probability of a pixel classified into a category on a picture to really belong to that category) are computed. They are associated with changes illumination (day, night, twilight, sunglint) and latitude (Nordic, mid-latitude).

The result of CT over each 5x5 target is compared with the class of the target given by the observer with the rules given in Table 20. There is an agreement if the most probable CT group class (i.e. the most frequent group class among the 9 central pixels) or the group class of the central pixel of the target is identical to the observer group class. Meta-classes are also considered by gathering very low and low into low, all semi-transparent clouds into a single semi-transparent, and high opaque clouds into a single high class. As clear and cloud confusions have been analysed in CMa validation section and explained also in Figure 21 we focus CT validation with interactive file on the analysis of the repartition of manually labelled

and CT group classes. Therefore the database is limited to cases identified as cloudy by the observer and CT, and CT fractional clouds are removed, to be studied separately.

We must keep in mind when analysing the results that most cases in interactive target database have been manually selected when presenting a difficulty for CMa or CT algorithm, therefore the statistical indicators are biased and must be handled with care when measuring the CT performance. On the other hand, this interactive target database will be useful to quantify the improvement when changing algorithm version.

Group Class name	Target type	CT type
Sea	Open sea, Sea with haze, Sea with shadow, Sea with sunglint	Sea not contaminated by clouds, aerosol or ice/snow
Land	Land, land with haze, land with shadow,	Land not contaminated by clouds, aerosol or snow
Ice	Ice, ice with shadow	Sea contaminated by ice/snow
Snow	Snow, snow with shadow	Land contaminated by snow
Very Low	Fog, stratus, small cumulus over land, small cumulus over sea	Very low clouds
Low	Stratocumulus, stratocumulus with shadow	Low clouds
Mid-level cloud	Altocumulus, Altostratus, cumulus congestus over land and sea	Medium clouds
Semitransparent Above lower clouds	Thin cirrus above stratus or stratocumulus or cumulus	Cirrus above lower clouds
Semitransparent Thin	Thin cirrus over sea, thin cirrus over land, thin cirrus over snow, thin cirrus over ice	Thin cirrus
Semitransparent Thick	Cirrostratus	Mean and thick cirrus
High opaque no cum	Cirrostratus over Altocumulus or Altostratus. Thin cirrus over Ac As	High opaque clouds
High opaque cum	Isolated or merged Cb	Very high opaque clouds

Table 20 Equivalence between manually labelled targets and CT types

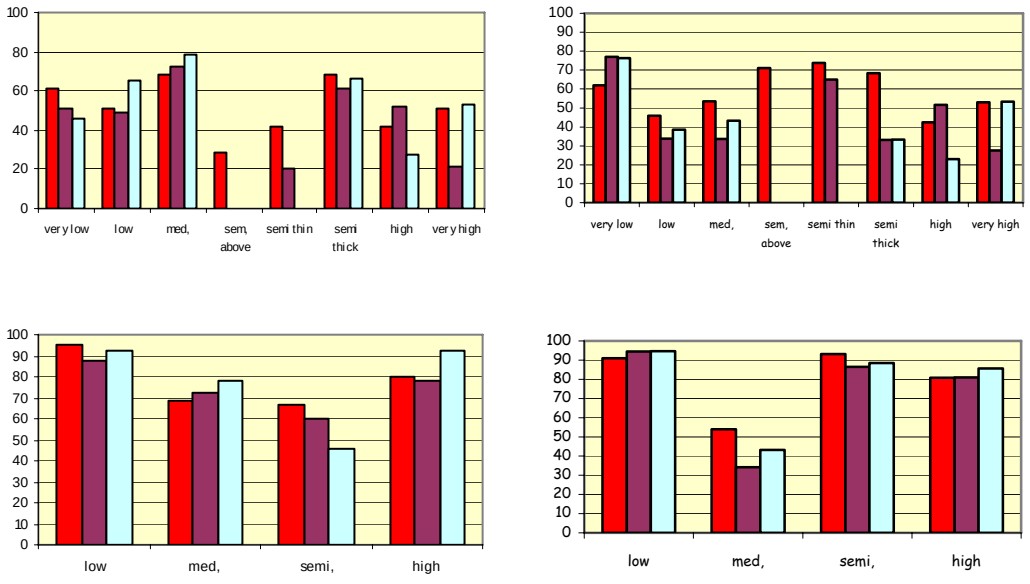

Figure 16 Top: Producer's(left) and User's(right) accuracy for grouped classes for mid-latitude targets of interactive database; Bottom: same for meta-classes. day (red), night (purple), twilight (blue)

Figure 16 shows that CT quality at mid-latitude regions is not dependent on illumination conditions (when the problems related to detection of clouds and snow have been removed). Low and high clouds have similar accuracy, semi-transparent clouds are not well produced, while medium are the least reliable for the user.

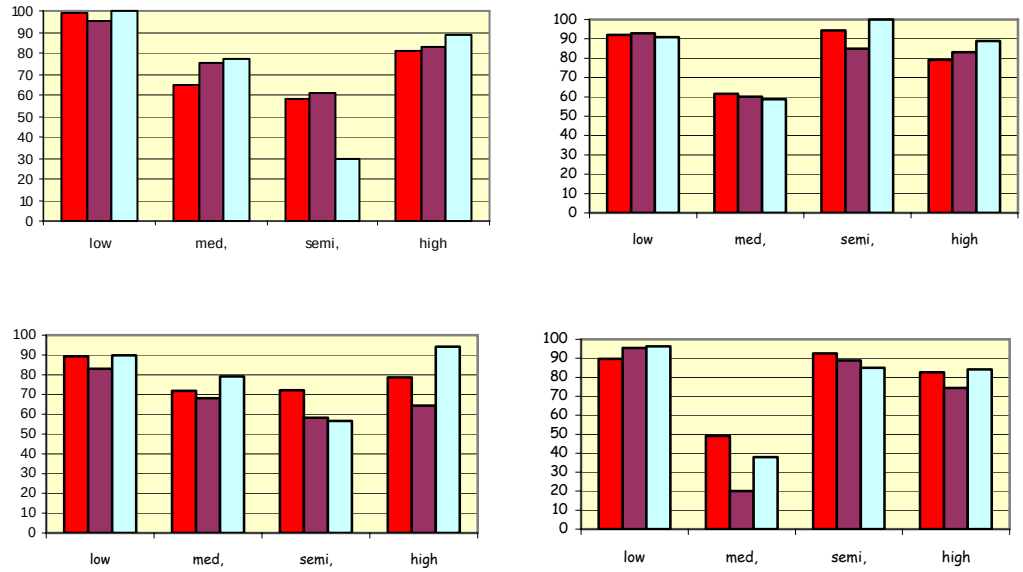

Figure 17 Top: Producer's(left) and User's(right) accuracy for meta-classes for mid-latitude sea targets of interactive database. Bottom: same for targets over land. day (red), night (purple), twilight (blue)

When comparing land/sea stratifications (Figure 17), we note over sea a slightly better identification of low clouds and less false alarms in medium clouds for similar producer's accuracy. One reason is that events with temperature inversion are more frequent over land thus increasing the confusion of low clouds with medium clouds, as shown by Figure 18. We must nevertheless keep in mind that most cases in interactive target database have been manually selected when presenting a difficulty for CMa or CT algorithm, which could explain the high frequency of low clouds confusion with medium clouds (this phenomena happens (see 3.4) but not as frequently). Figure 18 also indicates that one reason for rather low values for medium clouds' user accuracy is that cirrus clouds over a lower layer may be classified as medium clouds. This was also visually observed (see 3.4).

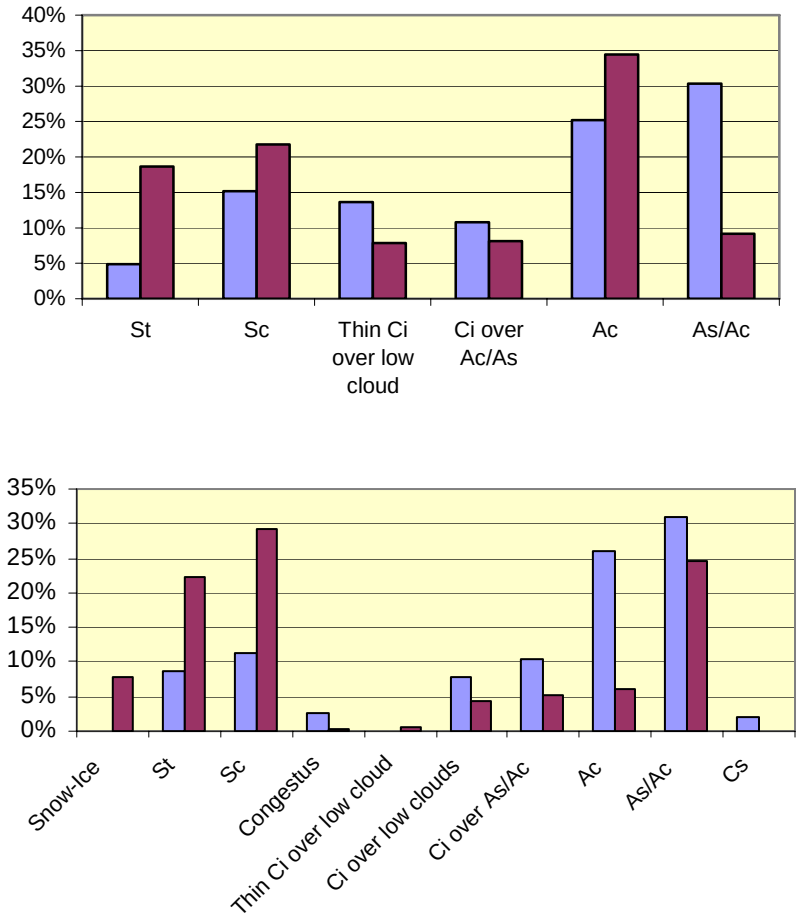

Figure 18 Repartition (in percentage) of manually-labelled classes for targets classified as medium clouds by CT. Top: all targets(1149 matchups,429 over sea 720 over land), Bottom: night targets(553 matchups, 197 over sea and 356 over land); blue over sea, purple over land.

As fractional cloud type cases have been removed from the previous set, we have also analysed how these clouds are labelled in interactive dataset (when not confused with clear targets). Figure 19 shows the percentage of fractional clouds that are in fact semi-transparent (thin cirrus, cirrus above low clouds): up to 50% at daytime but much less at night-time (less than 40% over land and around 20% over sea). This can be explained by the use at night-time of the 3.9µm channel which ease the identification of semi-transparency thanks to the Planck function non linearity in this channel.

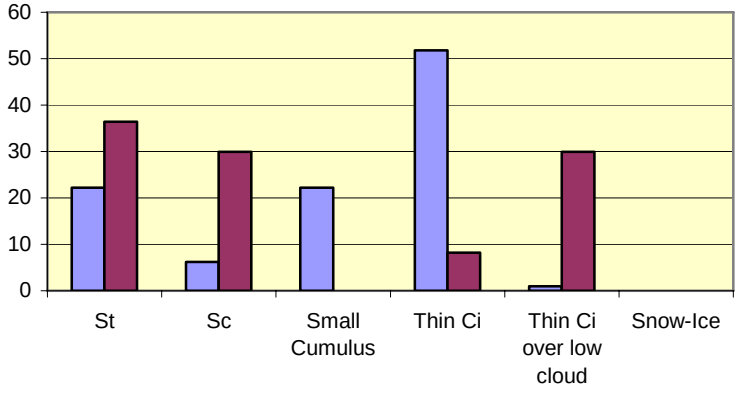

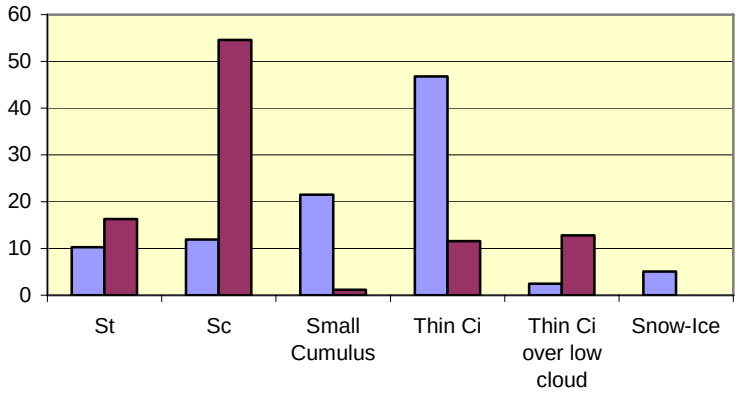

Figure 19 Repartition (in percentage) of manually-labelled classes for targets classified as fractional by CT, when clear are removed; Top over land (158 matchups), bottom over sea (165 matchups), day is blue and night purple.

3.3 COMPARISON WITH SURFACE OBSERVATION (SYNOP)

The quantitative comparison of the CT cloud types with surface synoptic observations is made possible thanks to the use of the coincident satellite targets and SYNOP data (available over Europe and North Africa, as shown in annex 3) gathered from 1st November 2003 up to 28th February 2005 (same as for CMa validation).

From the SYNOP data set, ground-based total cloud cover and partial cloud cover from low, medium and high clouds are available. To simulate the surface observations from the satellite pixels, no attempt is made to take into account the complexity of the observation. CT cloud type is estimated from the 25 pixels of the satellite target.

The most frequent type given by CT among the 25 pixels is retained as CT class of the target, except for cloud free where a threshold is used. How CT type and SYNOP cloud description are compared is given by Table 21 below.

The comparison between the CT and the cloud cover observed from the surface consists in building up contingency tables. The contingency tables are used to quantify producer's accuracy (probability of a target being correctly classified, it is a stratification by the ground truth given by the cloud description of the SYNOP report), and user's accuracy (probability of a pixel classified into a category on a picture to really belong to that category, it is a stratification by group of classes given by CT).

Contingency tables and associated statistical scores are computed for various illumination conditions, and different geographic areas.

Main class name	SYNOP cloud layers	CT types
cloud free	-Total cloudiness lower or equal 2 octas	-land not contaminated by cloud, -land contaminated by snow
low	-Sky not observed, due to fog -Stratus (except bad weather stratus) without overlying cloud layer reported -Stratocumulus without overlying cloud layer reported -Cumulus humilis	-very low clouds, -low clouds
mid-level cloud	-Dominant cloud layer: Cumulus mediocris -Dominant cloud layer: opaque altostratus or altocumulus (without cirrus clouds)	-medium clouds
high cloud	-Sky not observed due to rain or showers -Dominant cloud layer: cumulonimbus -Bad weather stratus -Altocumulus or altostratus overlaid by dense cirrus or cirrostratus	-high opaque clouds -very high clouds
semitransparent	-Dominant cloud layer: cirrus, cirrostratus or cirrocumulus -Dominant cloud layer: semitransparent altostratus or altocumulus	-thin, mean and thick cirrus
multi-layer	-Remaining cloud observations	
fractional		-fractional
cirrus above lower clouds		-cirrus above lower clouds

Table 21 Equivalence between CT classes and SYNOP dominant cloud classes derived from cloud layers description

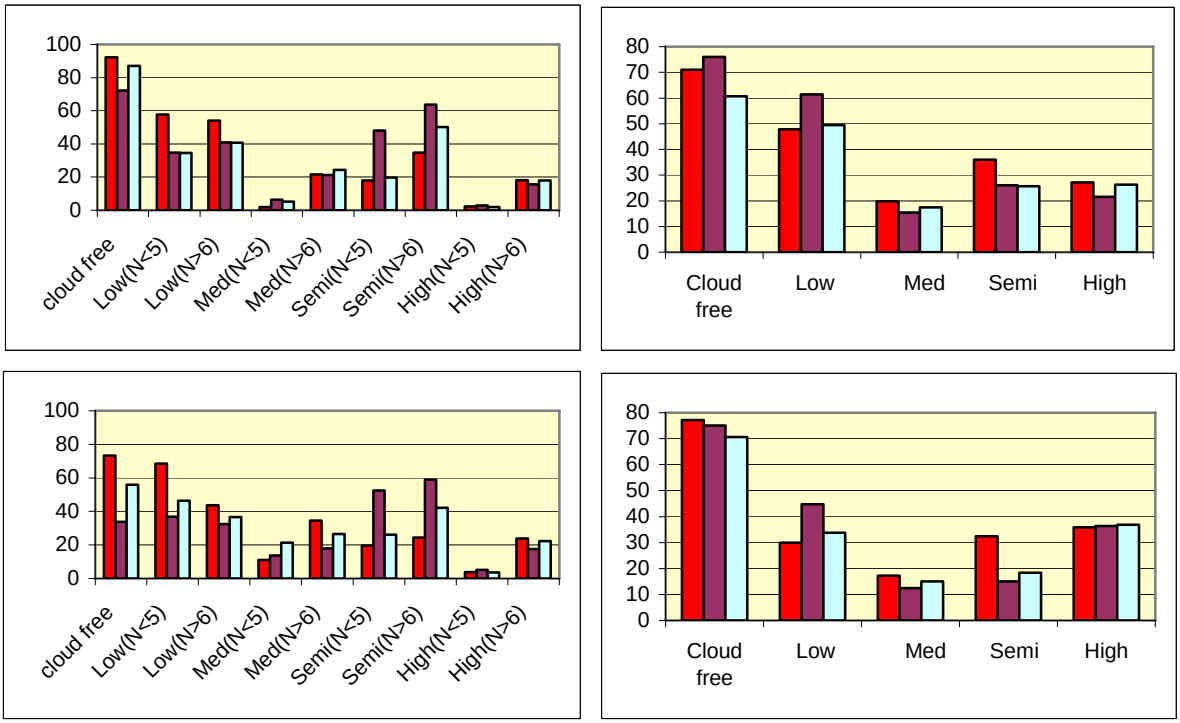

Figure 20 CT producer (left) and user (right) accuracy for midlatitude (top) and Nordic (bottom) according to illumination; day (red) , night (purple), twilight (blue) from November 1st 2003 till February 28th 2005

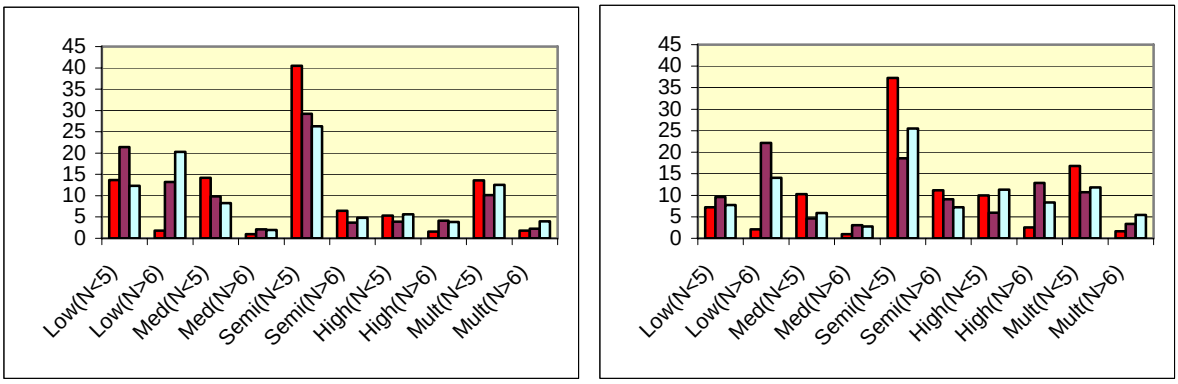

Figure 21 Percentage of occurrences of SYNOP classes corresponding to CMa cloud-free errors for midlatitude (left) and Nordic (right) according to illumination; day (red) , night (purple), twilight (blue) from November 1st 2003 till February 28th 2005

Figure 21 describes the distribution of SYNOP observations corresponding to erroneous CT Clear sky misclassifications per illumination and geographical area. It is a way to explain occurrences of ($1\text{-}POD_{Clear}$) defined in 2.3.2 with SYNOP comparison. Both for mid-latitude and Nordic cases, at daytime and twilight, the most frequent errors originate non detection of semitransparent clouds when N<5. At night, semitransparent clouds with N<5 still dominates errors for mid-latitude cases, while for Nordic the errors due to low clouds with high cloudiness become prevailing. At twilight for mid-latitude there is a noticeable increase due to low clouds with N>6. This agrees with what was observed in CMa validation.

3.4 PROBLEMS DETECTED BY VISUAL INSPECTION

A systematic long-term visual inspection of CT cloud types over Europe and adjacent seas allows to identify the main cloud misclassifications. Cloud and snow detection problems are not recalled here.

- Fog, St or Sc may be classified as medium clouds, in the event of strong thermal inversion, over cold grounds (confirmed by interactive database analysis)
- Thin cirrus may be classified as fractional clouds (confirmed by interactive database analysis)
- Thin cirrus over a lower cloud layer may be classified as medium clouds (confirmed by interactive database analysis)
- Minor changes in cloud classes may occur with day to night and night to day transition (semi-transparent over low cloud is available only at daytime)

3.5 CONCLUSION

3.5.1 Assessment of algorithm quality

A general assessment of the algorithm quality is given in this section.

CT classifier is very weakly sensitive to illumination conditions, except for semi-transparent over low clouds and other inheritances from CMa, as for instance snow detection not performed at night and at low solar elevations.

Its main problem is the medium clouds class which may include semi-transparent and low clouds, as shown by interactive database and SYNOP cloud cover analysis.

Fractional clouds are still not well typed as they contain both low clouds and high semi-transparent clouds.

4. CTTH VALIDATION

4.1 OVERVIEW

4.1.1 General objectives of the validation

The following validation of CTTH is performed:

- ✓ Cloud top height are validated for all seasons in all illumination conditions using measurements from ground-based radar and lidar located near Paris
- ✓ Low cloud top pressure errors, mainly due to the presence of atmospheric thermal inversions, are estimated for all seasons in European conditions at 0h and 12h UTC using radio-sounding measurements

In addition, the dependency of CTTH errors with viewing angle and time of the day is evaluated.

4.1.2 Methodology outline

Measurements of ground-based radar and lidar located near Paris gathered during one year (September 2003-October 2004) are used to evaluate cloud top height errors. Impact on the error of the time of the day or the method used during the retrieval is investigated.

Radio-sounding measurements, gathered all over Europe (see Annex 4) during ten months (March 2004-February 2005), are used to evaluate low cloud top pressure errors. Impact on the error of the viewing angles, the time of the day or the presence and strength of thermal inversion is investigated. The use of an automatic method to analyse the cloud cover (low clouds) from the radio-sounding allows an extensive comparison.

In all these comparisons, CTTH is retrieved using NWP fields forecast by the French model ARPEGE four times per day (0h, 6h, 12h and 18h) at a 1.5 degree horizontal resolution. Temperature and humidity are available on twenty pressure levels (10, 20, 30, 50, 70, 100, 150, 200, 250, 300, 400, 500, 600, 700, 800, 850, 900, 925, 950, 1000).

4.2 VALIDATION OF CTTH WITH GROUND-BASED LIDAR AND RADAR

A validation of the CTH (Cloud Top height) quality with measurements from ground-based lidar and radar located near Paris has been performed within the frame of a visiting scientist activity (see the visiting scientist report available on www.meteorologie.eu.org/safnwc for detailed results) from a dataset prepared using PGE03 from SAFNWC/MSG v1.0 software and covering the period September 2003-October 2004. Since then, this dataset has been updated by applying PGE03 from SAFNWC/MSG v1.2 and the validation procedure defined by the visiting scientist has been applied, leading to similar conclusions. Results obtained from PGE03 v1.2 are presented in this report.

The ground-based measurements used in this study are provided by SIRTA (Site Instrumental de Recherche par Télédétection Atmosphérique), an atmospheric observatory for cloud and aerosol research operated by the Institut Pierre Simon Laplace (IPSL). The SIRTA observatory is located on the campus of Ecole Polytechnique, Palaiseau, France with geographical coordinates: 48.7 N – 2.2 E. SIRTA is composed of an ensemble of state-of-the-art active and passive remote sensing instruments, including radars, lidars and radiometers. A detailed description of the radar and lidar measurements is given in Annex 7.

The following procedure is applied to SEVIRI, lidar and radar measurements to gather the validation dataset:

- Because of the difference in spatial resolution between the ground-based and satellite sensors, the approach is to perform a temporal average of the ground-based data over a period of time and compare with spatially averaged SEVIRI cloud top height retrievals. In the present work, the cloud properties derived from observations at SIRTA are averaged temporally over 30 minutes and the SEVIRI cloud properties are averaged spatially over 5x3 pixels.
- Because of inherent discrepancies in ground and spatial observational scales, focusing the comparison on homogeneous situations will minimize scale-induced variability. Hence, the comparison is restricted to the SEVIRI scenes showing a large homogenous cloud coverage (low/middle or high/semi-transparent cloud fractions must be larger than 80 % within an area of 11x7 pixels and 50% within an area of 5x3 pixels).
- When more than one cloud layer is detected by the radar or the lidar, the SEVIRI CTH is systematically compared with the nearest layer of ground-based instrument dataset.
- Suspect cases have been manually analysed by displaying the full SEVIRI images and the full lidar and radar measurements. They often corresponds to multilayer clouds where the upper semi-transparent cloud layer was not automatically detected from the radar/lidar measurements. These cases have been removed from the study. There certainly still remains such cases, therefore part of the comparison errors certainly comes from the ground-based radar/lidar measurements themselves.

Results are summarized for low opaque clouds, medium and high opaque clouds, semi-transparent clouds using either intercept or radiance ratioing methods. The influence of the illumination or the method used during the retrieval is investigated.

4.2.1 Low opaque clouds

In this section, we analyse SEVIRI CTH retrieval for low opaque clouds (corresponding to radar/lidar retrieved CTH lower than 3km). Although lidar is the best instrument to measure cloud boundaries, lidar measurements are strongly attenuated by most of opaque clouds and therefore, the signal often does not reach the cloud top. Radar measurements are therefore needed to measure the top height of opaque clouds. For low opaque clouds, we therefore use RALI measurements (synergie of radar and lidar, described in Annex 7) during radar time acquisition (operational mode 0). From a total of 13370 SEVIRI slot, only 1133 pairs are considered to be sufficiently suitable for this validation.

The comparison of SEVIRI and RALI CTH retrieval for low opaque clouds is summarized in Figure 22,

Figure 23 and Table 22. The following conclusions can be drawn:

- On average, SEVIRI CTH shows an overestimation of 320m as compared to radar/lidar retrieved CTH with a standard deviation of 1030m (see first line in Table 22).

However, an underestimation may be observed in case low quality retrieved SEVIRI CTH (see Table 22).

- Figure 23, which shows a SEVIRI CTH overestimation at night or at low solar elevation and an SEVIRI CTH underestimation at high solar elevation.

CTH Quality	Mean (km)	Standard deviation (km)	Median (km)	Number of cases
All QI	0.32	1.03	0.26	1133
IQ=100%	0.40	0.80	0.34	287
50%<IQ<100%	0.44	0.88	0.38	543
0%<IQ<50%	0.09	1.35	-0.34	271
IQ=0%	-0.34	1.40	-0.76	32

Table 22 Low opaque clouds statistical scores for (CTH_SEVIRI-CTH_RALI) as a function of an averaged quality index IQ. IQ is an averaged value on the 5x3 area of quality indices of individual SEVIRI pixels (1 for good quality, 0 for bad quality); therefore IQ=100% corresponds good quality for all pixels, IQ=0% to low quality for all pixels. Negative mean or median values correspond to SEVIRI CTH underestimation.

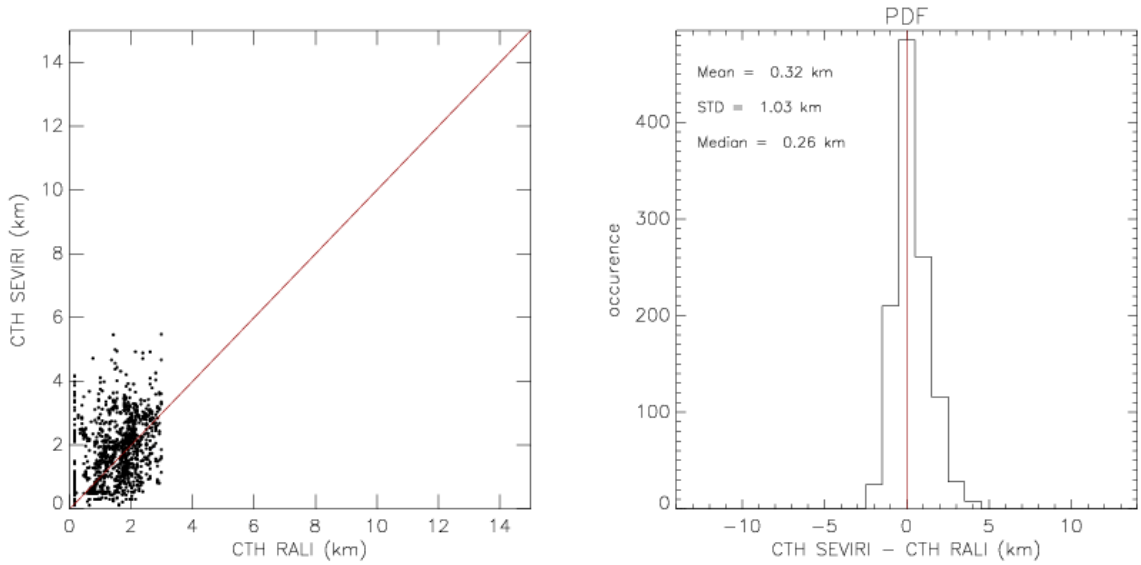

Figure 22 Comparison of CTH retrieved from SEVIRI and from Radar/lidar (RALI) for low opaque clouds. PDF is the probability Density Function.

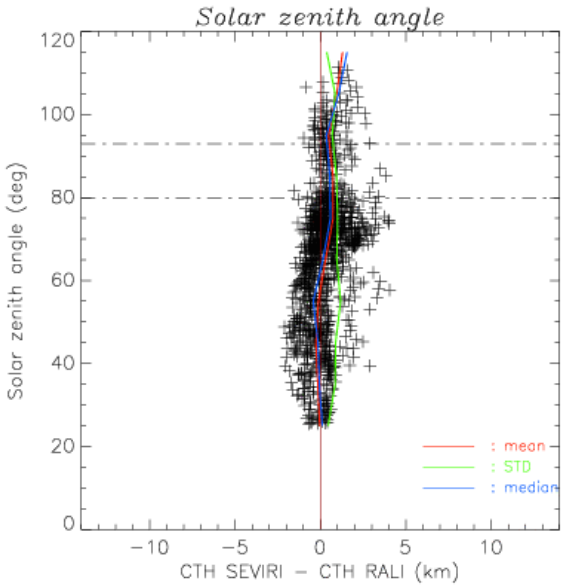

Figure 23 Influence of solar zenith angle on the comparison of CTH retrieved from SEVIRI and from Radar/lidar (RALI) for low opaque clouds.

4.2.2 Medium and high opaque clouds

In this section, we only analyse CTH retrieval for medium and high clouds (corresponding to radar/lidar retrieved CTH larger than 3km). Although lidar is the best instrument to measure cloud boundaries, lidar measurements are strongly attenuated by most of opaque clouds and therefore, the signal often does not reach the cloud top. Radar measurements are therefore needed to measure the top height of opaque cloud. For medium or high opaque clouds, we therefore use RALI measurements (synergie of radar and lidar, described in Annex 7) during radar time acquisition (operational mode 0). From a total of 13370 SEVIRI slot, only 1080 pairs are considered to be sufficiently suitable for this validation.

The comparison of SEVIRI and RALI CTH retrieval for medium and high opaque clouds is summarized in Figure 24, Figure 25 and Table 23. The following conclusions can be drawn:

- On average, SEVIRI CTH shows an underestimate of 400m as compared to radar/lidar retrieved CTH with a standard deviation of 1170m (see first line in Table 23).
- The underestimation seems stronger for low quality retrieved CTH (see Table 23).
- The solar zenith angle does not impact the SEVIRI CTH retrieval (see Figure 25)

CTH Quality	Mean (km)	Standard deviation (km)	Median (km)	Number of cases
All QI	-0.40	1.17	-0.46	1030
IQ=100%	0.01	0.63	-0.01	39
50%<IQ<100%	-0.39	1.03	-0.32	292
0%<IQ<50%	-0.47	1.22	-0.64	538
IQ=0%	-0.30	1.30	-0.46	161

Table 23 Medium and high opaque clouds statistical scores for (CTH_SEVIRI-CTH_RALI) as a function of an averaged quality index IQ. IQ is an averaged value on the 5x3 area of quality indices of individual SEVIRI pixels (1 for good quality, 0 for bad quality); therefore IQ=100%

corresponds good quality for all pixels, IQ=0% to low quality for all pixels. Negative mean or median values correspond to SEVIRI CTH underestimation.

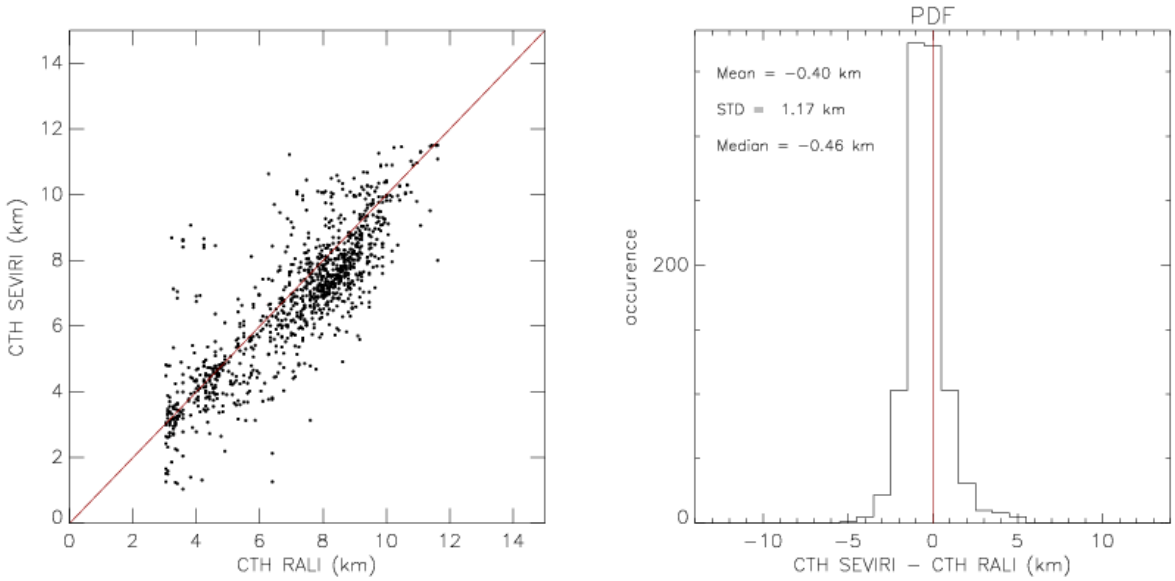

Figure 24 Comparison of CTH retrieved from SEVIRI and from Radar/lidar (RALI) for medium/high opaque clouds. PDF is the probability Density Function.

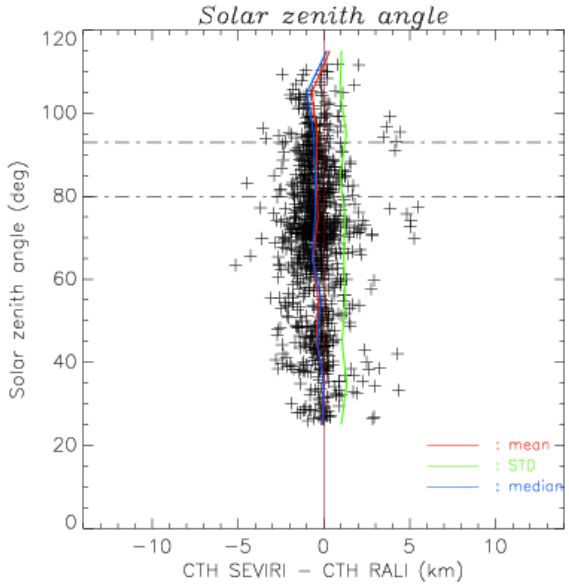

Figure 25 Influence of solar zenith angle on the comparison of CTH retrieved from SEVIRI and from Radar/lidar (RALI) for medium/high opaque clouds.

4.2.3 Semi-transparent clouds with intercept method

In general, radar instruments are able to detect most cloud, except thin cirrus and thin strato-cumulus, however the lidar is ideally suited to this task. For the study of semi-transparent cloud, we only used lidar measurements to perform the validation. In case of the presence of a low cloud layer with a high optical depth, a thin cirrus could be not detected by the lidar. Because the lidar is subject to attenuation, we imposed that the mean range of LNA instrument during the 30 minutes time period was higher than 8 km. Most of multi-layer cloudy scene are therefore excluded for

this study. From a total of 13370 processed SEVIRI data, 314 retrieved CTHs with intercept method were corresponding to a simultaneous LNA measurement.

The comparison of SEVIRI (using intercept method) and LNA CTH retrieval is summarized in Figure 26, Figure 27 and Table 24. The following conclusions can be drawn:

- On average, SEVIRI CTH shows an underestimate of 1080m as compared to lidar retrieved CTH with a standard deviation of 1090m (see first line in Table 24).
- The underestimation seems stronger when channel at 7.3µm is used (see Table 24).
- The underestimation seems independent of the semi-transparent cloud effective emissivity which may be associated to cloud thickness (see Figure 27)
- The solar zenith angle does not impact the SEVIRI CTH retrieval (see Figure 27).

SEVIRI sounding channels used	Mean (km)	Standard deviation (km)	Median (km)	Number of cases
Any	-1.08	1.09	-1.26	314
13.4µm	NA	NA	NA	0
6.2µm	-0.15	1.17	0.04	28
7.3µm	-1.13	1.20	-1.46	62
6.2µm & 7.3µm	-1.16	1.02	-1.28	153
6.2µm & 13.4µm	-0.33	0.72	-0.22	12
7.3µm & 13.4µm	-2.03	0.98	-2.52	11
13.4µm, 6.2µm & 7.3µm	-1.28	0.81	-1.40	48

Table 24 Statistical scores for (CTH_SEVIRI-CTH_LNA) as a function of the channels used in the intercept method. Negative mean or median values correspond to SEVIRI CTH underestimation.

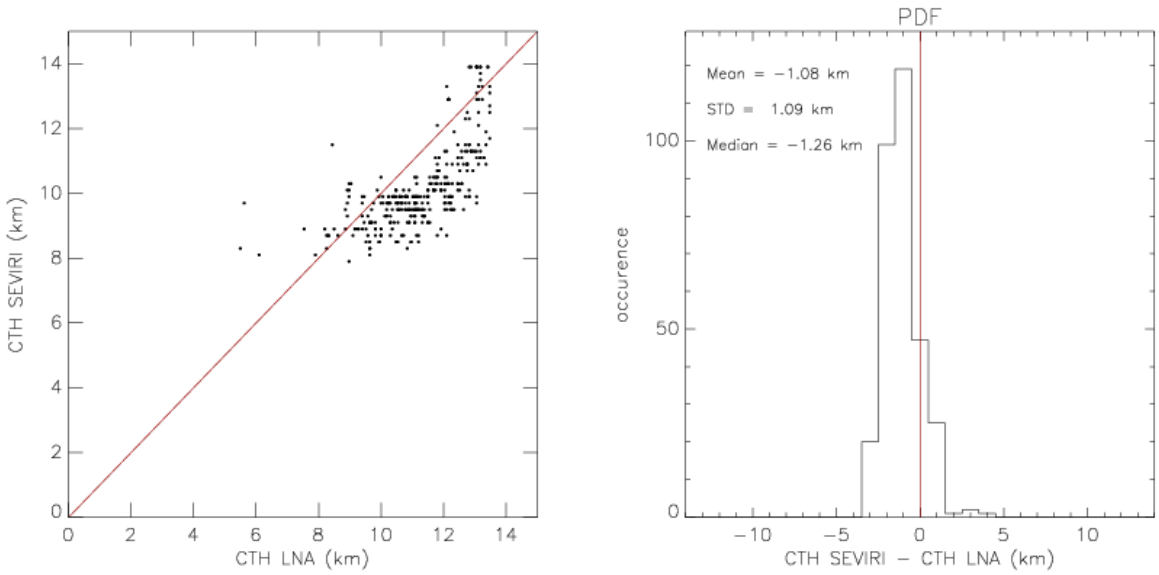

Figure 26 Comparison of CTH retrieved from SEVIRI and from lidar (LNA) for semi-transparent clouds (intercept method). PDF is the probability Density Function.

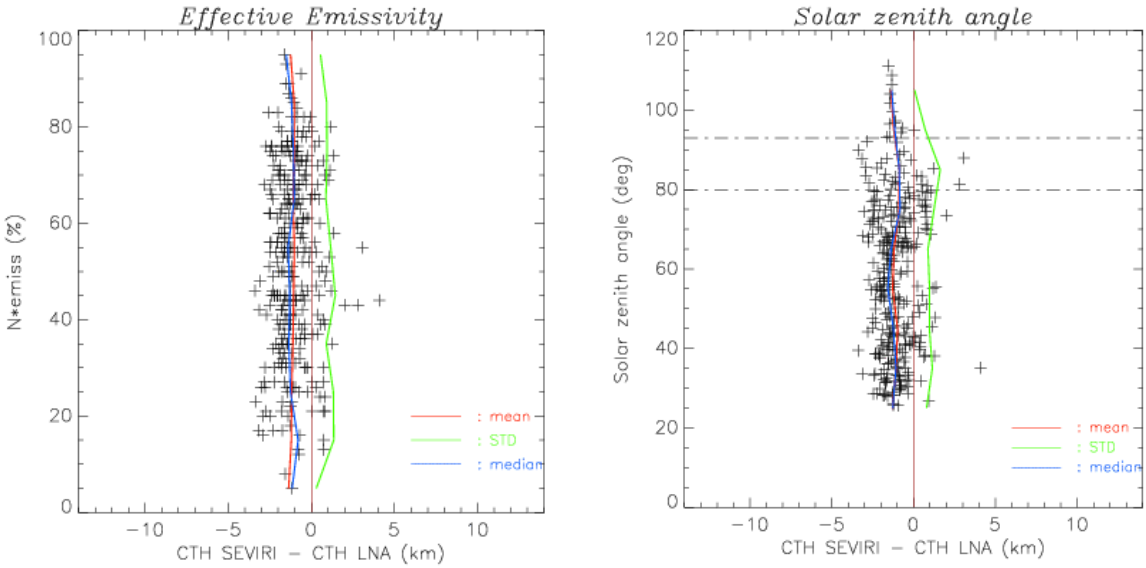

Figure 27 Influence of effective emissivity and solar zenith angle on the comparison of CTH retrieved from SEVIRI and from lidar (LNA) for semi-transparent clouds (intercept method).

4.2.4 Semi-transparent clouds with radiance ratioing method

The radiance ratioing method is applied to semi-transparent clouds whose effective emissivity is close to 100 % (nearly opaque cloud) and is giving results at pixel scale. This method is only applied to semi-transparent clouds if no reliable retrieved cloud top pressure is found using intercept method. Clouds analysed in this section are therefore much thicker than in case the cloud top is retrieved by intercept method. In order to increase the number of available cases, we used RALI ground-based measurements when at least one of the two instruments operated (optional mode 3). We found 214 coincidences between SEVIRI and RALI fully functioning for the semi-transparent cloud top height retrieved with radiance ratioing method.

The comparison of SEVIRI and RALI CTH retrieval, summarized in Figure 28, Figure 29 and Table 25, demonstrates the ability of the radiance ratioing method to perform fairly good agreement with radar and lidar retrievals for rather thick semi-transparent clouds:

- On average, SEVIRI CTH for semi-transparent clouds using the radiance ratioing method show an underestimate of 60m as compared to radar/lidar retrieved CTH with a standard deviation of 1180m (see first line in Table 25).
- Figure 29 illustrates that the radiance ratioing method is only applied to thick semi-transparent clouds.
- The solar zenith angle does not impact the SEVIRI CTH retrieval (see Figure 29).

SEVIRI sounding channels used	Mean (km)	Standard deviation (km)	Median (km)	Number of cases
Any	-0.06	1.18	-0.10	211
13.4µm	-0.56	0.94	-0.38	12
6.2µm	0.43	1.03	0.46	6
7.3µm	-0.06	1.18	-0.10	209

Table 25 Statistical scores for (CTH_SEVIRI-CTH_RALI) as a function of the channels used in the radiance ratioing method. Negative mean or median values correspond to SEVIRI CTH underestimation.

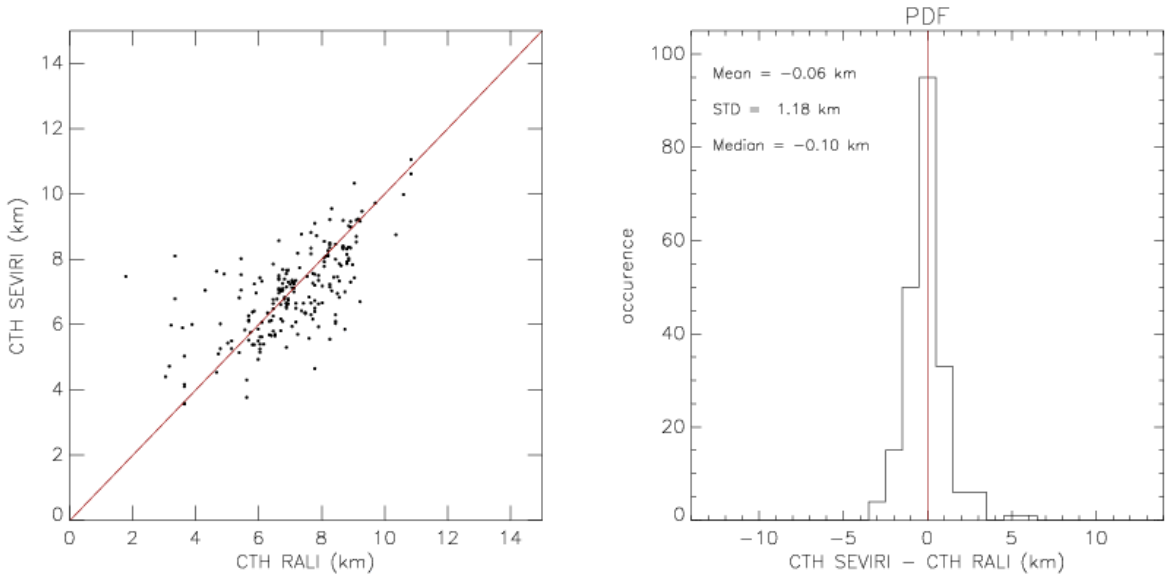

Figure 28 Comparison of CTH retrieved from SEVIRI and from Radar/lidar (RALI) for semi-transparent clouds (radiance ratioing method). PDF is the probability Density Function.

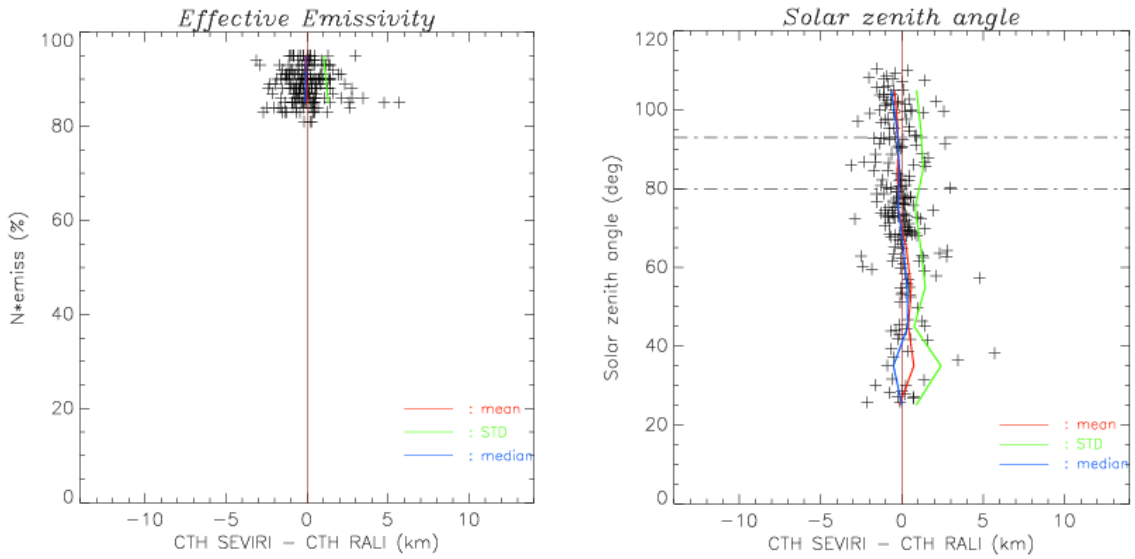

Figure 29 Influence of effective emissivity and solar zenith angle on the comparison of CTH retrieved from SEVIRI and from Radar/lidar (RALI) for semi-transparent clouds (radiance ratioing method).

4.3 VALIDATION OF CTTH FOR LOW CLOUDS WITH RADIO-SOUNDINGS

Opaque cloud top pressures or heights are retrieved from measured T10.8µm brightness temperatures through a vertical profile of brightness temperatures simulated from temperature and humidity vertical profile forecast by NWP. It often happens in the lower troposphere that the variation of temperature with height is not monotonous (in case of thermal inversion) and not well simulated by NWP. This explains why low cloud retrieved top pressure or height may present rather strong errors. Nevertheless, errors on retrieved low cloud top temperatures are not expected to be so large (at least in mid-latitude regions). In this validation, we focus on the cloud top pressure validation.

A systematic comparison of low cloud top pressure retrieved from SEVIRI imagery (using SAFNWC/MSG v1.2) and estimated from radio-sounding is performed over Europe (Figure 41) during nearly one year (from 3rd March 2004-14th February 2005). The impact of the atmospheric thermal inversion on the retrieval's quality is documented. The influence of the illumination and viewing angles' impact is investigated.

The following procedure is applied to gather the validation dataset:

- The cloud top pressure is estimated from each radio-soundings using Pone's rules (see Annex 6): stable and unstable layers are first looked for from surface up to the tropopause ; cloud layers are then derived depending on the stability of these layers. The Annex 4 illustrates the location of these radio-soundings in Europe.
- The cloud top pressures, computed from the SEVIRI imagery using the SAFNWC/MSG version 1.2, are averaged in an area of 9x9 IR SEVIRI pixels centred on each radio-sounding.
- The following filtering is then applied to select homogeneous cloud layers:
  - Only one cloud layer must be found in the radio-sounding (cloud layers separated by less than 50 hPa are merged).
  - At least 90% of the pixels inside the 9x9 satellite target must be classified as very low, low or medium clouds by CT.
  - The T10.8µm standard deviation computed in the 9x9 satellite target with these cloudy pixels must be less than 1K
- An additional filtering is applied to limits problems linked with the automatic method applied to radio-sounding: the cloud top temperature retrieved from satellite and estimated from radio-sounding must agree within 5K. In fact, even after the first filtering, strong differences between cloud top temperature estimated from radio-soundings and retrieved from satellite could be observed. A visual analysis of these situations shows that they usually correspond to limitations in the automatic radio-sounding analysis (if the radio-sounding was slightly different, a cloud layer more in agreement the satellite data would have been possible) or to a radio-sounding spatially very close to the edge of two cloud layers. This additional filtering is reasonable as for low or medium opaque clouds, provided the cloud classification is correct, the difference between the cloud top temperature and the IR10.8 brightness temperature is mainly due to atmospheric effects which are not very strong in European areas.

The cloud top pressure estimated from satellite and from radio-sounding using this procedure have been compared. Daytime and night-time observations have been analysed separately and are synthesised in Table 26 and in Figure 30, Figure 31 and Figure 32.

Time of day	Bias (Satellite-radio-sounding)	Standard deviation	Number of cases
0hUTC	-15.89 hPa	70.67 hPa	382
12hUTC	-30.06 hPa	71.77 hPa	344

Table 26 Comparison between cloud top pressure retrieved from satellite and estimated from radio-soundings: bias, standard deviation and number of cases at 0hUTC and 12hUTC.

Table 26 shows that on average, low clouds top pressures are underestimated by 15hPa at night-time and by 30hPa at daytime, but a large scatter is observed (70hPa standard deviation). Figure 30 suggests that clouds top pressures are generally underestimated by more than 50hPa for cloud pressures lower than 800hPa whereas both underestimation and overestimation are observed for cloud pressures larger than 800hPa. This can be linked to the presence and strength of a thermal inversion in the radio-sounding, as shown in Figure 31. The method to retrieve the cloud top pressure of low clouds is dependent on the presence of a thermal inversion in the forecast NWP fields. If a very strong inversion is observed in the radio-sounding, there is then a chance that this inversion is present in the forecast NWP fields even if its strength is not well simulated. In this

case, the retrieved cloud top pressure is usually set below the inversion, and Figure 31 indicates that a cloud pressure overestimation ranging around 50hPa is then observed. On the reverse, if no strong inversion is observed in the radio-sounding, there is a chance that no thermal inversion is simulated in the NWP fields and therefore a chance that the cloud top is set much to high in the atmosphere, thus leading to cloud pressure underestimation. The systematic underestimation by around 50-100hPa of cloud pressure below 800hPa is not observed in the comparison with lidar and radar which on the contrary shows that there is a tendency to underestimate opaque cloud top height, i.e. to overestimate opaque cloud top pressure (see 4.2).

These values are coherent with those obtained from radar/lidar (see 4.2.1) although the standard deviation observed with radar/lidar (1030m) corresponds a standard deviation of about 100hPa larger than the one derived from the comparison with radio-sounding.

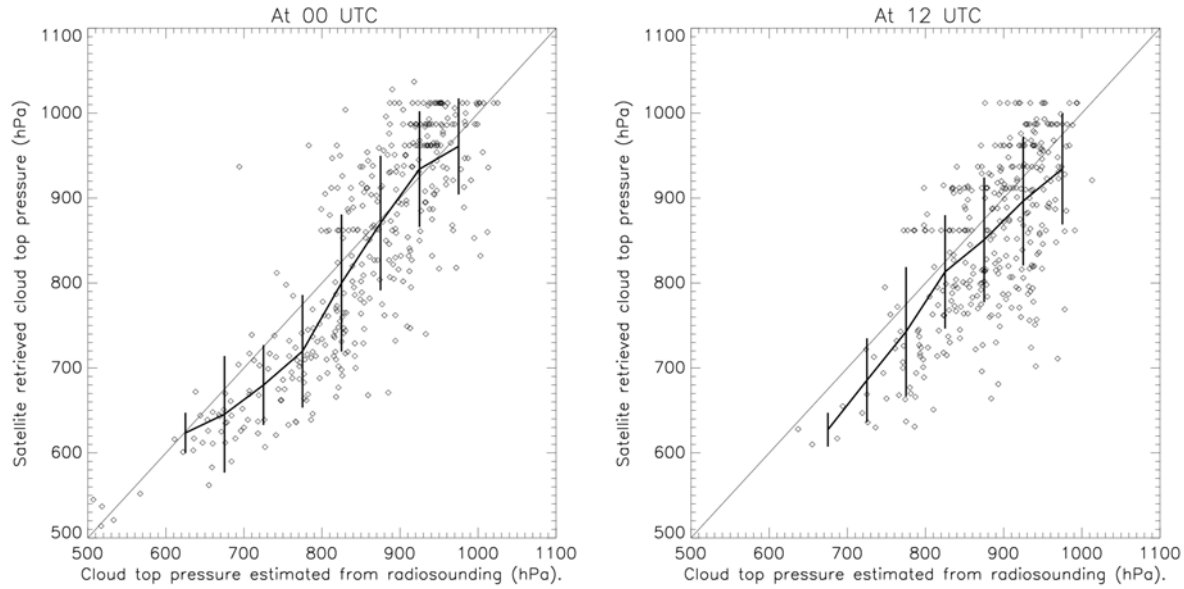

Figure 30 Comparison between cloud top pressure retrieved from satellite and estimated from radio-soundings. The solid lines corresponds to mean and standard deviation computed in 50hPa intervals.

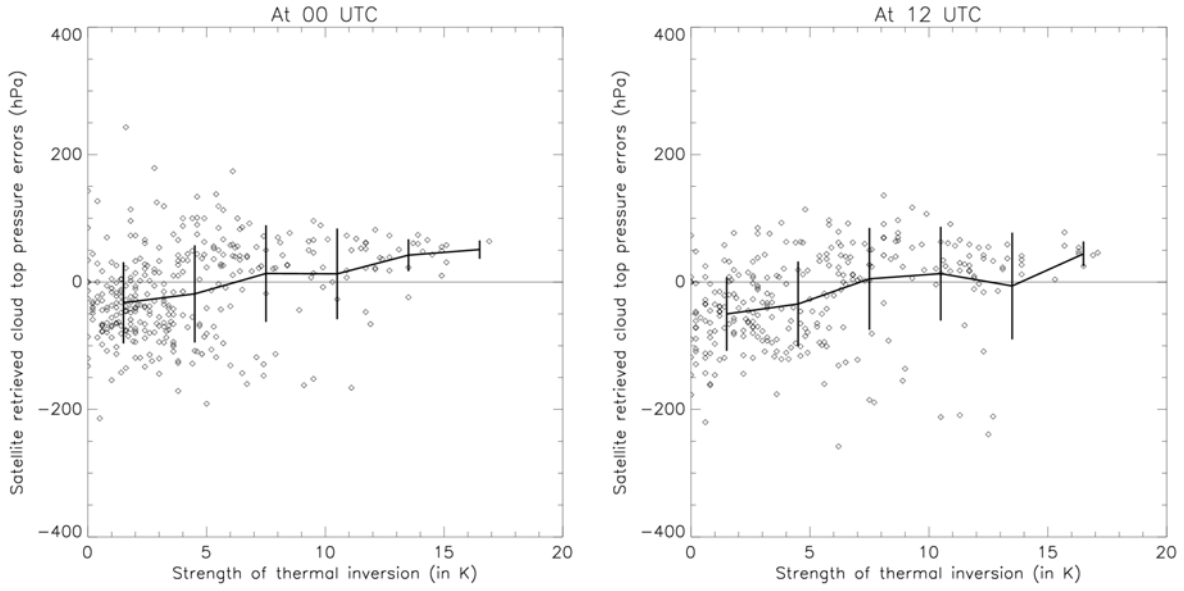

Figure 31 Satellite retrieved cloud top pressure error as a function of the thermal inversion strength. The error stands for the difference of cloud top pressures derived from satellite and

estimated from the collocated radio-sounding. The thermal inversion strength (observed in the radio-sounding) is defined as the difference between the cloud top temperature (estimated from radio-sounding) and the maximum air temperature observed above the cloud. The solid lines corresponds to bias and standard deviation computed in 2.5K intervals.

No clear errors' dependency with the time of day (0hUTC or 12UTC) can be observed. Therefore the tendency observed with radar/lidar to overestimate CTH at night-time as compared to daytime has not been found with radio-sounding.

An underestimation at large viewing angle is observed as shown on Figure 32: cloud top pressures measured at viewing angles larger than 70 degrees are lower by around 50hPa than those measured at viewing angles around 50-60 degrees. One reason is that RTTOV, used to simulate the atmospheric absorption above the clouds, is not valid at high viewing angle and therefore RTTOV simulations are performed using a satellite zenith angle limited to 65 degrees. The consequence is an underestimation of the atmospheric effects above the clouds at viewing angle larger than 65 degrees which can lead to too low retrieved cloud top pressures.

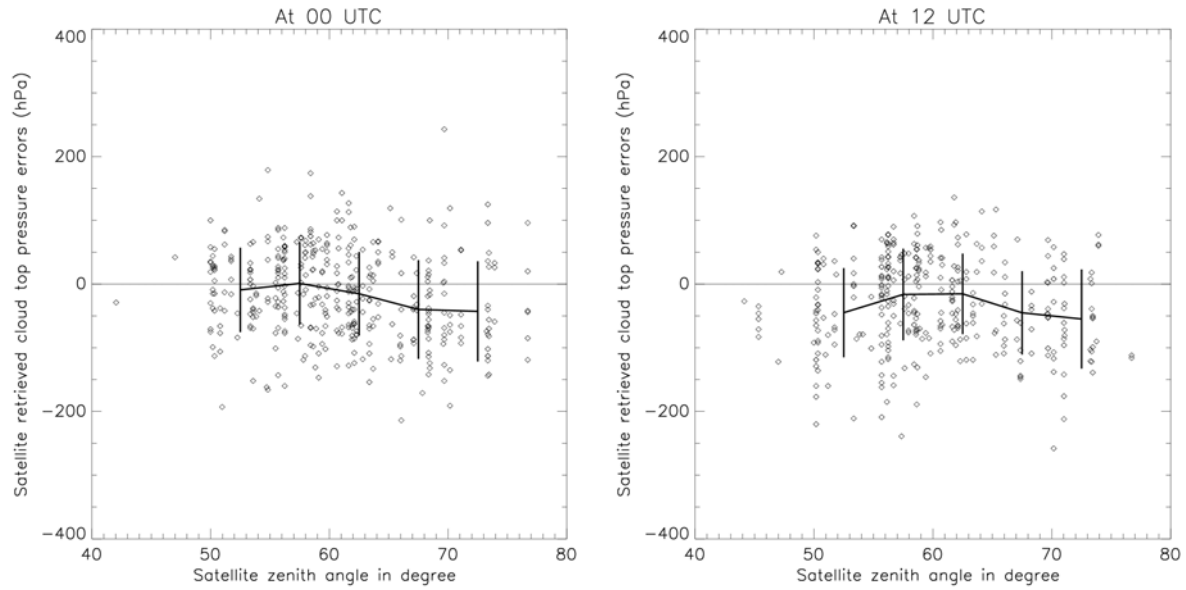

Figure 32 Satellite retrieved cloud top pressure error as a function of satellite zenith angle. The error stands for the difference of cloud top pressures derived from satellite and estimated from the collocated radio-sounding. The solid lines corresponds to bias and standard deviation computed in 5 degrees intervals.

4.4 INDEPENDENCY OF CTTH ERRORS WITH VIEWING ANGLE AND TIME OF DAY

We should normally check the dependency of CTTH errors with viewing angle and time of day from a dataset including collocated CTTH and in-situ cloud top observations for all cloud types. The validation datasets including measurements from radio-sounding, ground-based radar and lidar allow to draw partial conclusions on the dependency of CTTH errors with time of the day for all cloud types (see 4.2 and 4.3) and with viewing angles for low clouds only (see 4.3). To complement them, statistics on CTTH values are computed over a large area during one year: strong abnormal variations of CTTH with viewing angle or time of the day should indicate a dependency of CTTH errors.

To perform this statistical study, we use the dataset gathering SYNOP measurements and SEVIRI measurements and cloud products. This dataset does not allow the re-processing of CTTH (too small targets: 5*5 IR pixels whereas 32*32 is required for CTTH processing). Therefore, the dependency of CTTH errors with viewing angle and time of the day is estimated using the CTTH stored in the file which is computed with version v1.0. The differences between CTTH v1.2 and v1.0 mainly consist in the use of RTTOV7 instead RTTOV6, in an improved low clouds top height retrieval in case strong thermal inversion and an improved CMa and CT (see AD. 5).

Statistics are computed using data from 1st November 2003 up to 30th November 2004 covering Europe and north Africa (see Annex 3). These statistical characteristics are associated with changes in latitudes, (for Nordic (latitude larger than 55 degrees) and midlatitude (latitude between 20 and 55 degrees)), illumination conditions (day (sun zenith angle lower than 80 degrees), night (sun zenith angle larger than 93 degrees) or twilight), viewing angles (satellite zenith angle in the six following intervals: [0-40],[40-50],[50-60],[60-70],[70-80],[80,90]) and cloud types (very low and low clouds, medium clouds, high and very high clouds, semi-transparent clouds). Averaged cloud top pressure, temperature and height are displayed respectively in Figure 33, Figure 34 and Figure 35.

We focus the discussion on the cloud top pressure which is the first parameter retrieved by the CTTH software, the cloud top temperature and height being derived from the cloud top pressure through the use of forecast vertical temperature and humidity profiles.

The following conclusions can be drawn from the figures inspection:

- Cloud top pressure of low clouds are generally lower at night-time/twilight and at high viewing angles (especially if larger than 80 degrees), but also in Nordic areas. Two possible explanations can be put forward:
    - RTTOV, used to simulate the atmospheric absorption above the clouds, is not valid at high viewing angle. In case of viewing angles larger than 65 degrees, RTTOV simulations are performed using a satellite zenith angle of 65 degrees. The consequence is an underestimation of the atmospheric effects above the clouds at large viewing angle which can lead to too low retrieved cloud top pressures. This effect contributes to the decrease of cloud top pressure observed at high viewing angles (above 70 degrees) in all illumination conditions on Figure 33 (left), and also in Nordic areas characterized by high viewing angles.
    - In case strong thermal inversion is present and not well simulated by NWP model, the boundary layer clouds are retrieved above the inversion thus leading to too low cloud top pressure (this effect is less present in CTTH v1.2). This is more frequent in Nordic and continental areas and at night-time. This can partly explain lower cloud top pressure observed at daytime and in Nordic areas (Figure 33, right).

  Similar tendency with the viewing angle is observed from the comparison of low cloud CTTH (v1.2) with radio-sounding (see Figure 32): a 50hPa decrease is observed for viewing angles increasing from 55 up to 75 degrees.

  The lower low cloud top pressure observed at night-time/twilight are coherent with results obtained by comparing with radar/lidar (see 4.2.1) but not with radio-soundings (Table 26).

- Cloud top pressures of medium, high/very high clouds, medium and thick semi-transparent clouds are nearly independent on the time of the day, whereas a slight variation of less than 25hPa is observed for thin semi-transparent clouds. This is in agreement with the comparison with radar and lidar where no clear tendency with the time of the day can be seen (see 4.2).

- Cloud top pressures of high and very high clouds are lower in Nordic areas or in case high viewing angles; but this is coherent with a tropopause being higher at low latitude.
- Cloud top pressures of thin and medium semi-transparent clouds are higher by more than 80hPa at night-time and twilight for viewing angles larger than 70 degrees. This effect is not observed at daytime. The explanation could be a misclassification of snowy grounds as semi-transparent clouds in night-time conditions (all cloud pressures higher than 400hPa are observed in February).

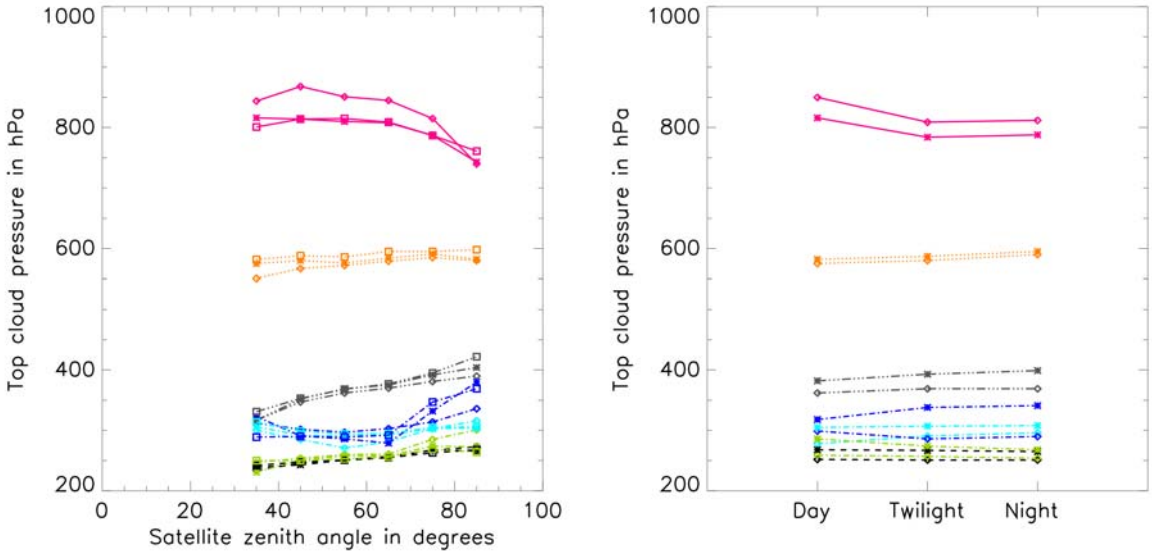

Figure 33 Illustration of Cloud top pressure (in hPa) for low clouds (red), medium clouds (orange), high and very high clouds (grey and black), and for semi-transparent clouds (thin (dark blue), medium (light blue) or thick (green)). Left: dependency on viewing angles for daytime (diamond), twilight (star) or night (square) conditions. Right: dependency on illumination for mid-latitude (diamond) and Nordic (star) areas.

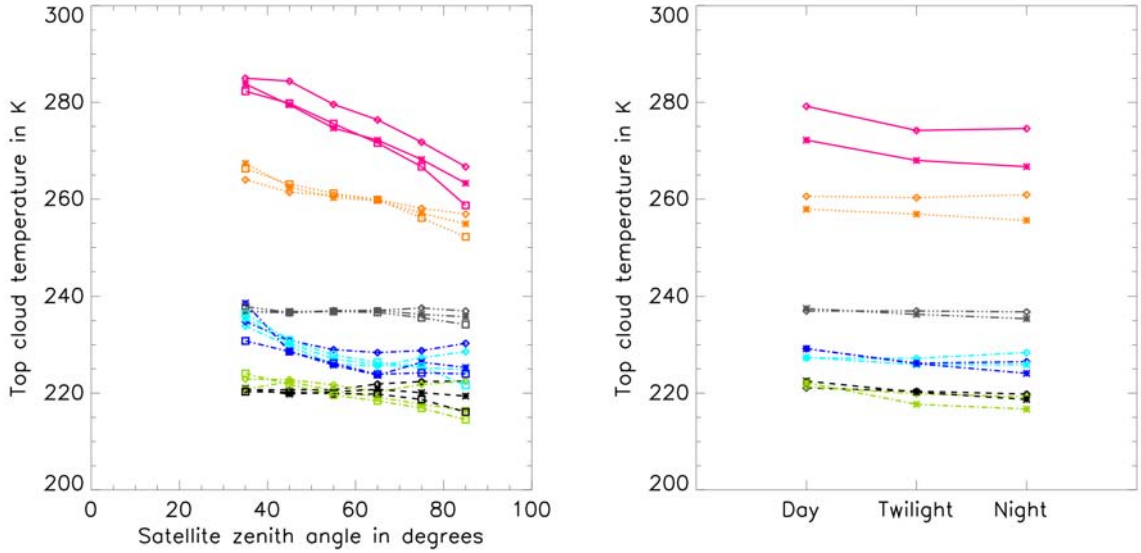

Figure 34 Illustration of Cloud top temperature (in Kelvin) for low clouds (red), medium clouds (orange), high and very high clouds (grey and black), and for semi-transparent clouds (thin (dark blue), medium (light blue) or thick (green)). Left: dependency on viewing angles for daytime

(diamond), twilight (star) or night (square) conditions. Right: dependency on illumination for mid-latitude (diamond) and Nordic (star) areas.

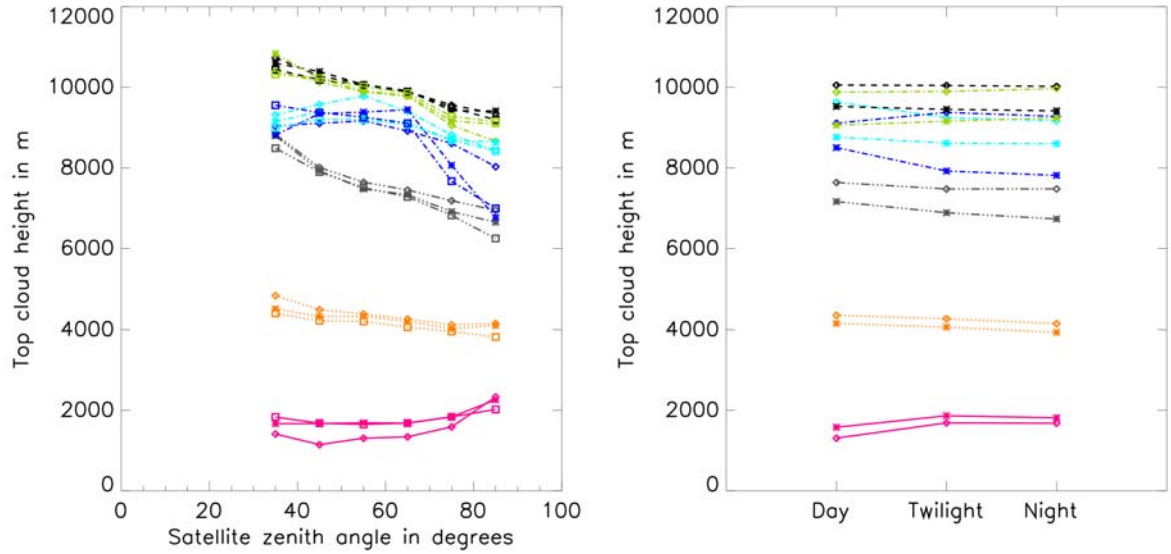

Figure 35 Illustration of Cloud top height (in meters) for low clouds (red), medium clouds (orange), high and very high clouds (grey and black), and for semi-transparent clouds (thin (dark blue), medium (light blue) or thick (green)). Left: dependency on viewing angles for daytime (diamond), twilight (star) or night (square) conditions. Right: dependency on illumination for mid-latitude (diamond) and Nordic (star) areas.

4.5 CONCLUSION

4.5.1 Assessment of algorithm quality

A general assessment of the algorithm quality is given in this section.

For all clouds except low opaque clouds:

- A general underestimation of cloud top height (400m for opaque medium or high clouds, up to 1000m for semi-transparent clouds retrieved using intercept method) associated with a rather high standard deviation (larger than 1000m) is observed from the comparison with radar/lidar measurements over Paris.
- An independency of retrieved cloud top height with illumination is observed from radar/lidar over Paris; the independency with illumination is likely over the whole Europe except perhaps for thin cirrus (see Figure 33).
- The dependency with viewing angle has not been checked.

For low opaque clouds:

- On average, a reasonable overestimation of cloud top height (320m with radar/lidar measurements, between –15 and -30hPa with radio-sounding) associated to a large standard deviation (1000m with radar/lidar measurement, 70hPa with radio-soundings) is observed.
- A dependency with thermal inversion is observed with radio-soundings.
- A dependency of retrieved cloud top height with illumination is observed with radar/lidar but not with radio-soundings.
- A dependency with viewing angles (above 60 degrees) is observed with radio-sounding.

4.5.2 Proposal for algorithm modification

Areas for algorithm improvement are given in this section.

For high opaque clouds:

- Try to decrease underestimation by applying radiance ratioing methods; check using the validation dataset radar/lidar/seviri.

For semi-transparent clouds:

- Try to decrease underestimation (both bias and standard deviation) by a better tuning of intercept/radiance ratioing using the validation dataset radar/lidar/seviri.

For low clouds:

- The observed limitations are inherent to the algorithm: brightness temperatures are measured and are converted into pressure or height through a forecast vertical profile. One way to improve the low clouds CTH retrieval is to allow the user to change the segment's size (currently a fixed value of 32 IR pixel), thus allowing the CTTH algorithm to make a better use of the NWP vertical profile input by the user. Another way is to wait RTTOV9 that should simulate the IR radiation using pressure levels input by the user and not fixed pressure levels.

ANNEX: TEST AND VALIDATION DATASET

ANNEX 1 INTERACTIVE TARGET DATABASE

An interactive tool, based on the use of the commercial image processing software WAVE, has been used by experienced operators for the extraction of visually identified satellite targets in SEVIRI images (area : full disk). The result of this work is a dedicated database for spectral signature studies that we call the Interactive Target Database. Such a database has been already been gathered from GOES during prototyping activities (AD. 1). The interactive procedure allows :

- the display of various channels combination full resolution in satellite projection,
- the zoom of an area
- the choice of small square targets (configurable size, by default: 5*5 SEVIRI IR pixels)
- the labelling of the targets through a menu

The Interactive Target Database gathers the following information (detailed below) for each satellite target:

- the label given by the operator to the target (list displayed in Table 27 below),
- the full satellite information in the square targets together with satellite & solar angles and time information,
- the collocated and nearest in time meteorological information extracted from ARPEGE forecast fields,
- collocated atlas values.

Open sea	Sea with shadow	Sea with sand aerosols	Sea with ash
Sea with haze	Sea with sunglint	Sea with volcanic plume	
Land	Land with shadow	Land with sand aerosol	Land with ash
Land with Haze	Land with volcanic plume	Ice	Ice with shadow
Snow	Snow with shadow	Unclassified (cloudy or cloudfree)	Cloudy (unknown)
fog	stratus	Stratocumulus	shadow over low clouds
small cumulus over sea	Cumulus congestus over sea	small cumulus over land	Cumulus congestus over land
Cumulonimbus	Extensive cumulonimbus	Thin cirrus over sea	Thin Cirrus over ice
Thin cirrus over land	Thin cirrus over snow	Thin cirrus over St/Sc	Thin cirrus over Cu
Thin cirrus over Ac/As	Altocumulus/Altrostratus	Altocumulus	Cirrostratus
Cirrostratus over Ac/As			

Table 27 List of cloud & earth types available in the Interactive Target Database

22619 targets have been gathered from SEVIRI images, mainly focusing on cloud free, low clouds and aerosols (as shown by the statistics of the data base sum up in Table 28).

	Sea	**Land**	**Snow**	**St/Sc**	**Ac/As**	**Cu**	**Cb**	**Ci over cloud**	**Ci**	**Cs over Ac,As**	**Aerosol**
SEVIRI 22619 targets	10.5 %	15.7%	2.1%	32.6%	3.7%	1.6%	2.4%	1.7%	4.3%	1.2%	23.0%

Table 28 Statistics on cloud and earth's types available in the SEVIRI Interactive test file

ANNEX 2 FORMAT FOR SEVIRI SATELLITE TARGET

Satellite targets are gathered, either manually with the Interactive Target Database, either automatically around synoptic meteorological stations.

Each satellite target window will be have a configurable size, the default size being 5 columns by 5 rows (3km IR pixel).

The satellite targets contains the following information:

Full satellite information in the square targets, together with satellite & solar angles and time information :

type	a*2 target type (in for interactive)
observer	a*10 user name of the person who has analysed the target
lat	i*4 latitude of the centre of the target (1000th of degrees)
lon	i*4 longitude of the centre of the target (1000th of degrees)
date	i*4 julian day (count from 00h, 1 Jan 1950)
hour	i*4 UTC time of day in milliseconds
idsat	i*4 satellite identification (1=MSG1, 2=MSG2, 3=MSG3)
nbp	i*2 number of columns expressed in 3km IR coordinates
nbl	i*2 number of rows expressed in 3km IR coordinates
nbc	i*2 number of channels (7,10 or 11, according to day/night consideration and HRV availability)
valcan_VIS06	I*2 indicator of VIS0.6 availability
valcan_VIS08	I*2 indicator of VIS0.8 availability
valcan_IR16	I*2 indicator of IR1.6 availability
valcan_IR38	i*2 indicator of IR3.8 availability [-1 =not in the file
valcan_WV62	i*2 indicator of WV62 availability [0 =is missingt
valcan_WV73	i*2 indicator of WV73 availability [>0 =mean value in the
valcan_IR87	i*2 indicator of IR87 availability [target(unit: 1/100 % or 1/100 K)]
valcan_IR97	i*2 indicator of IR97 availability
valcan_IR108	i*2 indicator of IR108 channel availability
valcan_IR120	i*2 indicator of IR120 channel availability
valcan_IR134	i*2 indicator of IR134 channel availability
valcan_HRV	I*2 indicator of HRV availability
canal VIS06	x i*2 window from VIS06 (x = nbp*nbl) in 1/100 %
canal VIS08	x i*2 window from VIS08 (x = nbp*nbl) in 1/100 %
canal IR6	x i*2 window from IR16 (x = nbp*nbl) in 1/100 %
canal IR38	x i*2 window from IR38 (x = nbp*nbl) in 1/100 K
canal WV62	x i*2 window from WV62 (x = nbp*nbl) in 1/100 K
canal WV73	x i*2 window from WV73 (x = nbp*nbl) in 1/100 K
canal IR87	x i*2 window from IR87 (x = nbp*nbl) in 1/100 K
canal IR97	x i*2 window from IR97 (x = nbp*nbl) in 1/100 K
canal IR108	x i*2 window from IR108 (x = nbp*nbl) in 1/100 K
canal IR120	x i*2 window from IR120 (x = nbp*nbl) in 1/100 K
canal IR134	x i*2 window from IR134 (x = nbp*nbl) in 1/100 K
canal HRV	x i*2 window from HRV (x = 3*nbp*3*nbl) in 1/100 %
solzen	i*2 solar zenith angle (100th of degrees)
satzen	i*2 satellite zenith angle (100th of degrees)
daz	i*2 local azimuth angle (100th of degrees)s
typ_cloud	i*2 target code (given by the observer , or –9999 if automatically fed)

Full CMa/CT/CTTH results in the square targets:

CMa main categories	x i*1 window from CMa main categories (x = nbp*nbl)
CMa tests	x i*2 window from CMa tests (x = nbp*nbl)
CMa quality flag	x i*2 window from CMa quality flag (x = nbp*nbl
CT main categories	x i*1 window from CT main categories (x = nbp*nbl)
CT quality flag	x i*2 window from CT quality flag (x = nbp*nbl
CTTH top pressure	x i*1 window from CTTH top pressure (x = nbp*nbl)
CTTH top temperature	x i*1 window from CTTH top temperature (x = nbp*nbl)
CTTH top height	x i*1 window from CTTH top height (x = nbp*nbl)
CTTH cloudiness	x i*1 window from CTTH cloudiness (x = nbp*nbl)
CTTH quality flag	x i*1 window from CTTH quality flag (x = nbp*nbl)

Collocated atlas values and climatological values :

land/sea	x i*1 land/sea atlas (space=0, sea=2, land=3), (x = nbp*nbl)
land/sea/coast	x i*1 land/sea/coast atlas (space=0, coast=1,sea=2, land=3), (x = nbp*nbl)
height	x i*2 height atlas value (in meters), (x = nbp*nbl)
stt	x i*2 sst climatological value (in 1/100 K), (x = nbp*nbl)
albedo	x i*2 visible reflectance climatological value (in 1/100 %), (x = nbp*nbl)
h2o	i*2 climatological integrated water vapor content (in 1/100 kg/m2)
T1000	i*2 climatological air temperature at 1000hPa (in 1/100 K)
T850	i*2 climatological air temperature at 850hPa (in 1/100 K)
T700	i*2 climatological air temperature at 700hPa (in 1/100 K)
T500	i*2 climatological air temperature at 500hPa (in 1/100 K)

Collocated and nearest in time meteorological information extracted from ARPEGE forecast fields (temperature & humidity vertical profile) [missing values : -9999] :

Modele a*7 name of modele (ARPEGE or ECMWF…)

Two set of forecast NWP fields are available (nearest in time before and after SEVIRI image):

date	i*4 julian day of forecast day (count from 00h, 1 Jan 1950)
res	i*4 hour of forecast
ech	i*4 forecast term (in hour)
HeightNWP	I*4 height of NWP grid (in meters)
psol	i*4 ground pressure (1/100 hPa)
tsol	i*4 ground temperature (1/100 K)
t2m	i*4 2m air temperature (1/100 K)
hu2m	i*4 2m air relative humidity (1/100 %)
nbniv	I*4 number of pressure levels on the vertical
pniv	20 i*4 nbniv pressure level (in hPa)
tniv	20 i*4 temperature at nbniv pressure levels (1/100 K)
huniv	20 i*4 relative humidity at nbniv pressure levels (1/100 %)
ptropo	i*4 pressure at tropopause level (1/100 hPa)
ttropo	i*4 temperature at tropopause level (1/100 K)
W	i*4 integrated water vapor content (in 1/100 kg/m2)

Spare values :

spare 30 i*4 spare data (not used)

ANNEX 3 SURFACE OBSERVATIONS (SYNOP)

The data used are the routine weather observations, coded by the observers into the WMO synoptic code, gathered at Toulouse and made available to users through a METEO-FRANCE data base. From this data base we extract all the synoptic reports (coded in BUFR) from a list of 535 selected land stations, over the European and Northern African area. These stations have been selected to cover European region. The SYNOP network status is permanently evolving because several nations are replacing human cloud cover observations by automatic systems delivering cloud covers. For this reason we decided to keep from the initial database only the SYNOP whose $i_x < 4$ (in $i_R i_x$hVV group of section 1 of SYNOP, coded according to table code 1860 of the WMO manual on codes) because they are assumed to be manned station. Another indicator of human observation is the anomaly at N=1 or N=7 in the N distribution (N1N7) of a station, as according to WMO standard for reporting cloud cover, a very small cloud in the sky leads human observer to code 1 octa, rather than 0, and, in a similar way, a small patch of clear sky gives rise 7 rather than 8 octas. We analyse these statistics by station and retain only those for which N1N7 anomaly is observed. We are aware that this distribution may change with time and that automatic observations may still enter our statistics. Our final set contains 302 stations, their spatial distribution is displayed on right part of Figure 36. This set is the basis retained for our statistics when we deal with "selected stations dataset" (SSD), otherwise we specify "no selection among stations" (NSASD). It is obvious that some countries are not covered by this geographical distribution, but considering the one-year duration and the dispersion of the stations, it should not hamper the study.

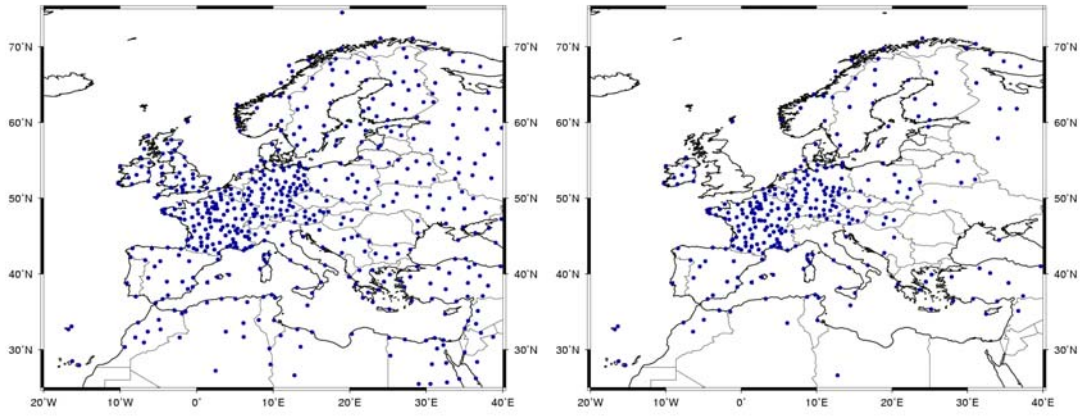

Figure 36 Geographical distribution of SYNOP stations, gathered from November, 1st 2004 till February, 28 th 2005; left initial set (NSASD set); right 302 selected stations(SSD set)

The database has been built as soon as MSG data were routinely available at CMS through EUMETCast diffusion with a stable geo-location and radiometric quality. We have used information from November 2003 till February 2005, with an interruption in January 2004 during the satellite positioning towards -3.4W. The SYNOP are selected with 3 hour intervals and gathered with MSG/SEVIRI information coming from the slot starting 15 minutes before.

To avoid cases where solar intrusion in IR 3.9 µm at night-time is significant, we also rejected from SSD selection all the matchups presenting a mean reflectance in SEVIRI VIS 0.6 µm greater than .9% with a sun zenithal angle greater than 93 degrees. Finally from a NSASD containing 1138432 samples, we get a SSD with 708793 usable sorted matchups. This dataset can be stratified according to station latitude. The Nordic subset (16%) contains stations with latitude higher than 55N. It can also be stratified in coastal (35.7%) and land (64.3%) subset for other analysis.

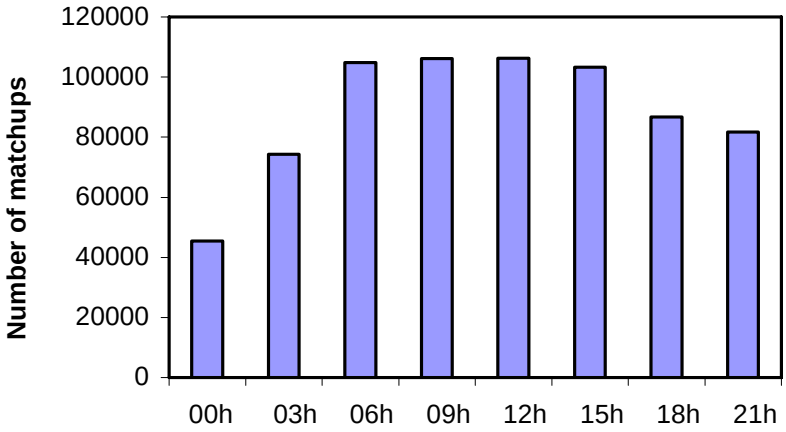

Figure 37 Frequency of 708793 SSD matchups according to their UTC observation hour.

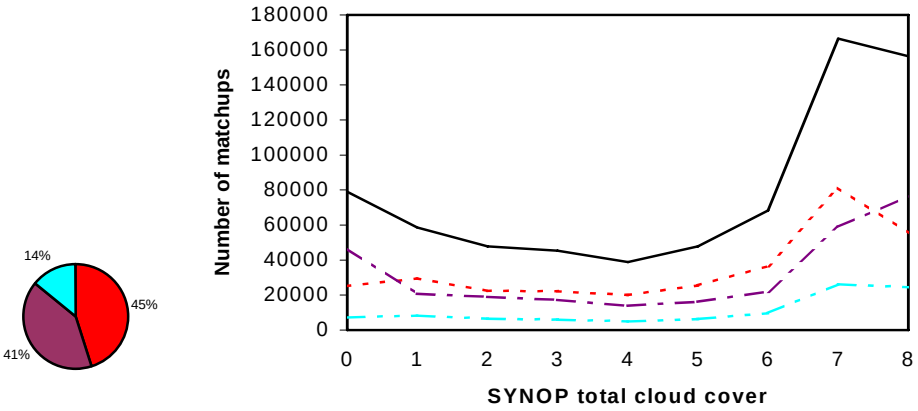

Figure 38 Left; SSD illumination conditions distribution; total (black), day (red), night (purple), twilight (blue) Right; SSD frequency of matchups according to their total cloud cover in octas, globally and detailed by illumination condition; total (black solid line) , day (red dotted), night (purple dashed), twilight (blue dash-dotted).

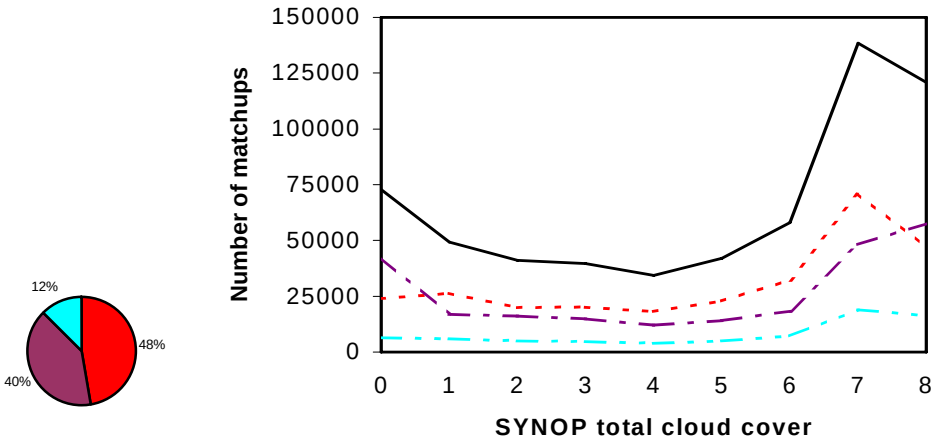

Figure 39 Same as figure above but for SSD midlatitude cases (total, day, night, twilight).

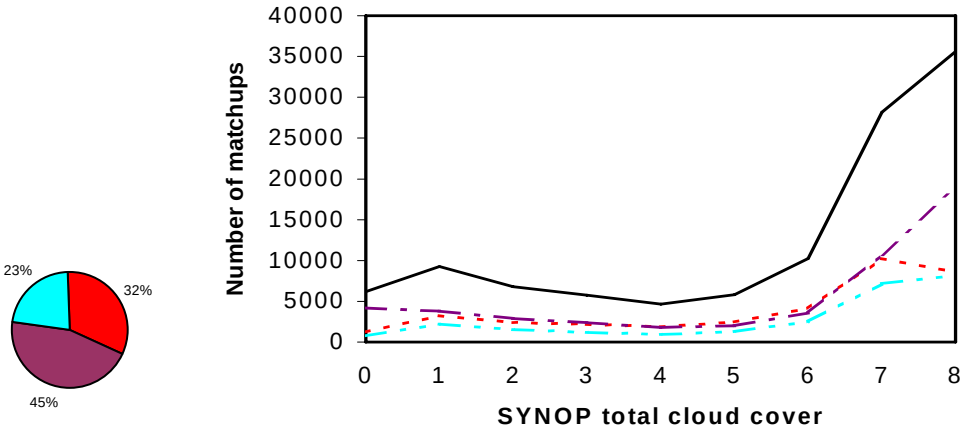

Figure 40 Same as figure above but for Nordic SSD cases (total, day, night, twilight).

The three figures above show that N1N7 anomaly is visible for daytime reports, that illumination distribution among dataset may vary. It is normal to see that geographical stratification changes slightly the illumination proportions, as twilight conditions become more numerous at northern latitudes.

ANNEX 4 RADIOSOUNDING OBSERVATIONS (TEMP)

The data used are the routine radiosounding observations, coded into the WMO temp code, gathered at Toulouse and made available to users through a METEO-FRANCE data base. From this data base we extract all the temp reports (coded in BUFR) from a list of 100 selected land stations, over the European area. The following figure illustrates the spatial coverage of the selected land stations.

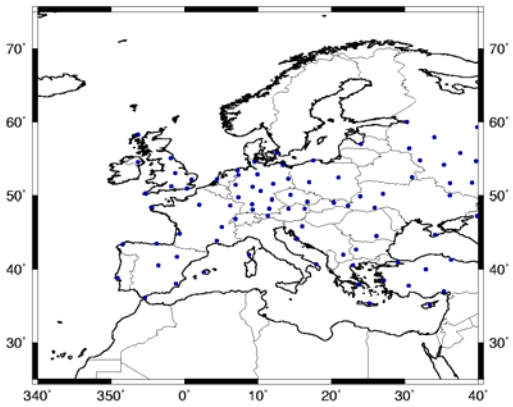

Figure 41Geographical distribution of validation TEMP stations

ANNEX 5 CONTINGENCY TABLES FOR CT VALIDATION WITH SYNOP

	Cloud free	Low	Med	Semi	High	Semi above	Fract	Total
Cloud free	158124	8997	1113	11557	345	260	5060	185456
Low (N≤5)	9608	11499	434	2128	151	107	2414	26341
Low (N≥6)	6355	79515	24505	29410	14521	5515	4958	164779
Med (N≤5)	7024	8612	765	2562	300	455	2131	21849
Med (N≥6)	1214	12454	12265	14281	12417	2713	1533	56877
Semi (N≤5)	21101	4556	1142	15585	696	1592	5003	49675
Semi (N≥6)	3605	5168	4398	22148	4785	4389	2798	47291
High (N≤5)	3339	3560	637	2438	314	478	1819	12585
High (N≥6)	2075	17974	14941	19623	14371	4531	2570	76085
Mult (N≤5)	7712	6446	600	3492	234	526	2651	21661
Mult (N≥6)	1732	12890	7473	10687	5684	3527	2248	44241
Total	221889	171671	68273	133911	53818	24093	33185	706840

Table 29 Validation of Cloud Type (CT) with SYNOP. Error matrix for all climatic and illumination conditions from collocated surface and MSG-1/SEVIRI observations from 01/11/2003 to 28/02/2005 when NWP are available (N stands for total cloud cover reported in SYNOP)

	Cloud free	Low	Med	Semi	High	Semi above	Fract	Total
Cloud free	70320	3801	151	906	40	260	1646	77124
Low (N≤5)	3710	6869	91	230	15	107	778	11800
Low (N≥6)	528	36815	9821	4839	5635	5515	581	63734
Med (N≤5)	3982	7234	304	826	72	455	1193	14066
Med (N≥6)	292	8063	5959	3733	5817	2713	485	27062
Semi (N≤5)	11457	2585	380	4433	179	1592	2912	23538
Semi (N≥6)	1880	2911	2036	8249	2329	4389	1600	23394
High (N≤5)	1642	2422	316	808	157	478	867	6690
High (N≥6)	492	9512	7186	5682	6489	4531	799	34691
Mult (N≤5)	3905	4562	212	986	58	526	1425	11674
Mult (N≥6)	537	8333	3901	3610	2839	3527	856	23603
Total	98745	93107	30357	34302	23630	24093	13142	317376

Table 30 Validation of Cloud Type (CT) with SYNOP. Error matrix for all day-time conditions for collocated surface and MSG-1/SEVIRI observations from 01/11/2003 to 28/02/2005 when NWP are available (N stands for total cloud cover reported in SYNOP)

	Cloud free	Low	Med	Semi	High	Semi above	Fract	Total
Cloud free	68288	4004	772	10131	260	0	2843	86298
Low (N≤5)	4480	3802	284	1803	117	0	1388	11874
Low (N≥6)	3378	33027	10886	19846	6426	0	3980	77543
Med (N≤5)	2098	984	329	1514	191	0	679	5795
Med (N≥6)	635	3066	4282	8334	4408	0	847	21572
Semi (N≤5)	6330	1153	500	9631	420	0	1303	19337
Semi (N≥6)	1023	1406	1505	10321	1744	0	708	16707
High (N≤5)	906	584	195	1249	103	0	588	3625
High (N≥6)	1032	5557	4999	9831	5139	0	1315	27873
Mult (N≤5)	2274	1153	219	2045	137	0	760	6588
Mult (N≥6)	632	2660	2089	4846	1802	0	904	12933
Total	91076	57396	26060	79551	20747	0	15315	290145

Table 31 Validation of Cloud Type (CT) with SYNOP. Error matrix for all night-time conditions for collocated surface and MSG-1/SEVIRI observations from 01/11/2003 to 28/02/2005 when NWP are available (N stands for total cloud cover reported in SYNOP)

	Cloud free	Low	Med	Semi	High	Semi above	Fract	Total
Cloud free	19516	1192	190	520	45	0	571	22034
Low (N≤5)	1418	828	59	95	19	0	248	2667
Low (N≥6)	2449	9673	3798	4725	2460	0	397	23502
Med (N≤5)	944	394	132	222	37	0	259	1988
Med (N≥6)	287	1325	2024	2214	2192	0	201	8243
Semi (N≤5)	3314	818	262	1521	97	0	788	6800
Semi (N≥6)	702	851	857	3578	712	0	490	7190
High (N≤5)	791	554	126	381	54	0	364	2270
High (N≥6)	551	2905	2756	4110	2743	0	456	13521
Mult (N≤5)	1533	731	169	461	39	0	466	3399
Mult (N≥6)	563	1897	1483	2231	1043	0	488	7705
Total	32068	21168	11856	20058	9441	0	4728	99319

Table 32 Validation of Cloud Type (CT) with SYNOP. Error matrix for all twilight conditions for collocated surface and MSG-1/SEVIRI observations from 01/11/2003 to 28/02/2005 when NWP are available (N stands for total cloud cover reported in SYNOP)

	Cloud free	**Low**	**Med**	**Semi**	**High**	**Semi above**	**Fract**	**Total**
Cloud free	143882	6501	513	8616	158	161	3375	163206
Low (N≤5)	9128	10562	320	1780	107	101	2257	24255
Low (N≥6)	5581	70726	19524	23734	11549	5252	4626	140992
Med (N≤5)	6685	7604	495	2154	215	369	1867	19389
Med (N≥6)	1042	10853	9319	10851	9417	2518	1345	45345
Semi (N≤5)	19795	3871	739	13759	527	1402	4487	44580
Semi (N≥6)	3156	4219	3141	18742	3619	4013	2522	39412
High (N≤5)	2870	2498	293	1761	192	380	1347	9341
High (N≥6)	1721	13395	9159	13987	9435	4116	2007	53820
Mult (N≤5)	7045	5324	313	2785	149	440	2314	18370
Mult (N≥6)	1538	10812	5369	8722	4186	3247	2040	35914
Total	202443	146365	49185	106891	39554	21999	28187	594624

Table 33 Validation of Cloud Type (CT) with SYNOP. Error matrix for mid-latitude subset with all illumination conditions for collocated surface and MSG-1/SEVIRI observations from 01/11/2003 to 28/02/2005 when NWP are available (N stands for total cloud cover reported in SYNOP)

	Cloud free	Low	Med	Semi	High	Semi above	Fract	Total
Cloud free	65115	2926	47	658	16	161	1336	70259
Low (N≤5)	3593	6440	74	218	10	101	748	11184
Low (N≥6)	494	34011	8124	4470	4802	5252	556	57709
Med (N≤5)	3824	6444	167	727	49	369	1101	12681
Med (N≥6)	276	7299	4681	3434	4751	2518	453	23412
Semi (N≤5)	10898	2262	234	4044	127	1402	2724	21691
Semi (N≥6)	1717	2523	1516	7512	1792	4013	1489	20562
High (N≤5)	1490	1812	159	665	105	380	751	5362
High (N≥6)	455	7665	4716	5096	4836	4116	719	27603
Mult (N≤5)	3647	3920	120	857	32	440	1295	10311
Mult (N≥6)	513	7323	2908	3302	2233	3247	802	20328
Total	92022	82625	22746	30983	18753	21999	11974	281102

Table 34 Validation of Cloud Type (CT) with SYNOP. Error matrix for mid-latitude subset with day-time conditions for collocated surface and MSG-1/SEVIRI observations from 01/11/2003 to 28/02/2005 when NWP are available (N stands for total cloud cover reported in SYNOP)

	Cloud free	Low	Med	Semi	High	Semi above	Fract	Total
Cloud free	62473	2974	401	7713	125	0	1754	75440
Low (N≤5)	4232	3437	207	1486	85	0	1279	10726
Low (N≥6)	2864	28939	8781	15670	5026	0	3706	64986
Med (N≤5)	1988	873	260	1261	146	0	561	5089
Med (N≥6)	524	2542	3368	6003	3301	0	720	16458
Semi (N≤5)	5945	972	381	8552	341	0	1118	17309
Semi (N≥6)	856	1070	1143	8522	1399	0	619	13609
High (N≤5)	757	353	85	867	59	0	346	2467
High (N≥6)	835	3977	3074	6260	3177	0	944	18267
Mult (N≤5)	2050	908	134	1618	99	0	633	5442
Mult (N≥6)	547	2149	1544	3805	1322	0	800	10167
Total	83071	48194	19378	61757	15080	0	12480	239960

Table 35 Validation of Cloud Type (CT) with SYNOP. Error matrix for mid-latitude subset with night-time conditions for collocated surface and MSG-1/SEVIRI observations from 01/11/2003 to 28/02/2005 when NWP are available (N stands for total cloud cover reported in SYNOP)

	Cloud free	Low	Med	Semi	High	Semi above	Fract	Total
Cloud free	16294	601	65	245	17	0	285	17507
Low (N≤5)	1303	685	39	76	12	0	230	2345
Low (N≥6)	2223	7776	2619	3594	1721	0	364	18297
Med (N≤5)	873	287	68	166	20	0	205	1619
Med (N≥6)	242	1012	1270	1414	1365	0	172	5475
Semi (N≤5)	2952	637	124	1163	59	0	645	5580
Semi (N≥6)	583	626	482	2708	428	0	414	5241
High (N≤5)	623	333	49	229	28	0	250	1512
High (N≥6)	431	1753	1369	2631	1422	0	344	7950
Mult (N≤5)	1348	496	59	310	18	0	386	2617
Mult (N≥6)	478	1340	917	1615	631	0	438	5419
Total	27350	15546	7061	14151	5721	0	3733	73562

Table 36 Validation of Cloud Type (CT) with SYNOP. Error matrix for mid-latitude subset with twilight conditions for collocated surface and MSG-1/SEVIRI observations from 01/11/2003 to 28/02/2005 when NWP are available (N stands for total cloud cover reported in SYNOP)

	Cloud free	Low	Med	Semi	High	Semi above	Fract	Total
Cloud free	14242	2496	600	2941	187	99	1685	22250
Low (N≤5)	480	937	114	348	44	6	157	2086
Low (N≥6)	774	8789	4981	5676	2972	263	332	23787
Med (N≤5)	339	1008	270	408	85	86	264	2460
Med (N≥6)	172	1601	2946	3430	3000	195	188	11532
Semi (N≤5)	1306	685	403	1826	169	190	516	5095
Semi (N≥6)	449	949	1257	3406	1166	376	276	7879
High (N≤5)	469	1062	344	677	122	98	472	3244
High (N≥6)	354	4579	5782	5636	4936	415	563	22265
Mult (N≤5)	667	1122	287	707	85	86	337	3291
Mult (N≥6)	194	2078	2104	1965	1498	280	208	8327
Total	19446	25306	19088	27020	14264	2094	4998	112216

Table 37 Validation of Cloud Type (CT) with SYNOP. Error matrix for nordic subset with all illumination conditions for collocated surface and MSG-1/SEVIRI observations from 01/11/2003 to 28/02/2005 when NWP are available (N stands for total cloud cover reported in SYNOP)

	Cloud free	Low	Med	Semi	High	Semi above	Fract	Total
Cloud free	5205	875	104	248	24	99	310	6865
Low (N≤5)	117	429	17	12	5	6	30	616
Low (N≥6)	34	2804	1697	369	833	263	25	6025
Med (N≤5)	158	790	137	99	23	86	92	1385
Med (N≥6)	16	764	1278	299	1066	195	32	3650
Semi (N≤5)	559	323	146	389	52	190	188	1847
Semi (N≥6)	163	388	520	737	537	376	111	2832
High (N≤5)	152	610	157	143	52	98	116	1328
High (N≥6)	37	1847	2470	586	1653	415	80	7088
Mult (N≤5)	258	642	92	129	26	86	130	1363
Mult (N≥6)	24	1010	993	308	606	280	54	3275
Total	6723	10482	7611	3319	4877	2094	1168	36274

Table 38 Validation of Cloud Type (CT) with SYNOP. Error matrix for nordic subset at day-time conditions for collocated surface and MSG-1/SEVIRI observations from 01/11/2003 to 28/02/2005 when NWP are available (N stands for total cloud cover reported in SYNOP)

	Cloud free	Low	Med	Semi	High	Semi above	Fract	Total
Cloud free	5815	1030	371	2418	135	0	1089	10858
Low (N≤5)	248	365	77	317	32	0	109	1148
Low (N≥6)	514	4088	2105	4176	1400	0	274	12557
Med (N≤5)	110	111	69	253	45	0	118	706
Med (N≥6)	111	524	914	2331	1107	0	127	5114
Semi (N≤5)	385	181	119	1079	79	0	185	2028
Semi (N≥6)	167	336	362	1799	345	0	89	3098
High (N≤5)	149	231	110	382	44	0	242	1158
High (N≥6)	197	1580	1925	3571	1962	0	371	9606
Mult (N≤5)	224	245	85	427	38	0	127	1146
Mult (N≥6)	85	511	545	1041	480	0	104	2766
Total	8005	9202	6682	17794	5667	0	2835	50185

Table 39 Validation of Cloud Type (CT) with SYNOP. Error matrix for nordic subset at night-time for collocated surface and MSG-1/SEVIRI observations from 01/11/2003 to 28/02/2005 when NWP are available (N stands for total cloud cover reported in SYNOP)

	Cloud free	Low	Med	Semi	High	Semi above	Fract	Total
Cloud free	3222	591	125	275	28	0	286	4527
Low (N≤5)	115	143	20	19	7	0	18	322
Low (N≥6)	226	1897	1179	1131	739	0	33	5205
Med (N≤5)	71	107	64	56	17	0	54	369
Med (N≥6)	45	313	754	800	827	0	29	2768
Semi (N≤5)	362	181	138	358	38	0	143	1220
Semi (N≥6)	119	225	375	870	284	0	76	1949
High (N≤5)	168	221	77	152	26	0	114	758
High (N≥6)	120	1152	1387	1479	1321	0	112	5571
Mult (N≤5)	185	235	110	151	21	0	80	782
Mult (N≥6)	85	557	566	616	412	0	50	2286
Total	4718	5622	4795	5907	3720	0	995	25757

Table 40 Validation of Cloud Type (CT) with SYNOP. Error matrix for nordic subset at twilight for collocated surface and MSG-1/SEVIRI observations from 01/11/2003 to 28/02/2005 when NWP are available (N stands for total cloud cover reported in SYNOP)

	Cloud free	Low (N<5)	Low (N>6)	Med (N<5)	Med (N>6)	Semi (N<5)	Semi (N>6)	High (N<5)	High (N>6)
All :	85.26	43.65	48.26	3.50	21.56	31.37	46.83	2.50	18.89
Day	91.18	58.21	57.76	2.16	22.02	18.83	35.26	2.35	18.71
Night	79.13	32.02	42.59	5.68	19.85	49.81	61.78	2.84	18.44
Twilight	88.57	31.05	41.16	6.64	24.55	22.37	49.76	2.38	20.29
Mid-latitude:	88.16	43.55	50.16	2.55	20.55	30.86	47.55	2.06	17.53
Day	92.68	57.58	58.94	1.32	19.99	18.64	36.53	1.96	17.52
Night	82.81	32.04	44.53	5.11	20.46	49.41	62.62	2.39	17.39
Twilight	93.07	29.21	42.50	4.20	23.20	20.84	51.67	1.85	17.89
Nordic:	64.01	44.92	36.95	10.98	25.55	35.84	43.23	3.76	22.17
Day	75.82	69.64	46.54	9.89	35.01	21.06	26.02	3.92	23.32
Night	53.55	31.79	32.56	9.77	17.87	53.21	58.07	3.80	20.42
Twilight	71.17	44.41	36.45	17.34	27.24	29.34	44.64	3.43	23.71

Table 41 CT Producer accuracy for SYNOP cloud classes for collocated surface and MSG-1/SEVIRI observations from 01/11/2003 to 28/02/2005 when NWP are available (N stands for total cloud cover reported in SYNOP)

	Cloud free	Low	Med	Semi	High
All :	71.26	53.02	19.09	28.18	27.29
Day	71.21	46.92	20.63	36.97	28.13
Night	74.98	64.17	17.69	25.08	25.27
Twilight	60.86	49.61	18.18	25.42	29.63
Mid-latitude:	71.07	55.54	19.95	30.41	24.34
Day	70.76	48.96	21.31	37.30	26.35
Night	75.20	67.18	18.72	27.65	21.46
Twilight	59.58	54.43	18.95	27.35	25.35
Nordic:	73.24	38.43	16.85	19.36	35.46
Day	77.42	30.84	18.59	33.93	34.96
Night	72.64	48.39	14.71	16.17	35.40
Twilight	68.29	36.29	17.06	20.79	36.21

Table 42 CT User accuracy for grouped cloud types for collocated surface and MSG-1/SEVIRI observations from 01/11/2003 to 28/02/2005 when NWP are available (N stands for total cloud cover reported in SYNOP)

	Cloud free	Low (N<5)	Low (N>6)	Med (N<5)	Med (N>6)	Semi (N<5)	Semi (N>6)	High (N<5)	High (N>6)
All :	78.64	45.56	44.86	4.54	22.46	30.33	46.17	2.89	18.27
Day	90.66	58.35	53.15	2.88	23.28	18.09	33.57	2.68	19.32
Night	67.35	34.94	39.60	7.30	20.44	48.47	62.87	3.57	16.25
Twilight	80.73	35.93	39.75	8.13	25.07	20.87	48.03	2.44	19.72
Mid-latitude:	82.44	45.38	46.31	3.42	21.76	29.88	46.92	2.43	17.26
Day	92.33	57.80	54.12	1.99	21.55	17.95	34.82	2.37	18.18
Night	72.14	34.74	40.97	6.41	21.22	48.00	63.76	2.87	15.59
Twilight	87.10	34.51	40.64	5.17	24.30	19.74	50.19	1.89	17.93
Nordic:	50.45	47.69	36.22	13.41	25.24	34.36	42.38	4.24	20.73
Day	73.37	68.56	43.79	11.11	34.50	19.75	24.37	3.91	23.85
Night	33.72	36.88	32.46	13.76	17.92	52.57	58.91	5.06	17.52
Twilight	55.89	46.46	36.59	21.29	26.60	26.06	42.18	3.55	22.30

Table 43 CT Producer accuracy for SYNOP cloud classes for collocated surface and MSG-1/SEVIRI observations from 01/11/2003 to 28/02/2005 without NWP (N stands for total cloud cover reported in SYNOP)

	Cloud free	Low	Med	Semi	High
All :	71.76	50.19	16.95	26.54	27.91
Day	71.38	45.81	19.22	35.73	28.91
Night	75.96	58.64	14.74	23.59	25.42
Twilight	61.88	45.29	16.46	23.54	30.33
Mid-latitude:	71.52	52.67	17.69	28.80	25.05
Day	70.98	47.85	19.83	36.07	27.15
Night	76.02	61.46	15.48	26.08	21.58
Twilight	60.64	49.44	17.41	25.73	26.28
Nordic:	74.91	36.50	14.89	17.75	36.31
Day	77.14	29.96	17.21	32.48	35.88
Night	75.06	44.72	12.48	15.06	36.33
Twilight	70.64	33.83	15.02	18.38	36.87

Table 44 CT User accuracy for grouped cloud types for collocated surface and MSG-1/SEVIRI observations from 01/11/2003 to 28/02/2005 without NWP (N stands for total cloud cover reported in SYNOP)

ANNEX 6 ESTIMATION OF LOW CLOUD TOP HEIGHT FROM RADIOSOUNDING

Pone's rules are applied to radio-sounding measurements to analyse the saturation and stability of each layer from surface up to the tropopause, and consequently deduce the likely cloud cover vertical extension. These rules are fully described in "Météorologie générale" from J.P.Triplet and G.Roche (Météo-France publication, ISBN: 2-11-085 176-7) and are summarized in this annex.

The saturation of each layer is analysed by comparing air and dew temperatures at the bottom and top of each layer. The stability of layers can be inferred from the comparison of the lapse rate of the air and wet-bulb temperature curves through the layer to the lapse rate of the dry adiabatic and saturated pseudo-adiabatic curves respectively. Seven types of layers are then defined as follows:

- **absolute stability (saturated or unsaturated):** air and wet-bulb temperature lapse rates less than dry adiabatic and saturated pseudo-adiabatic lapse rates respectively.
- **latent potential instability:** air temperature lapse rate less than dry adiabatic lapse rate and wet-bulb temperature lapse rate greater than saturated pseudo-adiabatic lapse rate. Temperature of particle lifted through the layer according saturated adiabatic is less than air temperature at the top of the layer.
- **selective potential instability:** air temperature lapse rate less than dry adiabatic lapse rate and wet-bulb temperature lapse rate greater than saturated pseudo-adiabatic lapse rate. Temperature of particle lifted through the layer according saturated adiabatic is greater than air temperature at the top of the layer.
- **absolute instability (saturated or unsaturated):** air and wet-bulb lapse temperature lapse rates greater than dry adiabatic and saturated pseudo-adiabatic lapse rates respectively.
- **dry instability:** air temperature lapse rate greater than dry adiabatic lapse rate and wet-bulb temperature lapse rate less than saturated pseudo-adiabatic lapse rate.

For each type of layer, the probable cloud cover is defined by its type (stratiform or cumuliform), its basis and its vertical extension (average, intermediate or maximum vertical extension) according to empirical rules:

- **saturated absolute stability:** stratiform cloud defined by its average vertical extension
- **unsaturated absolute stability:** usually no cloud cover
- **latent potential instability:** usually no cloud cover
- **selective potential instability:** two cloud layers are possible, one stratiform layer defined by its average vertical extension and a cumuliform cloud layer defined by its average and maximum vertical extension
- **saturated absolute instability:** cumuliform cloud defined by its average, intermediate and maximum vertical extension
- **unsaturated absolute instability:** cumuliform cloud defined by its average and maximum vertical extension
- **dry instability:** usually no cloud cover

Throughout the study, the cloud top pressures are obtained by using the average vertical extension.

ANNEX 7 GROUND-BASED RADAR AND LIDAR MEASUREMENTS AT SIRTA SITE (PARIS)

LIDAR instrument (LNA)

The lidar instrument, called Lidar Nuages Aerosols (LNA) is a backscattered lidar developed at LMD for cloud and aerosol remote sensing. It can detect aerosol and cloud layers with visible optical thickness ranging from 0.05 to 3, above which the signal is completely attenuated.

The LNA is an Nd-Yag pulsed lidar emitting at 532 and 1064 nm and linearly polarized. The pulse frequency is 20 Hz while the nominal temporal resolution is 10 s. Backscattered photons are collected through two telescopes: a narrow-field-of-view one (0.5 mrad) with range 2-15 km and a wide-field-of-view one (5 mrad) with range 0.1-5 km. The backscattered signal is sampled with a vertical resolution of 15 meters. Vertical distributions of particles are characterized from the ground to about 15 km and the structure of the atmosphere such as the boundary layer height and the altitudes of aerosol and cloud layer is derived by the STRAT algorithm (described below).

The LNA operates on routine schedules from Mondays through Fridays, 8am to 8pm local time. However, the LNA instrument is turned off in case of precipitation. Figure 42 shows the number of 15 min slots of LNA observation each month during the study period.

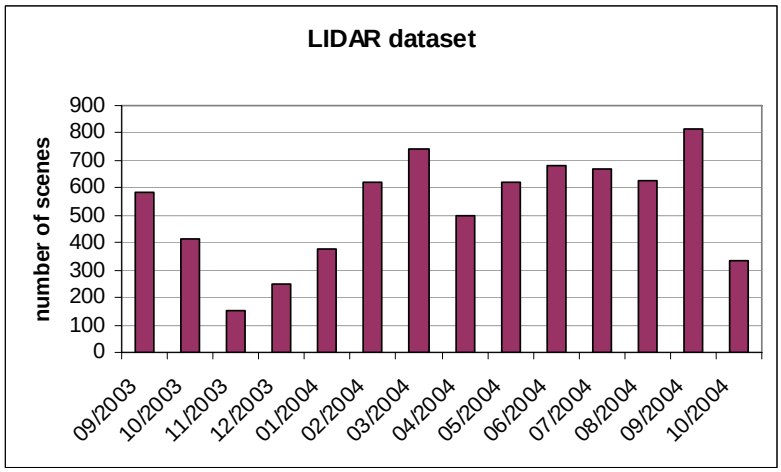

Figure 42 Distribution of LNA dataset (number of 15 min slots of observation each month).

Raw lidar data gives the amount of backscattered photons as a function of altitude for every profile. The LNA product used in this study is the output of the STRAT (STRucture of the ATmosphere) algorithm. It identifies the different layers crossed by the laser beam. In the v1 version of the STRAT algorithm, each pixel can be classified as:

- No significant power return (NSPR): the backscattered signal is considered too noisy for identification. A signal is considered too noisy when the signal to noise ratio is smaller than 3. The noise, caused by optical and electronic variations is considered constant along the profile. It is estimated by taking the standard deviation of the signal where there is no lidar return in the highest range (i.e. where the signal is totally due to sky radiance). The NSPR flag occurs in case the lidar beam is attenuated by the atmosphere underneath it.
- Boundary layer: the pixel is part of the boundary layer. It is the lowest layer of the atmosphere and is generally located between 1000 and 2000 meters altitude, depending on the intensity of the turbulent mixing (normally lower during night than during day). In this layer, where turbulence induced by the ground is very strong, the dynamics are different than in the higher layers. Most of the aerosols from the ground, mixed by turbulent flow,

are found inside this layer. In the STRAT algorithm, the boundary layer is identified by a threshold test applied on the ratio of the backscattering signal between two heights.

- Molecular: the atmosphere is cloud and aerosol free. A molecular backscattering profile is estimated from the comparison between pressure and temperature profiles (measured by daily atmospheric sounding or extracted from models) and the recording backscattered signal. Molecular layers correspond to zones that successfully passed a threshold test relevant of the similarity between the slopes of the simulated and measured profiles.
- Cloud or aerosol: the pixel is contaminated or filled by cloud or aerosol. Continuous Wavelet transform is used to detect singularities of the backscattering signal at layer boundaries (top, peak and base). A threshold test is also used to remove over detections due to noise fluctuations.
- Aerosol/cloud separation: based on the analysis of the particle backscatter distribution. A threshold on the average peak-to-base backscatter ratio of consistent particle layers is used to separate aerosol from cloud layers.

From this classification, a simplified cloud mask is derived as shown in Figure 43. The cloud mask reveals that the lidar provides a full characterization of the vertical extent of the cirrus cloud (07:00 to 12:00 UT), but as the cloud becomes optically thicker, the lidar signal is attenuated and the range is limited to the lowest 2 km of the cloud.

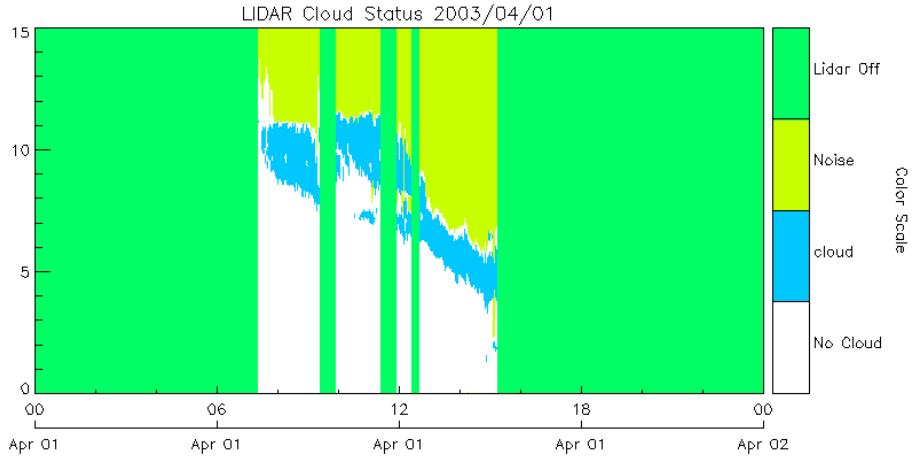

Figure 43 Cloud mask derived from the lidar backscattered power (green: lidar off, yellow: noise, blue: cloud, white: no cloud).

RADAR instrument (RASTA)

The cloud radar called RASTA (Radar Aéroporté et Sol de Télédétection Atmosphérique) is a vertically-pointing single beam 95GHz Doppler radar with a range resolution of 60 meters and the temporal resolution is 1 s. This instrument is devoted to the investigation of cloud processes, through the documentation of the microphysical, radiative and dynamical properties of all type of non-precipitating clouds.

The ground-based configuration of the RASTA cloud radar operates routinely at SIRTA since October 2002 until September 2004. RASTA ceased functioning in October 2004. Figure 44 shows the number of 15 min slots of RASTA observation each month during the study period.

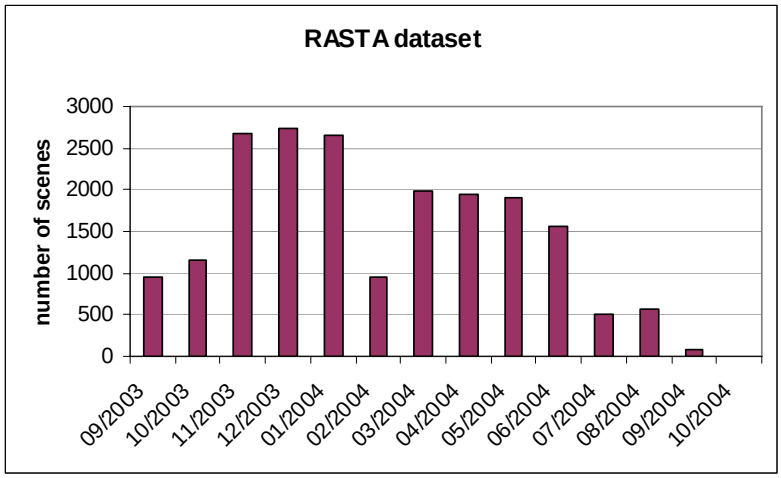

Figure 44 Distribution of RASTA dataset (number of 15 min slots of observation each month).

The radar products have been derived from an algorithm developed by the Department of Meteorology from the University of Reading (UK). This algorithm uses a multiple threshold tests on radar reflectivity and vertical Doppler velocity to classify pixels as : clear-sky, ice particles, melting ice particles, cloud liquid droplets, drizzle/rain, aerosols, or insects. We derive a simpler classification consisting of number 0 to 3 defined as :

0 : clear-sky, aerosol and insect pixels are deemed to be 'clear-sky'
1 : ice/water hydrometeor pixels are deemed to be 'cloud'
2 : precipitating hydrometeor pixels are deemed to be 'drizzle/rain'
3 : radar instrument turned off

Information of the retrieval algorithm can be found at
http://www.met.rdg.ac.uk/radar/cloudnet/data/products/categorize.html.

Figure 45 shows the cloud mask derived from this algorithm.

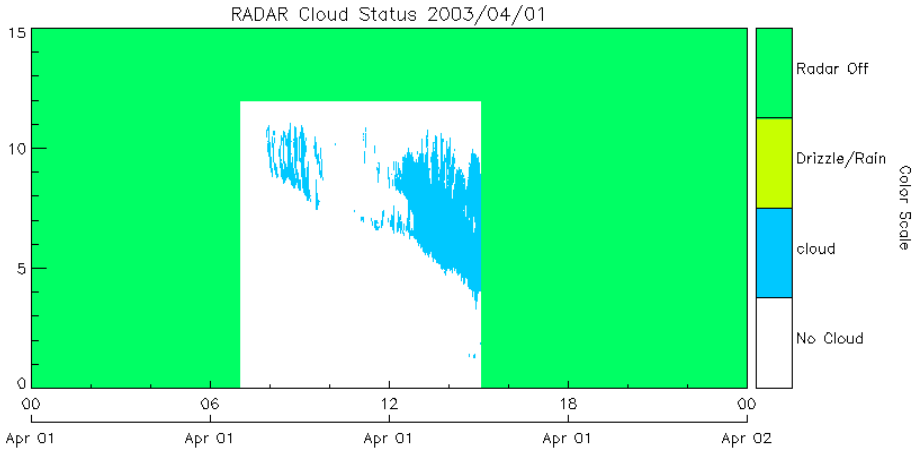

Figure 45 Cloud mask derived from the radar reflectivity (green: radar off, yellow: drizzle or rain, blue: cloud, white: no cloud)

Radar & Lidar synergy (RALI)

Data products retrieved from the synergy between the radar and lidar are called the RALI data in this study. The radar and lidar measurements are averaged over a 30 s timeframe and then are independently analysed to retrieve cloud mask product.

Figure 46 shows a cloud mask derived from the combined analysis of the radar reflectivity and the lidar backscattered power. Clouds shown in blue correspond to areas where one of the instruments detects clouds. The cloud mask reveals that radar-lidar synergy is particularly suited to extend the

range of observable cloud layers. The vertical resolution is 60 m and the RALI measurements give a maximum range of 15 km.

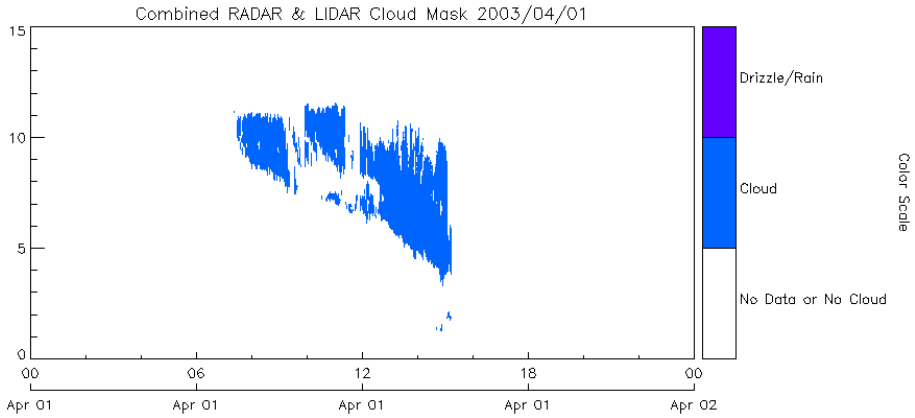

Figure 46 Cloud mask derived from radar-lidar synergy (violet: drizzle or rain, blue: cloud, white: no data or no cloud). The temporal resolution is 30 s.

RALI cloud mask datasets are available for 4 modes of measurement:

- Mode 0: measurement during radar data acquisition time
- Mode 1: measurement during simultaneous radar and lidar data acquisition time
- Mode 2: measurement during lidar data acquisition time
- Mode 3: measurement during radar and/or lidar data acquisition time

Remote sensing of clouds by lidar and radar : limitations

Active remote sensing by lidar only (mode 2):

Lidar back-scattering at 532 nm is sensitive to the number of scattering particles and second moment of the particle size distribution (D^2). The lidar beam is scattered by both liquid water and ice clouds. At each level of the atmosphere, scattering produces lidar signal (the back-scattered portion) but also lidar signal attenuation for the higher levels. For the LNA lidar we consider that the lidar signal is completely extinguished beyond an optical depth of about 3. We also consider that a cloud can be detected as long as its optical depth is greater than 0.01. According to Morille et al. (2005), for clouds with optical depth ranging between 0.01 and 3, the analysis of lidar back-scattered power by the STRAT algorithm will yield CTH values with a bias ranging from 0 to –60m (underestimation of CTH). In the following situations the lidar alone will not provide reliable CTH estimates for:

- Optically thick water clouds
- Ice clouds overlying a solid continuous layer of optically thick water clouds

Active remote sensing by radar only (mode 0):

Radar reflectivity at 94 GHz is driven by the number of particle and the sixth moment of the particle size distribution (D^6). The radar reflectivity is much more sensitive to particle size than particle concentration. Hence the radar will be efficient to detect clouds that contain a high amount of liquid or ice water in which cloud droplets and ice crystals have reached a significant size. Contrary to the lidar, the radar signal in clear air (outside the cloud) is virtually zero hence the cloud boundaries are easily found with a signal threshold. The only ambiguity is that if the cloud particles are too small or if the cloud is too thin and too far (> 10 km), the sensitivity of the radar is not sufficient to produce a reflectivity above the threshold. In the following situations the radar alone will not provide reliable CTH estimates for:

- Optically thin clouds above 10 km
- Fair weather cumulus clouds at the top of the boundary layer

Active remote sensing by lidar and radar (mode 1):

By combining the retrievals from lidar and radar observations, we are able to significantly decrease the number of clouds that are missed by the ground-based station. The combination of wavelengths allows us to observe the entire range of optical depth and cloud types. However, in the following situations the combination of lidar and radar at the ground may not be able to provide reliable CTH estimates for:

- Multi-layer situation with solid continuous layer of optically thick water clouds underlying a layer of optically thin ice clouds at a high altitude.

For all CTH validation studies, mode 1 is by far the most reliable data source, but the number of combined lidar/radar observation is smaller than lidar alone (mode 2) or radar alone (mode 0). Hence, to validate CTH values for:

- Opaque clouds, we use the mode 0 dataset.
- Semi-transparent clouds: we use the mode 2 dataset